



Measurement of J/ψ -jet correlations in pp and Pb+Pb collisions at $\sqrt{s_{NN}} = 5.02$ TeV with the ATLAS detector

The ATLAS Collaboration

Yields of charmonia, bound states of $c\bar{c}$ quarks, are observed to be strongly suppressed in heavy-ion collisions relative to proton-proton collisions as a result of their interaction with the quark-gluon plasma produced in such collisions. Understanding the mechanisms responsible for this suppression requires a detailed understanding of charmonium production. To constrain the production mechanisms, it is essential to quantify how charmonium production correlates with jet activity. Measurements of J/ψ production in the dimuon decay channel are presented for inclusive J/ψ mesons and for J/ψ mesons that are either isolated or not isolated from jets, separately for prompt and non-prompt production. Non-isolated J/ψ mesons are defined by matching J/ψ candidates to anti- k_t jets with $R = 0.2$ and $p_T > 20$ GeV, reconstructed without signal from the J/ψ meson, allowing the quantification of jet activity accompanying J/ψ production. The analysis uses Pb+Pb and pp collisions at $\sqrt{s_{NN}} = 5.02$ TeV recorded by the ATLAS experiment at the LHC, corresponding to integrated luminosities of 1.82 nb^{-1} and 0.26 fb^{-1} , respectively. The J/ψ yields in Pb+Pb, cross sections in pp , and nuclear modification factors are presented for non-isolated, isolated, and inclusive J/ψ up to $p_T = 60$ GeV. Isolated fractions and non-prompt fractions are reported in both pp and Pb+Pb collisions. Strong J/ψ suppression is observed to persist up to the highest measured p_T values, with differences observed between non-isolated, isolated, and inclusive J/ψ . These results provide new constraints on charmonium production mechanisms and their in-medium suppression.

Contents

1	Introduction	3
2	ATLAS detector	4
3	Data and simulated event samples	5
4	Data analysis	6
4.1	Corrections of raw J/ψ distributions	7
4.2	Dimuon–jet association	8
4.3	J/ψ signal extraction	9
4.4	Definition of observables	12
5	Systematic uncertainties	14
5.1	Acceptance uncertainty	14
5.2	Muon reconstruction efficiency uncertainty	14
5.3	Muon trigger efficiency uncertainty	15
5.4	Fit model uncertainty	15
5.5	Jet correction uncertainty	15
5.6	Background subtraction uncertainty	16
5.7	pp luminosity and $\langle T_{AA} \rangle$ uncertainties	16
6	Results	17
7	Conclusion	24
	Appendix	26

1 Introduction

High-energy heavy-ion collisions at the Relativistic Heavy Ion Collider (RHIC) [1] and the Large Hadron Collider (LHC) [2] create conditions under that strongly interacting matter transitions into the deconfined phase of quantum chromodynamics (QCD), the quark-gluon plasma (QGP) [3, 4]. In this environment, hard probes – particles or partonic systems produced in large-momentum-transfer scatterings that precede the formation of the medium – serve as sensitive tools for characterising the medium. Energetic partons undergo substantial energy loss, giving rise to the well-established phenomenon of jet quenching [5–7], while heavy quark–antiquark bound states (quarkonia) are modified through colour screening, in-medium dissociation, and regeneration [8]. The resulting suppression of quarkonium production is found to be pronounced and to persist up to transverse momenta of several tens of GeV [9–16]. In the case of $c\bar{c}$ bound states (charmonia), besides the conventional suppression mechanisms associated with colour screening and in-medium dissociation, it has also been suggested that charmonia with high transverse momenta (p_T) may be affected by medium-induced gluon radiation, leading to an energy-loss mechanism analogous to that responsible for jet quenching [17–19].

Understanding the origin of charmonia suppression requires a clear picture of how charmonia are produced in high-energy collisions. Charmonium states may be created directly in the hard scattering and subsequently evolve as either colour-singlet or colour-octet configurations [8, 20–22], or they may be formed during a parton-shower evolution [23, 24]. Although extensive theoretical work is devoted to charmonia production, the dominant production mechanism and the possible interplay among different production mechanisms remain unresolved [25]. Additional complexity arises from the distinction between prompt charmonia, formed on the time scale of the strong interaction, and non-prompt charmonia, which appear much later through b -hadron decays. To constrain the production mechanisms, it is therefore important to experimentally quantify how charmonium production correlates with jet activity.

To quantify the correlation between the charmonium production and jet activity, the CMS and LHCb collaborations measured the J/ψ –jet fragmentation function in 5.02 TeV pp collisions [26] and 13 TeV pp collisions [27], respectively. In those measurements, the fragmentation function corresponds to the distribution of z , with z defined as the ratio of the J/ψ p_T to the p_T of the jet into which the J/ψ is clustered. The prompt J/ψ mesons were found to have more surrounding jet activity, i.e., to populate lower values of z than predicted by PYTHIA 8 [28] simulations, suggesting that J/ψ production late in the parton shower is generally underestimated in the model [24]. The correlation between the J/ψ production and jet activity was also studied at the level of yields in 8 TeV pp collisions by CMS [29]. That measurement used events where at least one jet with $p_T > 25$ GeV was observed and evaluated the angular separation between the J/ψ meson and the jet, finding that most prompt J/ψ mesons with energy above 15 GeV and rapidity $|y| < 1$ are contained in jets.

While the existing J/ψ –jet correlation measurements provide important constraints to the theoretical models describing charmonia production, they still do not give complete information. In particular, the definition of whether the J/ψ is contained in a jet depends on the jet definition. As the jet four-momentum is constructed from a sum containing the four-momentum of the J/ψ , an otherwise isolated J/ψ with high enough p_T is by definition a jet, thus in a jet, whereas the isolated J/ψ with p_T lower than the minimum value used to define a jet is not in a jet [25]. In addition, studying the J/ψ in an event sample that is triggered by the presence of a jet can introduce a possible event selection bias.

The first goal of the measurement presented in this paper is to bring new information into the quantification of the J/ψ –jet correlation by separating the kinematics of J/ψ from the kinematics of jets and by analysing

the J/ψ -jet correlations in all J/ψ events rather than in events a priori containing jets. The second goal is to measure possible differences between the suppression of isolated J/ψ and J/ψ produced in association with jets in Pb+Pb collisions.

The measurement presented in this paper uses data collected by the ATLAS experiment in Pb+Pb collisions in 2015 and 2018, and in pp collisions collected in 2017, both at a centre-of-mass energy of 5.02 TeV per colliding nucleon pair. The Pb+Pb and pp data samples contain 1.82 nb^{-1} and 0.26 fb^{-1} of collision data, respectively. The measurement thus presents the quantification of J/ψ suppression using the full LHC Run 2 data sample of Pb+Pb collisions.

2 ATLAS detector

The ATLAS detector [30] at the LHC covers nearly the entire solid angle around the collision point.¹ It consists of an inner tracking detector surrounded by a thin superconducting solenoid, electromagnetic and hadronic calorimeters, and a muon spectrometer incorporating three large superconducting air-core toroidal magnets.

The inner-detector system (ID) is immersed in a 2 T axial magnetic field and provides charged-particle tracking in the range of $|\eta| < 2.5$. The high-granularity silicon pixel detector covers the vertex region and typically provides four measurements per track, the first hit generally being in the insertable B-layer (IBL) installed before Run 2 [31, 32]. It is followed by the SemiConductor Tracker (SCT), which usually provides eight measurements per track. These silicon detectors are complemented by the transition radiation tracker (TRT), which enables radially extended track reconstruction up to $|\eta| = 2.0$. The TRT also provides electron identification information based on the fraction of hits (typically 30 in total) above a higher energy-deposit threshold corresponding to transition radiation.

The calorimeter system covers the pseudorapidity range $|\eta| < 4.9$. Within the region $|\eta| < 3.2$, electromagnetic calorimetry is provided by barrel and endcap high-granularity lead/liquid-argon (LAr) calorimeters, with an additional thin LAr presampler covering $|\eta| < 1.8$ to correct for energy loss in material upstream of the calorimeters. Hadronic calorimetry is provided by the steel/scintillator-tile calorimeter, segmented into three barrel structures within $|\eta| < 1.7$, and two copper/LAr hadronic endcap calorimeters. The solid angle coverage is completed with copper/LAr and tungsten/LAr calorimeter modules (FCal), covering the forward regions of $3.1 < |\eta| < 4.9$. The zero-degree calorimeters (ZDC) [33] measure neutral particles at pseudorapidities $|\eta| \geq 8.3$ and consist of layers of alternating quartz rods and tungsten plates. ZDC modules are positioned symmetrically at $z = \pm 140 \text{ m}$.

The muon spectrometer (MS) comprises separate trigger and high-precision tracking chambers measuring the deflection of muons in a magnetic field generated by the superconducting air-core toroidal magnets. The field integral of the toroids ranges between 2.0 and 6.0 T m across most of the detector. Three layers of precision chambers, each consisting of layers of monitored drift tubes (MDTs), cover the region $|\eta| < 2.7$, complemented by cathode-strip chambers (CSCs) in the forward region, where the background is highest.

¹ ATLAS uses a right-handed coordinate system with its origin at the nominal interaction point (IP) in the centre of the detector and the z -axis along the beam pipe. The x -axis points from the IP to the centre of the LHC ring, and the y -axis points upwards. Polar coordinates (r, ϕ) are used in the transverse plane, ϕ being the azimuthal angle around the z -axis. The pseudorapidity is defined in terms of the polar angle θ as $\eta = -\ln \tan(\theta/2)$ and is equal to the rapidity $y = \frac{1}{2} \ln \left(\frac{E+p_z}{E-p_z} \right)$ in the relativistic limit.

Angular distance is measured in units of $\Delta R \equiv \sqrt{(\Delta y)^2 + (\Delta \phi)^2}$.

The muon trigger system covers the range $|\eta| < 2.4$ with resistive-plate chambers (RPCs) in the barrel, and thin-gap chambers (TGCs) in the endcap regions.

The luminosity is measured mainly by the LUCID-2 [34] detector that records Cherenkov light produced in the quartz windows of photomultipliers located close to the beam pipe.

A two-level trigger system is used to select events of interest. The first-level (L1) trigger system is implemented in custom hardware, followed by selections made by software algorithms in the high-level trigger (HLT) [35]. The L1 trigger accepts events from the 40 MHz bunch crossings at a rate below 100 kHz, which the high-level trigger further reduces to record complete events to disk at about 1 kHz. The L1 muon trigger requires coincidences between hits on different RPC or TGC planes, which are used as a seed for the HLT algorithms. The HLT uses dedicated algorithms to incorporate information from both the MS and the ID, achieving position and momentum resolution close to that provided by the offline muon reconstruction [36].

A software suite [37] is used in data simulation, in the reconstruction and analysis of real and simulated data, in detector operations, and in the trigger and data acquisition systems of the experiment.

3 Data and simulated event samples

Events in the Pb+Pb and pp collisions are collected using a trigger requiring the presence of at least two muons, both with $p_T^\mu > 4$ GeV. In the pp sample, both muons must generate a spatially separated L1 muon trigger region of interest (RoI) and be confirmed by the HLT, while in the Pb+Pb sample, only one muon is required to be seen by the L1 muon trigger and confirmed by the HLT, the second muon is only required to satisfy the HLT requirements [36]. In addition to the muon trigger, two triggers are used in Pb+Pb collisions to select minimum-bias events. These are based on the presence of at least 50 GeV of transverse energy in all sections of the calorimeter system ($|\eta| < 4.9$) or, for events that do not meet this condition, on the presence of energy deposition above a one neutron threshold in both ZDC arms.

Both Pb+Pb and pp data also contain signal from multiple inelastic interactions per bunch crossing, also referred to as pile-up. The average number of inelastic interactions per bunch crossing reaches a maximum value of 0.004 in Pb+Pb collisions, and it varies between 1.4 and 4.4 in pp collisions. Although only a small fraction of the Pb+Pb events ($< 0.5\%$) contain pile-up events, these were suppressed utilising the observed anti-correlation, expected from the nuclear geometry, between the total transverse energy deposited in both of the forward calorimeters, ΣE_T^{FCal} , and the energy in the ZDC. Pile-up collisions are not rejected in pp collisions.

Monte Carlo (MC) simulated event samples are used for performance studies and to correct for detector effects. Prompt ($pp \rightarrow J/\psi \rightarrow \mu\mu$) and non-prompt ($pp \rightarrow b\bar{b} \rightarrow J/\psi \rightarrow \mu\mu$) samples of J/ψ were produced using PYTHIA 8.2 [38] for event generation and PHOTOS [39] for electromagnetic radiation corrections. The A14 set of tuned parameters [40] is used together with CTEQ6L1 parton distribution function set [41]. The response of the ATLAS detector is simulated using GEANT4 [42, 43]. To simulate the J/ψ production in the high multiplicity environment of Pb+Pb collisions, the simulated pp events are overlaid with dedicated minimum-bias Pb+Pb data events [44]. The minimum-bias data events from Pb+Pb collisions are combined with the signal from the PYTHIA 8 simulation of hard scattering events at the digitisation stage, and then reconstructed as a combined event.

In Pb+Pb collision data and MC samples, the transverse energy at the electromagnetic scale deposited in the forward calorimeter, ΣE_T^{FCal} , is used to estimate the centrality of the collision. Centrality describes the degree of geometric overlap of two colliding nuclei in the plane perpendicular to the beam, with large overlap in central collisions and small overlap in peripheral collisions. The measurement is performed in four exclusive centrality intervals, 0–10%, 10–20%, 20–40%, 40–80%, and an inclusive 0–80% centrality interval. The centrality is defined such that smaller percentiles label more central collisions. A weight is assigned to each MC event, ensuring that the event sample obtained from the minimum-bias trigger entering the MC overlay has the same centrality distribution as that measured in the data. The TGLAUBERMC v3.2 package [45], providing improved implementation of the MC Glauber model [46], is used to calculate the mean nuclear overlap function, $\langle T_{AA} \rangle$ [46, 47], as well as its uncertainty, for each centrality interval as presented in Table 1. The quantity $\langle T_{AA} \rangle$ is proportional to the mean number of binary nucleon–nucleon collisions divided by the inelastic nucleon–nucleon cross section, and accounts for the nuclear overlap geometry in a given centrality interval.

The number of minimum-bias events, N_{evt} , is used to normalise the yield in the respective centrality interval. Minimum-bias events are selected by requiring that they pass at least one of the two minimum-bias triggers. The analysed data sample corresponds to 11.15×10^9 Pb+Pb collisions after correction for the trigger prescale factor.

Table 1: The $\langle T_{AA} \rangle$ values and corresponding uncertainties for each centrality interval. The centrality-inclusive $\langle T_{AA} \rangle$ corresponds to the weighted sum of $\langle T_{AA} \rangle$ in individual centrality intervals.

Centrality	$\langle T_{AA} \rangle$ [mb $^{-1}$]	$\sigma(\langle T_{AA} \rangle)$ [mb $^{-1}$]
0–10%	23.22	0.06
10–20%	14.38	0.12
20–40%	6.93	0.13
40–80%	1.23	0.06
0–80%	7.05	0.08

4 Data analysis

The J/ψ mesons are reconstructed in the dimuon ($\mu^+ \mu^-$) decay channel. The reconstructed muons are required to satisfy the Medium muon working point, ignoring the TRT requirements [48], have $p_T^\mu > 4$ GeV, $|\eta^\mu| < 2.4$, and be matched to the muons reconstructed at the trigger level. Pairs of muons with opposite charges are used to construct dimuon objects. The transverse momentum of the dimuon, $p_T^{\mu\mu}$, is required to be larger than 9 GeV, and the rapidity of the dimuon, $y_{\mu\mu}$, is required to have an absolute value of less than 2. In addition, the invariant mass of the dimuon, $m_{\mu\mu}$, has to be within an interval of 2.5 GeV and 3.5 GeV. The selected dimuon is refitted to a common vertex. The yields entering the evaluation of observables are extracted using two-dimensional unbinned maximum-likelihood fits [49] in dimuon invariant mass $m_{\mu\mu}$ and pseudo-proper lifetime $\tau_{\mu\mu}$ defined as [11]

$$\tau_{\mu\mu} = \frac{L_{xy} m_{\mu\mu}}{p_T^{\mu\mu}}, \quad (1)$$

where L_{xy} is the distance between the reconstructed primary vertex and the reconstructed dimuon vertex in the event on the transverse plane. The $\tau_{\mu\mu}$ is introduced to separate prompt and non-prompt J/ψ in the

fitting procedure.

The raw dimuon kinematic distributions entering the fitting procedure are corrected for detector-related effects, as described in Section 4.1. The dimuon candidates are tagged for the presence of jets, which is described in Section 4.2. The fit model and the extraction of corrected yields are described in Section 4.3. Final observables extracted using corrected yields are defined in Section 4.4.

4.1 Corrections of raw J/ψ distributions

Before the dimuon $m_{\mu\mu}$ and $\tau_{\mu\mu}$ distributions are fit to extract J/ψ yields, each candidate dimuon is corrected using a weight that accounts for the J/ψ dimuon acceptance, trigger efficiency, and reconstruction efficiency. The dimuon acceptance $\mathcal{A}(\psi(nS))(|y^{\mu\mu}|, p_T^{\mu\mu})$ is defined as the probability that the $\psi(nS)$ decay products fall within the fiducial volume ($p_T^\mu > 4$ GeV, $|\eta^\mu| < 2.4$). The acceptance is obtained from a generator-level ‘accept-reject’ simulation as described in Ref. [50]. Finite detector and reconstruction resolution might lead to the application of the J/ψ acceptance correction to the $\psi(2S)$ candidates and vice versa, therefore the upper mass boundary for the J/ψ candidates of 3.5 GeV is used and the lower mass boundary for the $\psi(2S)$ candidates is set to be 3.2 GeV, resulting in the overlap range of 0.3 GeV. The interpolation of the acceptances is then performed as

$$\mathcal{A}(|y^{\mu\mu}|, p_T^{\mu\mu}) = \begin{cases} \mathcal{A}(J/\psi) & \text{if } m_{\mu\mu} \leq 3.2 \text{ GeV} \\ \mathcal{A}(J/\psi) \cdot \frac{3.5 - m_{\mu\mu} [\text{GeV}]}{0.3} + \mathcal{A}(\psi(2S)) \cdot \frac{m_{\mu\mu} [\text{GeV}] - 3.2}{0.3} & \text{if } 3.2 < m_{\mu\mu} < 3.5 \text{ GeV}. \end{cases} \quad (2)$$

To account for the final state radiation (FSR) of the J/ψ decay products, an additional correction is derived using the comparison of the acceptance from the accept-reject simulation and the acceptance obtained from the PYTHIA 8 samples. In principle, the acceptance could also depend on the spin alignment of the J/ψ . In this analysis, J/ψ mesons are assumed to be produced unpolarised, following Refs. [51–53]. The effects of variations to this assumption are considered and discussed in Section 5.

The dimuon reconstruction efficiency, $\varepsilon_{\text{reco}}(\mu_1, \mu_2)$, is determined as the product of two single-muon reconstruction efficiencies. Muon reconstruction in ATLAS is performed independently in the ID and MS. The total single-muon reconstruction efficiency can be factorised into the ID track reconstruction efficiency and MS reconstruction efficiency. The single muon reconstruction efficiency for the pp data is obtained from the $J/\psi \rightarrow \mu^+ \mu^-$ PYTHIA 8 simulation. The additional data-to-MC scale factors are derived using $J/\psi \rightarrow \mu^+ \mu^-$ tag and probe method [54] using 13 TeV pp data, as the previous study showed no dependence of the MS efficiency on the pile-up conditions [55]. The combined ID+MS muon reconstruction efficiency for the Pb+Pb data is obtained using the tag and probe method in $J/\psi \rightarrow \mu^+ \mu^-$ PYTHIA 8 events overlaid with dedicated minimum-bias Pb+Pb data events as described in Section 3. Data-to-MC scale factors are determined in Pb+Pb data to account for the small differences between data and simulation. The scale factors are close to unity in the barrel region and reach values of 1.05 at low p_T in the endcap regions. The MS+ID efficiency at $p_T^\mu = 4$ GeV is about 55% in the barrel region ($|\eta^\mu| < 1.05$) and 70% in the endcap region ($1.05 < |\eta^\mu| < 2.4$). The efficiency saturates around 95% at $p_T^\mu = 9$ GeV for both barrel and endcap regions. The performance of the muon reconstruction at low p_T^μ in the barrel region is affected mainly by the muon energy loss in the calorimeter system and the presence of multiple scattering.

The dimuon trigger efficiency, $\varepsilon_{\text{trig}}(\mu_1, \mu_2)$, is constructed from the single-muon trigger efficiencies in the input. The single-muon trigger employs two distinct logic schemes: a) a L1-seeded muon trigger, which requires the formation of a L1 RoI of the muon candidate that is subsequently confirmed in the

HLT trigger sequence, and b) a HLT-only muon trigger, which is only performed at the HLT level without any L1 trigger requirement. The single-muon trigger efficiency is determined in PYTHIA MC simulation. Data-to-MC scale factors are determined as the ratio of the trigger efficiency evaluated in the pp data to that evaluated in the MC, to correct for differences between the data and the simulation. Both scale factors and efficiencies are evaluated using a $J/\psi \rightarrow \mu^+ \mu^-$ tag-and-probe method [54]. The dimuon trigger efficiency in pp collisions is factorised as the product of two L1-seeded muon trigger efficiencies. For the L1-seeded single-muon trigger efficiency, an additional centrality-dependent correction is determined as the ratio of the single-muon trigger efficiency measured in the Pb+Pb data as a function of centrality to the single-muon trigger efficiency measured in pp data. The L1-seeded single-muon trigger efficiency varies from 60% at $p_T^\mu = 4$ GeV to 70% at higher p_T^μ ($p_T^\mu = 10$ GeV) in the barrel region, and it varies from 50% at $p_T^\mu = 4$ GeV to 90% at higher p_T^μ ($p_T^\mu = 10$ GeV) in the endcaps. The inefficiency originates primarily from the L1 trigger, where the RoI formation requires hit coincidences across multiple RPC and TGC stations. In 0–10% central collisions, the centrality-dependent correction corresponds to 0.7 at $p_T^\mu = 4$ GeV, and it reaches unity at $p_T^\mu = 10$ GeV and $p_T^\mu = 15$ GeV in the barrel and endcap, respectively. In 40–80%, the centrality-dependent correction is unity in both barrel and endcap regions. The centrality dependence arises from reduced tracking resolution in the trigger turn-on region, especially in central collisions, where the tracking resolution worsens due to an increase in random hit density from other tracks. The HLT-only single-muon trigger is only used in Pb+Pb collisions, and its efficiency is again determined using the tag and probe method. The HLT-only single-muon trigger efficiency plateau is found to be 90% in both the barrel and endcap regions, regardless of energy threshold. The dimuon trigger efficiency in Pb+Pb collisions is factorised into a form consisting of both L1-seeded and HLT-only muon trigger efficiencies, as previously used in Refs. [11, 14, 56].

The total weight applied to raw dimuon distributions is then

$$w = \frac{1}{\mathcal{A} \times \varepsilon_{\text{trig}}(\mu_1, \mu_2) \times \varepsilon_{\text{reco}}(\mu_1, \mu_2)}. \quad (3)$$

The denominator of this weight is multiplied by jet-related corrections defined in the next section.

4.2 Dimuon–jet association

Jets entering this analysis are reconstructed using the anti- k_t algorithm [57, 58] with a radius parameter of $R = 0.2$, which provides superior performance over the $R = 0.4$ jets in Pb+Pb collisions in terms of the jet energy resolution (JER) and jet reconstruction efficiency. The jet reconstruction procedure follows that used previously in Pb+Pb collisions [59, 60], and is summarised here. Calorimeter cells in all calorimeter layers, with their energy at the electromagnetic scale, are grouped into $\Delta\eta \times \Delta\phi = 0.1 \times \pi/32$ calorimetric towers. The towers are used as the input to the initial jet-finding. After the initial jet-finding, the contribution from the underlying event (UE) to the energy deposited in the towers is estimated on an event-by-event basis. This is done by averaging over energies deposited in towers at a given η position. During the averaging and subsequent subtraction, the ϕ dependence arising from the collective flow in Pb+Pb collisions is also taken into account. Information from towers within $\Delta R = 0.4$ of jet candidates is excluded from the estimate of UE energy. The energies in towers inside jets are updated to subtract the estimated UE contribution, and the UE procedure is iterated using a better-defined set of jets to define the exclusion regions. The resulting jet kinematics are corrected using p_T - and η -dependent factors, determined from simulation, to account for the response of the calorimeter to jets [61]. An additional correction for the absolute response in data is based on *in situ* studies of pp collisions where jets recoil against photons, Z bosons, or jets in other regions

of the calorimeter [61]. This calibration is followed by a cross-calibration that relates the jet energy scale (JES) in high-luminosity 13 TeV pp collisions [62], used for *in situ* studies, to that of jets reconstructed in the 5.02 TeV data. The same jet reconstruction procedure, without the azimuthal modulation of the UE, is also applied to pp collisions. The UE subtraction in pp collisions removes the pile-up contribution to the jet. ‘Truth’-level jets are defined in the MC samples before detector simulation by applying the anti- k_t algorithm with $R = 0.2$ to stable particles with a proper lifetime greater than 30 ps, but excluding muons and neutrinos, which do not leave significant energy deposits in the calorimeter. After the detector simulation, the truth jets are matched to the nearest reconstructed jet in $\Delta R < 0.15$.

Jets are used to tag dimuon candidates before the J/ψ signal extraction by the fitting procedure described in Section 4.3. For each dimuon candidate passing the selection criteria, a search for a reconstructed jet with transverse momentum $p_T > 20$ GeV matching the angular distance $\Delta R(\text{dimuon}, \text{jet}) < 0.4$ is performed. The ΔR requirement is chosen to associate J/ψ candidates with nearby jets using a cone size comparable to a jet radius commonly used in LHC jet measurements [63, 64].

Presence of the matching jet then allows the dimuon candidates to be separated into three classes: *non-isolated*, *isolated*, and *inclusive*. Non-isolated dimuon candidates refer to those with a matched jet, while the inclusive class refers to all dimuon candidates. The yield in the isolated class is calculated using the yield differences between inclusive and non-isolated classes as determined in the fit procedure described in Section 4.3.

To correct the dimuon tagging for finite jet momentum resolution and jet reconstruction efficiencies, jet p_T threshold correction factors are derived using the non-prompt J/ψ MC samples defined in Section 3. The correction factors are obtained as a ratio of the yield of reconstructed dimuons associated with the truth jet to the yield of reconstructed dimuons associated with the reconstructed jet in bins of reconstructed jet p_T and reconstructed dimuon p_T . These factors are applied as an additional weight w_{jet} on non-isolated dimuon candidates entering the fitting described in Section 4.3. The reconstructed jet p_T spectra entering the correction factors are reweighted to account for the difference in the shape of the reconstructed jet p_T spectrum between data and MC, and the associated systematic uncertainty is evaluated. These correction factors also account for muon energy deposits in the calorimeter. The procedure is validated by an MC closure test, with the closure consistent with unity.

4.3 J/ψ signal extraction

The yields of prompt and non-prompt J/ψ mesons are determined using unbinned maximum-likelihood fits to the weighted (as defined in Equation 3) dimuon $m_{\mu\mu}$ and $\tau_{\mu\mu}$ distributions, following the same procedure for both pp and Pb+Pb data. The fits are done separately for each $p_T^{\mu\mu}$ and centrality interval, non-isolated, and inclusive class. The yield of the isolated J/ψ , N_{iso} , is extracted from the yield of the non-isolated J/ψ , $N_{\text{non-iso}}$, and inclusive yield, N_{incl} using the difference

$$N_{\text{iso}} = N_{\text{incl}} - N_{\text{non-iso}}. \quad (4)$$

The probability distribution function (PDF) for the fit, as previously validated in Refs. [11, 50], is defined as a normalised sum of five terms corresponding to the one prompt signal source, one non-prompt signal source, one prompt background source and two non-prompt background sources. Each term is factorised into dimuon $m_{\mu\mu}$ -dependent and $\tau_{\mu\mu}$ -dependent functions. The compact form of the PDF can be written

as

$$\text{PDF}(m_{\mu\mu}, \tau_{\mu\mu}) = \sum_{i=1}^5 \mathcal{N}_i h_i(m_{\mu\mu}) \cdot t_i(\tau_{\mu\mu}) * g_i(\tau_{\mu\mu}), \quad (5)$$

where \mathcal{N}_i is the normalisation factor, $h_i(m_{\mu\mu})$ is a function describing the dimuon $m_{\mu\mu}$ signal or background distribution, $t_i(\tau_{\mu\mu})$ is a function describing the dimuon $\tau_{\mu\mu}$ signal or background distribution, and $g_i(\tau_{\mu\mu})$ is a function describing the detector resolution defined as a double Gaussian distribution. The symbol ‘*’ denotes the convolution. The distribution functions h_i and t_i are defined using the following distribution functions: the Crystal Ball (CB) function [65], the Gaussian (G) distribution function, and the exponential (E) distribution function. All individual components are fully defined in Table 2. The fit is performed using the RooFit framework [66]. To stabilise the fit model and reduce parameter correlation, a number of component terms listed in Table 2 share common parameters. Some terms are scaled to each other by a multiplicative parameter, while others are fixed to the values observed in the MC simulation.

The signal mass shape is modelled as the sum of the Crystal-Ball distribution and a single Gaussian distribution for the prompt ($i = 1$ in Table 2) and non-prompt ($i = 2$) signal. These CB and Gaussian distributions share a common mean. The α parameter represents the fractional contribution of the CB and Gaussian signal distributions. The width term in the CB distribution corresponds to the width of the Gaussian distribution multiplied by the scaling factor. The tail parameters of the CB distribution, as well as the width-scaling factor, are fixed based on the MC simulations. Variations of these parameters are considered as part of the fit model systematic uncertainties. The background mass shape is divided into prompt ($i = 3$) and two non-prompt parts ($i = 4, i = 5$), modelled by three exponentials. No separate $\psi(2S)$ signal component is included in the fit, since the fitted mass range ends well below the $\psi(2S)$ mass. Any residual contribution from its low-mass tail is absorbed by the smooth background parameterisation.

The $\tau_{\mu\mu}$ distribution is composed of the prompt and non-prompt components. The prompt component is modelled as a delta function ($i = 1$ in Table 2) convolved with the double-Gaussian resolution function. The resolution function has a fixed mean at $\tau = 0$. The width terms are free but connected by the scaling term between two Gaussian distributions, whose value is fixed. The variation of this parameter is considered part of the fit model systematic uncertainty. The non-prompt pseudo-proper decay time is described as a single-sided exponential distribution ($i = 2$) convolved with a double-Gaussian resolution function. The background $\tau_{\mu\mu}$ distribution is also composed of the prompt and non-prompt components. The prompt component is described by a delta function convolved with the double-Gaussian resolution function ($i = 3$). The non-prompt component is modelled by a single-sided exponential distribution for positive values of τ ($i = 4$), and by a double-sided exponential ($i = 5$) that accounts for mis-reconstructed dimuons or Drell–Yan muons and combinatorial background. The single-sided and double-sided exponential distributions are convolved with the same double-Gaussian resolution distributions that are used for the signal part.

An example of the fit for the 0–80% centrality interval of Pb+Pb collisions projected onto the binned representation of data distributions is shown in panels (a,b) in Figure 1, a corresponding example of the fit for the pp data is presented in panels (c,d) in Figure 1.

The UE in Pb+Pb collisions, pile-up in pp collisions, and the multi-parton interactions (MPI) in both Pb+Pb and pp collisions may lead to the presence of jets produced in $\Delta R < 0.4$ from the J/ψ , but not originating from the same hard process as the J/ψ . The yield of these background jets is estimated by using the orthogonal cone method [67]. Using that method, the background jet yield is estimated as a yield of jets in the event with J/ψ in a cone of radius $R = 0.4$ centred at coordinates $(\phi_{J/\psi}, -\eta_{J/\psi})$ in the azimuth-pseudorapidity space. In the region near $\eta = 0$ where the background cone would overlap with the signal cone, the η coordinate is shifted by a constant value and the yield is re-weighted by a factor

Table 2: PDFs of the individual components corresponding to the prompt (P) and non-prompt (NP) sources of the fit model used in this analysis. The α represents the fractional contribution of the Crystal-Ball (CB) and Gaussian (G) signal distributions, the $\delta(\tau_{\mu\mu})$ is the Dirac delta function, and the E denotes the exponential function.

i	Type	Source	$h_i(m_{\mu\mu})$	$t_i(\tau_{\mu\mu})$
1	Signal	P	$\alpha\text{CB}_1(m_{\mu\mu}) + (1 - \alpha)\text{G}_1(m_{\mu\mu})$	$\delta(\tau_{\mu\mu})$
2	Signal	NP	$\alpha\text{CB}_1(m_{\mu\mu}) + (1 - \alpha)\text{G}_1(m_{\mu\mu})$	$E_1(\tau_{\mu\mu})$
3	Background	P	$E_2(m_{\mu\mu})$	$\delta(\tau_{\mu\mu})$
4	Background	NP	$E_3(m_{\mu\mu})$	$E_4(\tau_{\mu\mu})$
5	Background	NP	$E_5(m_{\mu\mu})$	$E_6(\tau_{\mu\mu})$

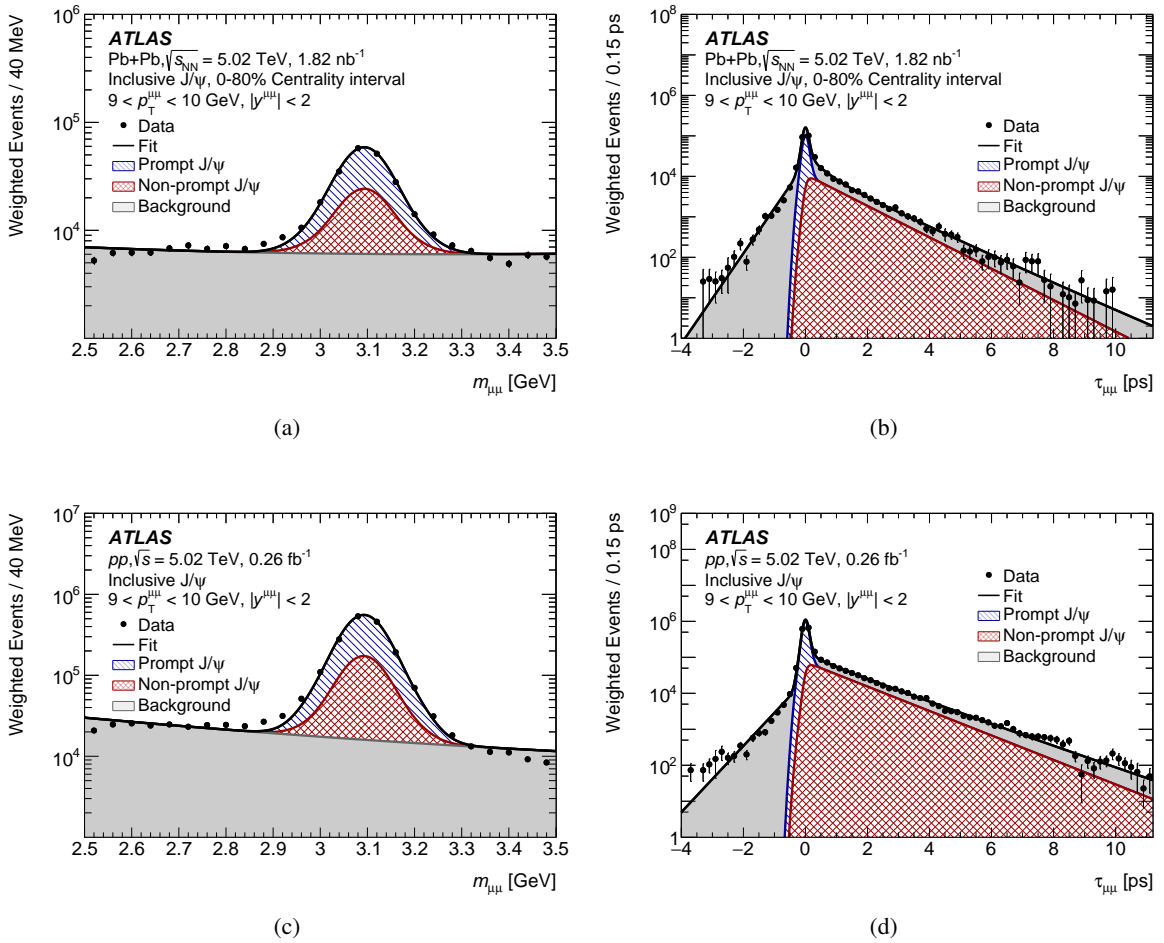


Figure 1: Binned representation of (a,c) the weighted dimuon invariant-mass $m_{\mu\mu}$ distribution and (b,d) the dimuon pseudo-proper decay-time $\tau_{\mu\mu}$ distribution in the fitted range for candidates in the transverse-momentum interval $9 \text{ GeV} < p_T^{\mu\mu} < 10 \text{ GeV}$ and $|y^{\mu\mu}| < 2$ in (a,b) 0–80% Pb+Pb collisions and in (c,d) pp collisions. The fit results are shown as solid lines, while the coloured filled areas indicate the extracted signal and background components. The error bars correspond to the statistical uncertainties of the data points.

compensating for the difference in the average yields taken from simulation. The estimated background jet yield is applied as an additive correction to transfer the corresponding yield from the non-isolated to the isolated category, as described by Equation 4. The yield of background jets is estimated to be less than 1% of the isolated J/ψ yield in pp collisions and less than 10% in 0–10% central Pb+Pb collisions. The procedure is tested on jet-tagged dimuon candidates in MC, resulting in full recovery of the jet-tagged signal distributions. The difference in the background yield magnitude between data and MC is less than 2%.

To connect the results of this paper with previous publications [26, 27, 29] and to do a qualitative test of the jet association procedure, the raw fragmentation function of J/ψ , i.e. the fragmentation function not corrected for the detector response, is evaluated. In this case, the fraction z of J/ψ momentum to the momentum of the jet is estimated as

$$z = \frac{p_T^{\mu\mu}}{p_T^{\text{jet}} + p_T^{\mu\mu}}, \quad (6)$$

where p_T^{jet} represents the momentum of the jet reconstructed without the signal from the J/ψ meson, and the denominator of Equation 6 thus follows the definition used by the previous measurements [26, 27, 29]. The raw fragmentation function is then defined as

$$D(z) = \frac{1}{N_{\text{jet}}} \frac{dN(z)}{dz}, \quad (7)$$

representing the yield (N) of J/ψ mesons carrying a fraction of momentum z normalised by the number of jets (N_{jet}) containing a J/ψ . The raw fragmentation functions are evaluated for non-isolated prompt J/ψ candidates selected based on conditions $3.0 < m_{\mu\mu} < 3.2$ GeV, $-0.3 < \tau_{\mu\mu} < 0.3$ ps and $9 < p_T^{\mu\mu} < 60$ GeV, and they are not unfolded for the detector response and not corrected for the background. The resulting raw fragmentation functions evaluated in pp collisions are shown in Figure 2. The raw fragmentation function evaluated in pp collisions is directly compared to the raw fragmentation functions with the same kinematic cuts evaluated using leading-order (LO) QCD PYTHIA 8 samples as defined in Section 3. The measured raw fragmentation functions for prompt dimuon candidates are qualitatively consistent with the fragmentation function simulated in PYTHIA 8 for non-prompt J/ψ production and differ significantly from those simulated for prompt J/ψ production. This confirms earlier findings by CMS Collaboration published in Ref. [26].

4.4 Definition of observables

The measurement presented in this paper quantifies J/ψ cross-section and yields in pp and Pb+Pb collisions, respectively. Using cross-section and yields, the nuclear modification factor of the J/ψ meson is evaluated. These observables are evaluated for prompt and non-prompt J/ψ , which also allows the determination of the fraction of non-prompt J/ψ mesons. These observables are also evaluated for non-isolated, isolated, and inclusive J/ψ mesons, which allows the determination of the fraction of isolated J/ψ mesons. The definition of all observables is given in this section.

The differential cross section for $J/\psi \rightarrow \mu^+ \mu^-$ production in pp collisions is defined as

$$\mathcal{B} \cdot \frac{d^2 \sigma_{J/\psi}}{dp_T^{\mu\mu} dy_{\mu\mu}} = \frac{N_{J/\psi}^{\text{corr}}}{\Delta p_T^{\mu\mu} \times \Delta y_{\mu\mu} \times L}, \quad (8)$$

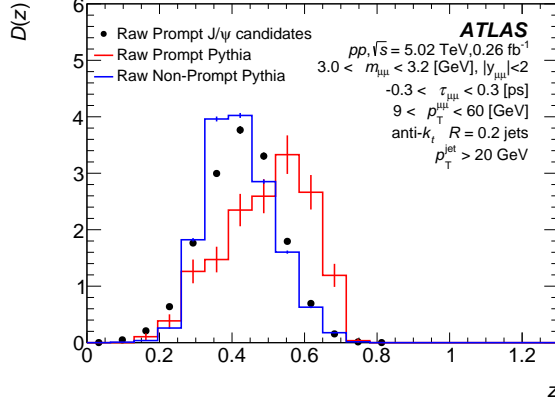


Figure 2: Raw fragmentation function evaluated for non-isolated prompt J/ψ candidates in pp collisions. The J/ψ candidates were selected requiring $2.5 < m_{\mu\mu} < 3.5$ GeV, $-0.3 < \tau_{\mu\mu} < 0.3$ ps and $9 < p_T^{\mu\mu} < 60$ GeV. Jets with $p_T^{\text{jet}} > 20$ GeV are used. Results are compared with the LO QCD PYTHIA prediction of raw distributions for prompt and non-prompt dimuon candidates with the same kinematic requirements as those applied to the data. The vertical lines represent statistical uncertainties. The statistical uncertainties of the black markers are negligible and thus not visible.

where $\mathcal{B}(J/\psi \rightarrow \mu^+ \mu^-) = (5.93 \pm 0.06)\%$ [68] is the J/ψ dimuon decay branching fraction, $N_{J/\psi}^{\text{corr}}$ is the corrected J/ψ yield estimated by using the procedure discussed in Section 4.3, $p_T^{\mu\mu}$ and $y_{\mu\mu}$ are the dimuon transverse momentum and rapidity, respectively, and L is the integrated luminosity of the pp data sample.

The yield characterising the $J/\psi \rightarrow \mu^+ \mu^-$ production in Pb+Pb collisions is defined as

$$\mathcal{B} \cdot \left. \frac{d^2 N_{J/\psi}}{dp_T^{\mu\mu} dy_{\mu\mu}} \right|_{\text{cent}} = \left. \frac{N_{J/\psi}^{\text{corr}}}{\Delta p_T^{\mu\mu} \times \Delta y_{\mu\mu}} \right|_{\text{cent}}, \quad (9)$$

where ‘cent’ refers to a specific centrality interval.

In nucleus–nucleus collisions, the suppression of J/ψ production is quantified using the nuclear modification factor, R_{AA} , which is defined for each centrality interval as

$$R_{AA}|_{\text{cent}} = \frac{\frac{1}{N_{\text{evt}}} \left. \frac{d^2 N_{J/\psi}}{dp_T^{\mu\mu} dy_{\mu\mu}} \right|_{\text{cent}}}{\langle T_{AA} \rangle |_{\text{cent}} \times \left. \frac{d^2 \sigma_{J/\psi}}{dp_T^{\mu\mu} dy_{\mu\mu}} \right|_{\text{cent}}}, \quad (10)$$

where N_{evt} is the total number of minimum-bias events for a given centrality interval and the values of the mean nuclear overlap function $\langle T_{AA} \rangle$ are provided in Section 3.

The non-prompt fraction, $f_{\text{NP}}^{J/\psi}$, is defined as the ratio of corrected yield of non-prompt (NP) J/ψ mesons to the sum of corrected prompt (P) and non-prompt J/ψ yields,

$$f_{\text{NP}}^{J/\psi} = \frac{N_{J/\psi}^{\text{NP,corr}}}{N_{J/\psi}^{\text{NP,corr}} + N_{J/\psi}^{\text{P,corr}}}. \quad (11)$$

The isolated fraction, $f_{\text{iso}}^{J/\psi}$, is defined as the ratio of corrected yield of isolated (iso) J/ψ mesons to the corrected inclusive J/ψ yields (inc),

$$f_{\text{iso}}^{J/\psi} = \frac{N_{J/\psi}^{\text{iso,corr}}}{N_{J/\psi}^{\text{inc,corr}}}. \quad (12)$$

To obtain statistical uncertainties of $f_{\text{NP}}^{J/\psi}$ and $f_{\text{iso}}^{J/\psi}$, the binomial error propagation is used.

5 Systematic uncertainties

The following sources of systematic uncertainties are considered in this measurement: J/ψ kinematic acceptance uncertainty, muon reconstruction efficiency uncertainty, muon trigger efficiency uncertainty, fit model uncertainty, jet-related uncertainties, UE/MPI subtraction uncertainty, uncertainty in pp luminosity, and $\langle T_{\text{AA}} \rangle$ uncertainty. Systematic uncertainties in the measured distributions can be categorised into two classes: bin-wise correlated uncertainties and uncertainties that affect the overall normalisation of distributions. Uncertainties due to the determination of $\langle T_{\text{AA}} \rangle$ and pp luminosity belong to the second class, all other uncertainties belong to the first. The systematic uncertainties are propagated using knowledge of the correlations among sources, leading to an appropriate reduction in systematic uncertainties in ratios.

5.1 Acceptance uncertainty

The uncertainty in acceptance has three components. The first component evaluates the impact of spin alignment on the acceptance. To measure that, six alternative scenarios are evaluated corresponding to extreme cases of spin-alignment as described in Ref. [50]. The uncertainty is calculated as the maximum deviation from the assumption of unpolarised production. Since the polarisation of charmonia in pp collisions is measured to be small [51–53], its modification due to the nuclear environment is neglected, and the spin-alignment uncertainty is assumed to cancel out in ratios involving pp and Pb+Pb yields. This uncertainty is presented on the cross-sections and yields separately from other uncertainties. The second source is the acceptance interpolation by Equation 2, which may introduce an artificial slope to the background when the signal-to-background ratio is low. To address this potential bias, an alternative set of weights is derived without the interpolation. The last component is connected to the FSR as described in Section 4.1. The FSR correction is derived in the full rapidity bin $|y| < 2$, and its systematic uncertainty arises from the residual rapidity dependence, which is studied. The acceptance uncertainties are fully cancelled in all ratios, they manifest themselves only in the per-event yields in Pb+Pb and cross-section in pp collisions. The dominant systematic uncertainty corresponds to the FSR uncertainty.

5.2 Muon reconstruction efficiency uncertainty

The systematic uncertainty associated with the muon reconstruction efficiency in pp collisions accounts for possible biases in the tag-and-probe method used to evaluate it. The uncertainty is lower than 1%, and more details of its estimation are given in Ref. [54].

Several sources of uncertainty are considered in evaluating the total muon reconstruction efficiency uncertainty in Pb+Pb collisions. The muon reconstruction efficiency uncertainty is evaluated following Ref. [54] by changing the tag-muon selection criteria and modifying the line shapes in the extraction fit procedure. The statistical uncertainties of the scale factors are also included as a source of the systematic uncertainty. Due to the small probe yield in the Pb+Pb data, the statistical uncertainties of the scale factors dominate the uncertainty in the muon reconstruction efficiency correction. The final systematic uncertainty is evaluated as a quadrature sum of individual sources and propagated through the data-to-MC scale factors.

5.3 Muon trigger efficiency uncertainty

The systematic uncertainty in the trigger efficiency correction is estimated in a similar manner to the uncertainty in the muon reconstruction efficiency. The fit model and tag-muon selection criteria are modified in the tag-and-probe method. For the muon trigger efficiency in the Pb+Pb, an additional uncertainty associated with the centrality-dependent correction is added to the total systematic uncertainty. Statistical uncertainties in the muon trigger efficiency scale factors are also propagated to the final result. All sources of muon trigger systematic uncertainties are combined in quadrature and propagated through the data-to-MC scale factors.

5.4 Fit model uncertainty

The uncertainty associated with the fit model is obtained by relaxing its parameter constraints and introducing alternative PDFs. In each modification of the fit model, all measured quantities are recalculated and compared with the nominal fit. In total, ten variations of the fit model are considered. The weighted sum of the CB distribution and the Gaussian distribution is changed to the weighted sum of two Gaussian distributions, and the parameters of the CB distribution, which were originally fixed, are left free. The scaling factor connecting the width of Gaussian distribution with the width parameter of CB distribution is varied. For the background $m_{\mu\mu}$ PDF, the single exponential distribution is replaced by the first-order Chebyshev polynomial. For the time-resolution PDF, the double Gaussian distribution is replaced with a single Gaussian distribution, and the width parameter is varied. The dominant source of uncertainty is the variation in the signal mass shape. The root-mean-square of all variations is then assigned as the fit model systematic uncertainty.

5.5 Jet correction uncertainty

The jet-related uncertainties have three sources: JES, JER, and the shape of the jet p_T spectrum. The JES uncertainty has three components. The first component is a centrality-independent baseline determined from calorimetric studies [61] plus relative energy-scale differences between heavy-ion and 13 TeV pp jet reconstruction [62]. The second component accounts for the quark/gluon composition of parton showers [59]. The third, centrality-dependent component, accounts for a different calorimetric response to jets with a modified parton shower due to quenching in Pb+Pb collisions [59, 62]. The JER uncertainty is derived from dijet energy-balance studies in 13 TeV pp data [61] and includes additional contributions to account for the different heavy-ion jet reconstruction procedure. The JES and JER uncertainties are propagated by modifying the jet p_T threshold correction factors. Since the jet p_T threshold correction

is sensitive to the shape of the jet p_T spectrum, the reconstructed jet p_T spectrum generated in MC is reweighted to match the jet p_T spectrum measured in data as described in Section 4.2. To assess the sensitivity of the result to this difference, the evaluation of the jet p_T threshold correction is repeated with the unweighted jet p_T spectrum. The dominant jet-related uncertainty is JER.

5.6 Background subtraction uncertainty

The uncertainty in the jet background subtraction, described in Section 4.3, is evaluated by a variation of the background jet rate within the overall statistical uncertainty. For pp collisions, this uncertainty is also studied and found to be negligible.

5.7 pp luminosity and $\langle T_{AA} \rangle$ uncertainties

The uncertainty in $\langle T_{AA} \rangle$ arises from geometric modelling uncertainties (e.g. nucleon–nucleon inelastic cross section, Woods–Saxon parameterisation of the nucleon distribution) and the uncertainty in the fraction of selected inelastic Pb+Pb collisions. The values of these uncertainties are presented in Table 1. The integrated luminosity of pp data is calibrated using data from dedicated beam separation scans and is determined using procedures described in Ref. [69]. The relative systematic uncertainty is 1.0%.

Table 3 summarises the magnitude of bin-wise correlated systematic uncertainties in measured prompt J/ψ yields in pp and Pb+Pb collisions. The corresponding uncertainties for non-prompt J/ψ production are of similar magnitude. Figure 3 summarises the magnitudes of bin-wise systematic uncertainties for the inclusive prompt and non-prompt J/ψ R_{AA} , whereas Figure 4 summarises the magnitudes of bin-wise systematic uncertainties for the non-isolated prompt and non-prompt J/ψ R_{AA} .

Table 3: Summary of the sources of bin-wise correlated systematic uncertainty for the prompt J/ψ yields.

Collision type	Source	Inclusive J/ψ [%]	Isolated J/ψ [%]	Non-isolated J/ψ [%]
pp collisions	Acceptance	< 3	< 3	< 3
	Trigger eff.	1.1–3.4	1.1–3.4	1.0–3.4
	Reconstruction eff.	0.1–0.2	0.1–0.2	0.1–0.2
	Signal extraction	1.5–2.2	1.5–2.4	1.6–2.5
	Jet correction	–	0.0–5.4	10–36
	Background	–	–	–
Pb+Pb collisions	Acceptance	< 3	< 3	< 3
	Trigger eff.	0.2–1.3	0.2–1.3	0.2–2.0
	Reconstruction eff.	2.1–12	2.5–12	1.2–12
	Signal extraction	1.2–2.8	1.1–2.9	0.3–3.4
	Jet correction	–	0.1–6.3	11–42
	Background	–	0.1–0.3	0.1–30

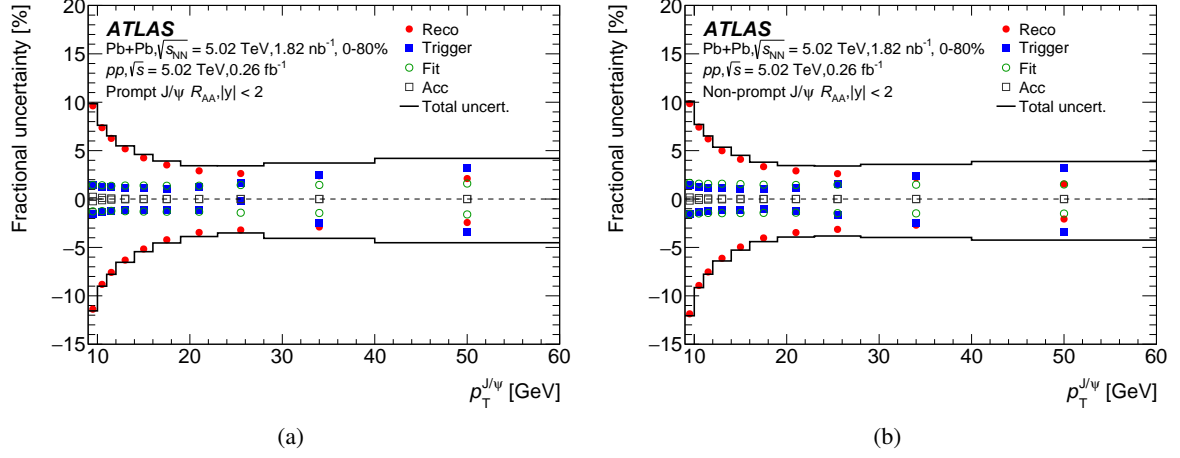


Figure 3: Summary of the sizes of different sources of bin-wise systematic uncertainty for (a) the inclusive prompt J/ψ R_{AA} and for (b) the inclusive non-prompt J/ψ R_{AA} evaluated in the 0–80% centrality interval. The solid line denotes total uncertainty.

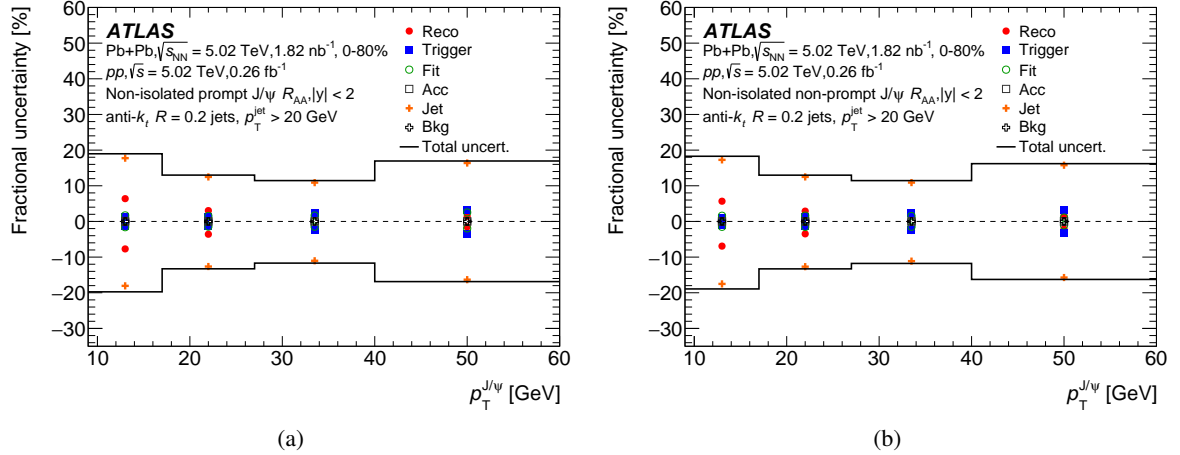


Figure 4: Summary of the sizes of different sources of bin-wise systematic uncertainty for (a) the non-isolated prompt J/ψ R_{AA} and for (b) the non-isolated non-prompt J/ψ R_{AA} evaluated in the 0–80% centrality interval. The solid line denotes total uncertainty.

6 Results

To study the J/ψ production mechanism, yields normalised by N_{evt} and $\langle T_{AA} \rangle$, measured in four centrality intervals of Pb+Pb collisions, and cross sections measured in pp collisions are shown in Figure 5. Yields and cross sections evaluated as a function of J/ψ p_T are reported for prompt and non-prompt J/ψ and for three classes characterising the correlation of J/ψ production with the jet production: non-isolated, isolated, and inclusive. A similar power-law-like decrease in measured distributions can be seen for inclusive and isolated J/ψ mesons, while an increasing trend in the distributions with increasing p_T in the region of $p_T < 20$ GeV is seen for non-isolated J/ψ mesons. This increasing trend may be interpreted as a consequence of the increasing phase-space accessibility of the selected J/ψ +jet topology, which is

restricted by the requirement of an accompanying jet with $p_T > 20$ GeV. This requirement becomes less restrictive with increasing J/ψ p_T .

Yields and cross-sections reported in Figure 5 are used to evaluate the fraction of isolated J/ψ (isolated fraction) defined in Section 4.4, which is reported in Figure 6. Overall, the isolated fraction starts at a value of 1 for J/ψ with $p_T \approx 10$ GeV and decreases with increasing p_T , reaching a value between 0.6 and 0.8 at $p_T \approx 50$ GeV. The increasing trend in distributions in Figure 5 attributed to the opening of the phase-space accessibility suggests that full isolation seen for J/ψ with $p_T < 20$ GeV is largely connected with the requirement on minimum jet p_T of 20 GeV.

The upper panels of Figure 6 compare the isolated fraction between prompt and non-prompt J/ψ showing that it is systematically 10–20% larger for prompt compared to non-prompt J/ψ mesons. No differences in the magnitude of the isolated fraction are found between Pb+Pb and pp collisions and among different centrality intervals of Pb+Pb as shown in the middle panels and lower panels of Figure 6, respectively. The middle panels also show a comparison with the LO QCD prediction from PYTHIA 8. This generator-level study is performed using the same kinematic selection criteria as those applied to the data. It is shown that PYTHIA 8 overestimates the isolated fraction for the prompt J/ψ , but provides a good prediction of the isolated fraction for the non-prompt J/ψ .

The non-prompt fraction for inclusive J/ψ measured in four centrality intervals of Pb+Pb collisions is shown in the left panel of Figure 7. The non-prompt fraction starts at a value of ≈ 0.3 at J/ψ p_T of 10 GeV, then it increases, reaching a value of approximately 0.6 at J/ψ $p_T \approx 50$ GeV. No significant centrality dependence is observed as previously measured in Ref. [11]. The non-prompt fraction for inclusive J/ψ measured in pp collisions and 0–80% Pb+Pb collisions is shown in the right panel of Figure 7. The non-prompt fraction measured in Pb+Pb collisions has a slightly different slope from the one measured in pp collisions, as observed before in Ref. [11]. Left and right panels of Figure 8 show the non-prompt fraction in pp and 0–80% Pb+Pb collisions, respectively, evaluated for non-isolated, isolated, and inclusive J/ψ mesons. While the non-prompt fraction is consistent between isolated and inclusive classes, it is significantly different for the case of non-isolated J/ψ . For $p_T > 15$ GeV, the non-prompt fraction of non-isolated J/ψ is consistent with no p_T dependence, and it reaches a value of approximately 0.7. These results provide complementary information to the evaluation of the isolated fraction presented in Figure 6.

The R_{AA} constructed from yields measured in Pb+Pb collisions and cross sections in pp collisions evaluated as a function of J/ψ p_T , is shown for inclusive prompt and non-prompt J/ψ in Figure 9. These new results improve the quantification of J/ψ suppression for $p_T > 30$ GeV with the R_{AA} values reaching approximately 0.6 and 0.4 at $p_T \approx 50$ GeV for prompt and non-prompt J/ψ , respectively, in the 0–10% centrality interval.

The R_{AA} evaluated as a function of J/ψ p_T for non-isolated, isolated and inclusive J/ψ in the 0–80% centrality interval is shown in Figure 10, and figures of the R_{AA} for other centrality intervals are presented in the Appendix of this paper. The two panels of Figure 10 compare prompt and non-prompt J/ψ . In both cases, one can see that the R_{AA} is consistent between the isolated and the inclusive case in the whole p_T range. For $p_T > 30$ GeV, the central values of R_{AA} of non-isolated prompt J/ψ appear to be systematically lower than those for isolated prompt J/ψ . To measure this difference, the p_T dependence of R_{AA} is fitted separately for the isolated and non-isolated samples using polynomial functions. The quadratic and higher-order terms are consistent with zero within uncertainties, indicating that linear functions provide a good description of the data in the kinematic range considered. The slopes extracted for the isolated and non-isolated samples differ by 3.3 standard deviations for the 0–80% centrality interval as well as for the individual centrality intervals excluding the most peripheral one. As a cross-check, Stouffer’s test [70, 71]

is applied directly to the data points, yielding a significance of 3.5 standard deviations. Such a difference might be interpreted as a larger suppression of J/ψ produced in association with more developed parton shower or fragmentation system. In the case of non-prompt J/ψ , no differences among the three isolation classes of J/ψ mesons are seen. A difference between non-isolated and isolated J/ψ is also seen in R_{AA} for $p_T < 20$ GeV for both prompt and non-prompt cases with a smaller significance than in the prompt high- p_T case. The R_{AA} in that region tends to grow, which may be connected with a complex interplay between phase-space opening and quenching of jets used to tag the J/ψ .

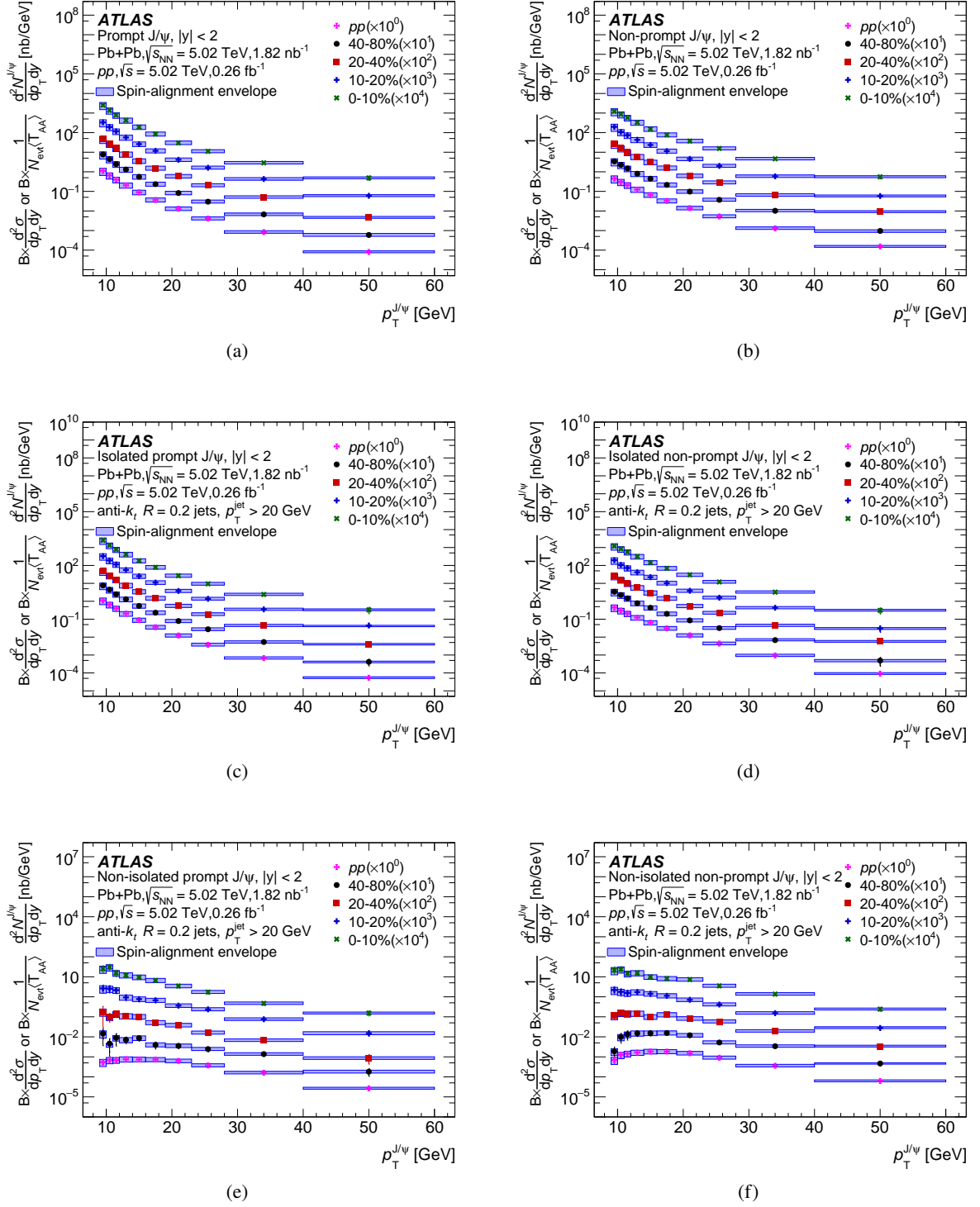


Figure 5: N_{evt} - and $\langle T_{\text{AA}} \rangle$ -normalised yields in different centrality intervals of Pb+Pb collisions and cross-section in pp collisions for (a,b) Inclusive, (c,d) Isolated, (e,f) Non-isolated, (a,c,e) Prompt, and (b,d,f) Non-prompt J/ψ production measured as a function of J/ψ p_T . Each distribution is scaled by an additional factor 10^n , indicated in the legend, to improve visibility. The vertical error bars denote combined statistical and systematic uncertainties. The boxes represent the variation in the results for various J/ψ spin polarisations.

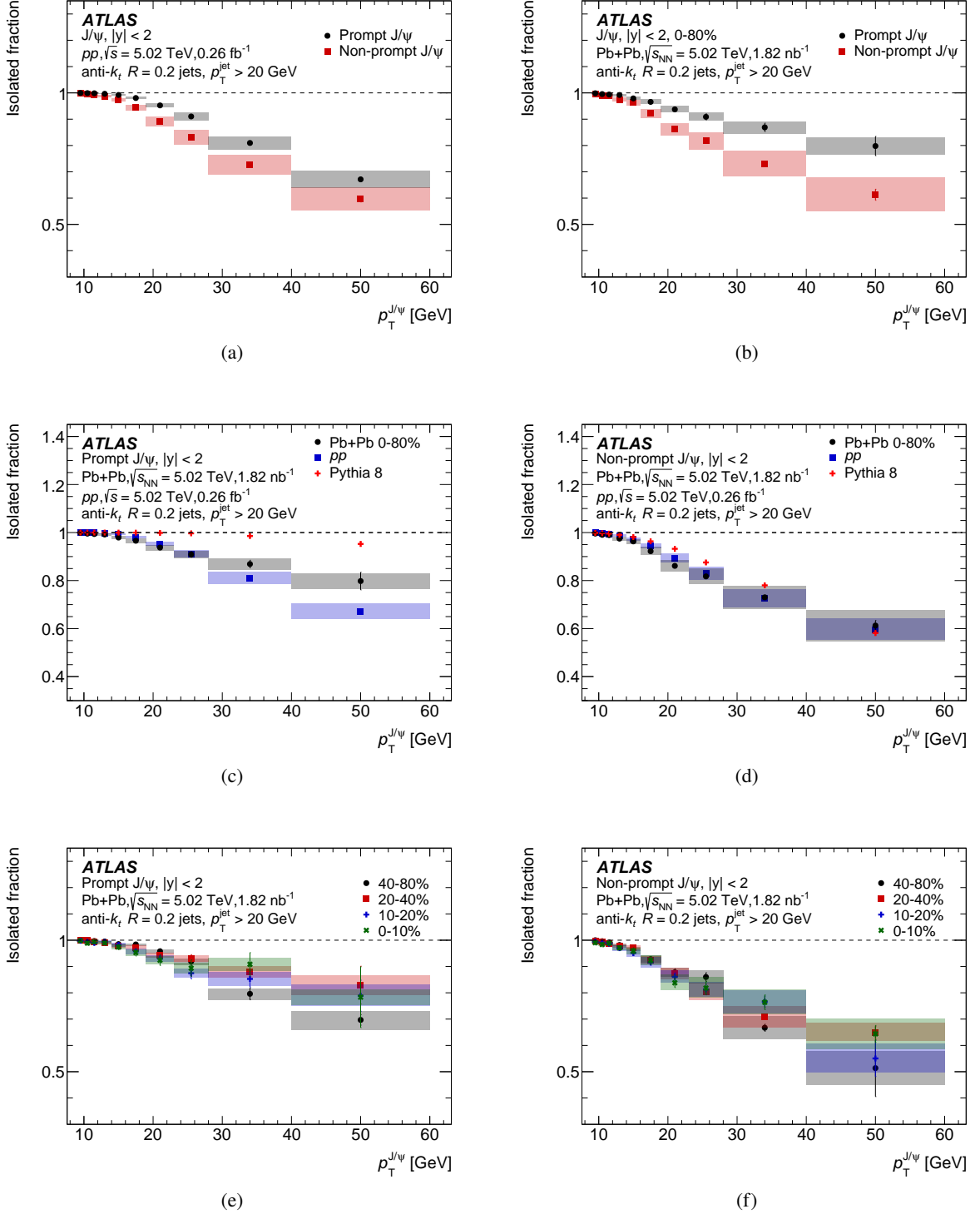


Figure 6: Isolated fraction evaluated as a function of J/ψ p_T for Prompt and Non-prompt J/ψ in (a) pp and (b) $Pb+Pb$ collisions in 0–80% centrality interval. Comparison of the Isolated fraction evaluated as a function of J/ψ p_T for (c) Prompt and (d) Non-prompt J/ψ in pp and $Pb+Pb$ collisions in 0–80% centrality interval compared to the LO prediction from the PYTHIA 8. Isolated fraction evaluated as a function of J/ψ p_T for (e) Prompt and (f) Non-prompt J/ψ in $Pb+Pb$ collisions for various centrality intervals. The error bars denote the statistical uncertainties, and the boxes represent the systematic uncertainties.

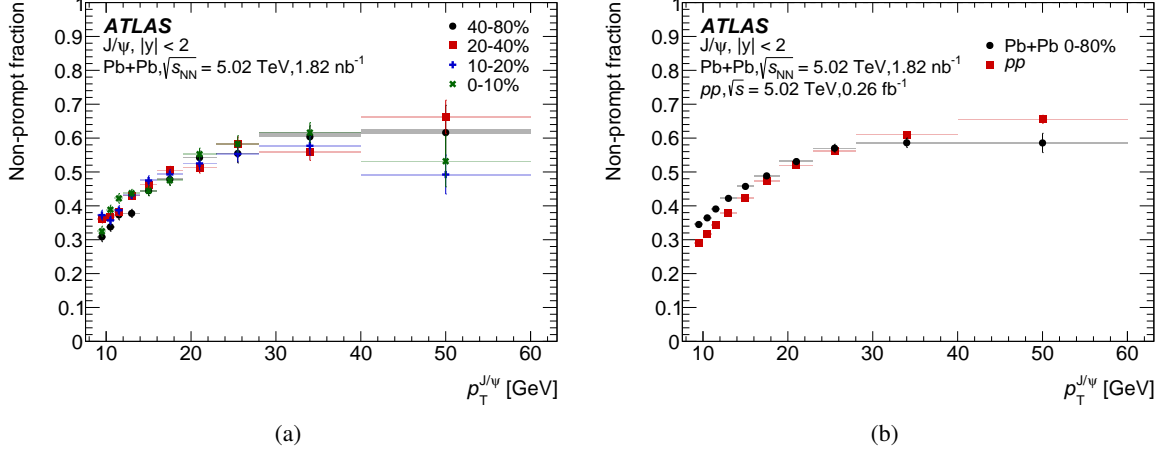


Figure 7: (a) Non-prompt fraction of Inclusive J/ψ production as a function of J/ψ p_T in Pb+Pb collisions for various centrality intervals. (b) Non-prompt fraction of Inclusive J/ψ production as a function of J/ψ p_T in pp and Pb+Pb in the 0–80% centrality interval. The error bars denote the statistical uncertainties, and the boxes represent the systematic uncertainties.

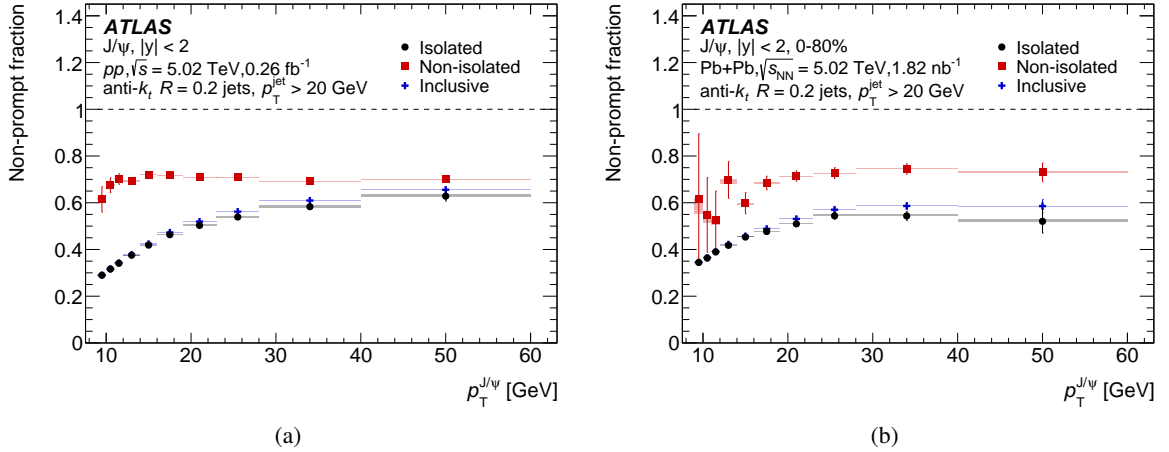


Figure 8: Non-prompt fraction of Inclusive, Isolated and Non-isolated J/ψ production as a function of J/ψ p_T in (a) pp and (b) Pb+Pb collisions in the 0–80% centrality interval. The error bars denote the statistical uncertainties, and the boxes represent the systematic uncertainties.

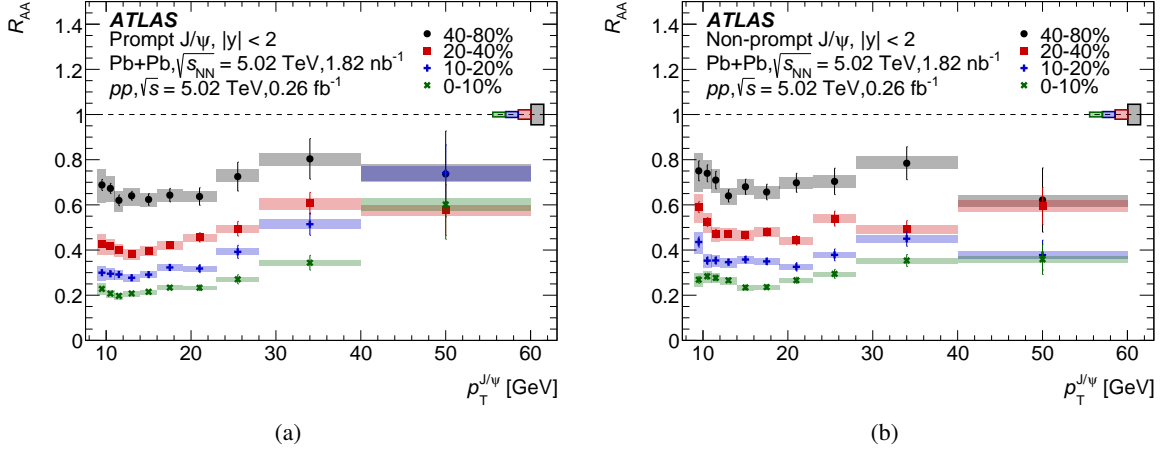


Figure 9: The nuclear modification factor as a function of J/ψ p_T for (a) Prompt and (b) Non-prompt J/ψ evaluated for different centrality intervals. The error bars denote the statistical uncertainties, and the boxes represent the systematic uncertainties. Boxes at $R_{AA} = 1$ represent global scale uncertainties, namely the pp luminosity uncertainty and $\langle T_{AA} \rangle$ uncertainty.

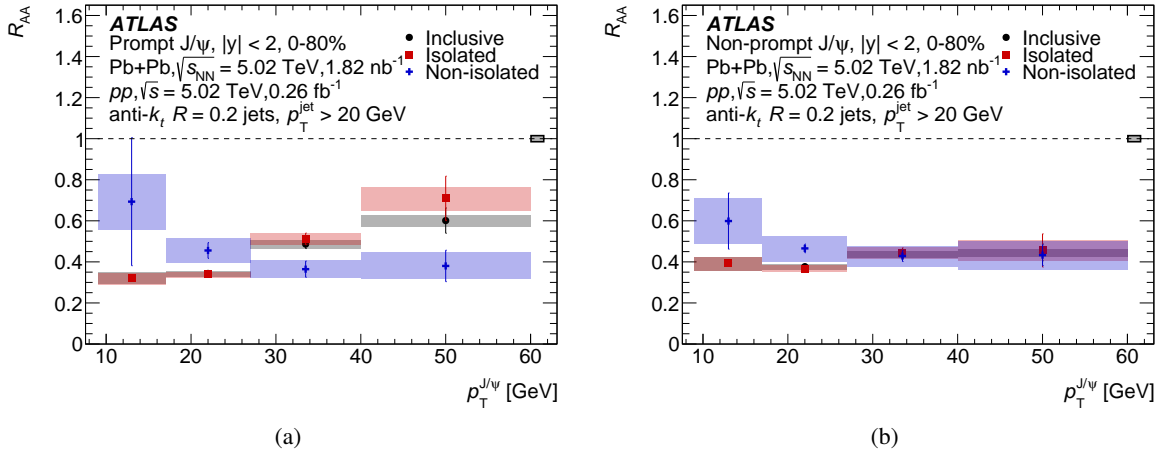


Figure 10: The nuclear modification factor as a function of p_T for Inclusive, Isolated and Non-isolated (a) Prompt and (b) Non-prompt J/ψ evaluated for 0–80% centrality interval. The error bars denote the statistical uncertainties, and the boxes represent the systematic uncertainties. Boxes at $R_{AA} = 1$ represent global scale uncertainties, namely the pp luminosity uncertainty and $\langle T_{AA} \rangle$ uncertainty.

7 Conclusion

This paper presents ATLAS measurements of J/ψ meson production in the dimuon decay channel in 5.02 TeV pp and Pb+Pb collisions, for the J/ψ mesons with $9 < p_T < 60$ GeV and $|y| < 2$. The measurements are performed for three classes of J/ψ mesons classified according to the presence of a $R = 0.2$ jet as non-isolated, isolated, and inclusive. Each of these classes is further divided into prompt and non-prompt J/ψ . The J/ψ non-isolation is defined by the presence of a jet with $p_T > 20$ GeV within $\Delta R < 0.4$ from J/ψ . The jet p_T is corrected to the MC truth level and does not include the p_T of J/ψ . The presence of jets from multi-parton interactions, or from the underlying event, which may correlate the J/ψ with a jet not originating from the same hard process, is corrected for using the orthogonal-cone method. In this set-up, more than 60% of non-prompt J/ψ are found to be isolated from jets at the highest measured p_T of J/ψ . The isolated fraction increases systematically with decreasing p_T of J/ψ and reaches unity for J/ψ with $p_T = 9$ GeV. For J/ψ $p_T \geq 20$ GeV, the isolated fraction is found to be approximately 10 – 20% larger for prompt compared to non-prompt J/ψ with no differences found between pp and Pb+Pb collisions. The R_{AA} of J/ψ is measured to be consistent between the isolated and the inclusive case. The observed difference in J/ψ R_{AA} between the non-isolated J/ψ and isolated J/ψ class has a significance of 3.5σ .

These new results complement previous measurements of quarkonia–jet correlations, where events required the presence of a jet and the p_T of jets included the p_T of the J/ψ meson. Results presented here provide new input to constrain theoretical models describing J/ψ production in pp and Pb+Pb collisions, and provide new information for modelling J/ψ suppression in Pb+Pb collisions.

Acknowledgements

We thank CERN for the very successful operation of the LHC and its injectors, as well as the support staff at CERN and at our institutions worldwide without whom ATLAS could not be operated efficiently.

The crucial computing support from all WLCG partners is acknowledged gratefully, in particular from CERN, the ATLAS Tier-1 facilities at TRIUMF/SFU (Canada), NDGF (Denmark, Norway, Sweden), CC-IN2P3 (France), KIT/GridKA (Germany), INFN-CNAF (Italy), NL-T1 (Netherlands), PIC (Spain), RAL (UK) and BNL (USA), the Tier-2 facilities worldwide and large non-WLCG resource providers. Major contributors of computing resources are listed in Ref. [72].

We gratefully acknowledge the support of ANPCyT, Argentina; YerPhI, Armenia; ARC, Australia; BMWFW and FWF, Austria; ANAS, Azerbaijan; CNPq and FAPESP, Brazil; NSERC, NRC and CFI, Canada; CERN; ANID, Chile; CAS, MOST, NSFC and FRFCU, China; Minciencias, Colombia; MEYS CR, Czech Republic; DNRF and DNSRC, Denmark; IN2P3-CNRS and CEA-DRF/IRFU, France; SRNSFG, Georgia; BMFTR, HGF and MPG, Germany; GSRI, Greece; RGC and Hong Kong SAR, China; ICHEP and Academy of Sciences and Humanities, Israel; INFN, Italy; MEXT and JSPS, Japan; CNRST, Morocco; NWO, Netherlands; RCN, Norway; MNiSW, Poland; FCT, Portugal; MNE/IFA, Romania; MSTDI, Serbia; MSSR, Slovakia; ARIS and MVZI, Slovenia; DSI/NRF, South Africa; MICIU/AEI, Spain; SRC and Wallenberg Foundation, Sweden; SERI, SNSF and Cantons of Bern and Geneva, Switzerland; NSTC, Taipei; TENMAK, Türkiye; STFC/UKRI, United Kingdom; DOE and NSF, United States of America.

Individual groups and members have received support from BCKDF, CANARIE, CRC and DRAC, Canada; CERN-CZ, FORTE and PRIMUS, Czech Republic; COST, ERC, ERDF, Horizon 2020 and Marie Skłodowska-Curie Actions, European Union; Investissements d’Avenir Labex, Investissements d’Avenir

IDEX and ANR, France; DFG and AvH Foundation, Germany; Herakleitos, Thales and Aristeia programmes co-financed by EU-ESF and the Greek NSRF, Greece; BSF-NSF and MINERVA, Israel; NCN and NAWA, Poland; La Caixa Banking Foundation, CERCA and AGAUR programs from Generalitat de Catalunya and PROMETEO and GenT Programmes Generalitat Valenciana, Spain; Göran Gustafssons Stiftelse, Sweden; The Royal Society and Leverhulme Trust, United Kingdom; Eric and Wendy Schmidt Fund for Strategic Innovation, United States of America.

In addition, individual members wish to acknowledge support from Chile: Agencia Nacional de Investigación y Desarrollo (ANID FONDECYT reg. 1230987, FONDECYT 1230812, FONDECYT 1240864, Fondecyt 3240661, Fondecyt Regular 1240721); China: Fundamental Research Funds for the Central Universities (010-63263105), Chinese Ministry of Science and Technology (MOST-2023YFA1605700, MOST-2023YFA1609300), National Natural Science Foundation of China (NSFC 12275265, NSFC-W2543005); Czech Republic: Czech Science Foundation (GACR - 24-11373S), Ministry of Education Youth and Sports (ERC-CZ-LL2327, FORTE CZ.02.01.01/00/22_008/0004632); EU: H2020 European Research Council (ERC - 101002463); European Union: European Research Council (BARD No. 101116429, ERC - 101219398, ERC 101089007), European Regional Development Fund (HE COFUND GA No.101081355, ERDF), Marie Skłodowska-Curie Actions (GAP-101168829); France: Agence Nationale de la Recherche (ANR-21-CE31-0013, ANR-22-EDIR-0002, ANR-24-CE31-0504-01); Germany: Deutsche Forschungsgemeinschaft (DFG - 469666862); China: Research Grants Council (GRF); Italy: Istituto Nazionale di Fisica Nucleare (LHC-MIUR - 28003/2025), Ministero dell'Università e della Ricerca (NextGenEU I53D23000820006 M4C2.1.1, SOE2024_0000023); Japan: Japan Society for the Promotion of Science (JSPS KAKENHI JP25H0063, JSPS KAKENHI JP22H04944, JSPS KAKENHI JP24K23939, JSPS KAKENHI JP24KK0251, JSPS KAKENHI JP25H00650, JSPS KAKENHI JP25H01291, JSPS KAKENHI JP25K01011, JSPS KAKENHI JP25K01023, JSPS KAKENHI JP25KK0047); Poland: Polish National Science Centre (NCN 2021/42/E/ST2/00350, NCN OPUS 2023/51/B/ST2/02507, NCN OPUS nr 2022/47/B/ST2/03059, NCN UMO-2019/34/E/ST2/00393, UMO-2022/47/O/ST2/00148, UMO-2023/49/B/ST2/04085, UMO-2023/51/B/ST2/00920, UMO-2024/53/N/ST2/00869); Spain: Agència de Gestió d'Ajuts Universitaris i de Recerca. (AGAUR - 2023 BP 00141), Ministry of Science and Innovation (RYC2019-028510-I, RYC2020-030254-I, RYC2021-031273-I, RYC2022-038164-I), Ministerio de Ciencia, Innovación y Universidades/Agencia Estatal de Investigación (EU NextGenerationEU (PRTR-C17.I1), PID2022-142604OB-C22); Sweden: Carl Trygger Foundation (Carl Trygger Foundation CTS 22:2312), Swedish Research Council (Swedish Research Council 2023-04654, VR 2021-03651, VR 2022-03845, VR 2022-04683, VR 2023-03403, VR 2024-05451, VR 2025-05940), Knut and Alice Wallenberg Foundation (KAW 2023.0366); United Kingdom: The Binks Trust, Royal Society (NIF-R1-231091); United States of America: U.S. Department of Energy (ECA DE-AC02-76SF00515), John Templeton Foundation (John Templeton Foundation 63206), Neubauer Family Foundation.

Appendix

The R_{AA} evaluated as a function of J/ψ p_T for non-isolated, isolated, and inclusive J/ψ in individual centrality intervals is presented for prompt and non-prompt production in Figures 11 and 12, respectively. These figures complement the corresponding results for the 0–80% centrality interval shown in Figure 10.

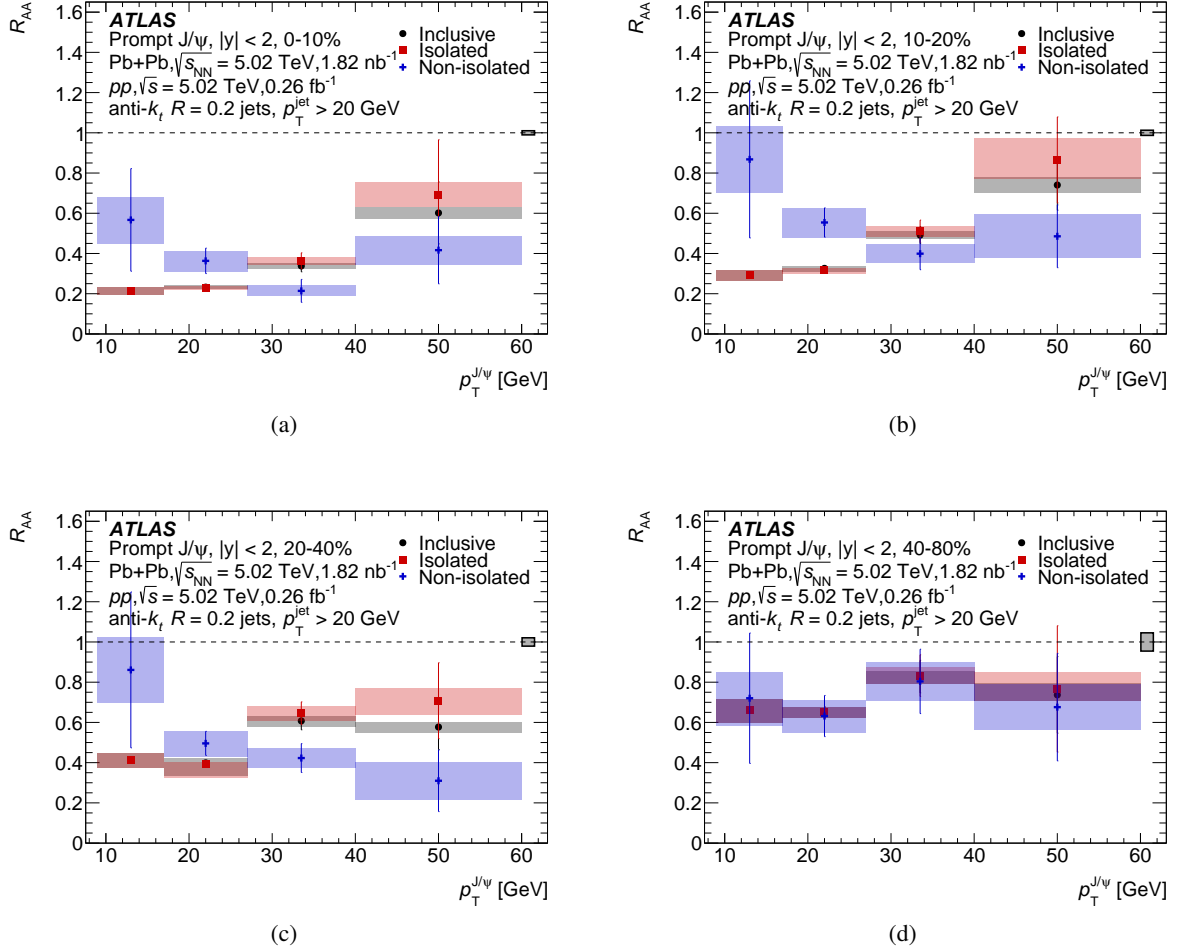


Figure 11: The nuclear modification factor as a function of p_T for Inclusive, Isolated and Non-isolated prompt J/ψ evaluated for four centrality intervals, namely (a) 0–10%, (b) 10–20%, (c) 20–40%, and (d) 40–80%. The error bars denote the statistical uncertainties, and the boxes represent the systematic uncertainties. Boxes at $R_{AA} = 1$ represent global scale uncertainties, namely the pp luminosity uncertainty and $\langle T_{AA} \rangle$ uncertainty.

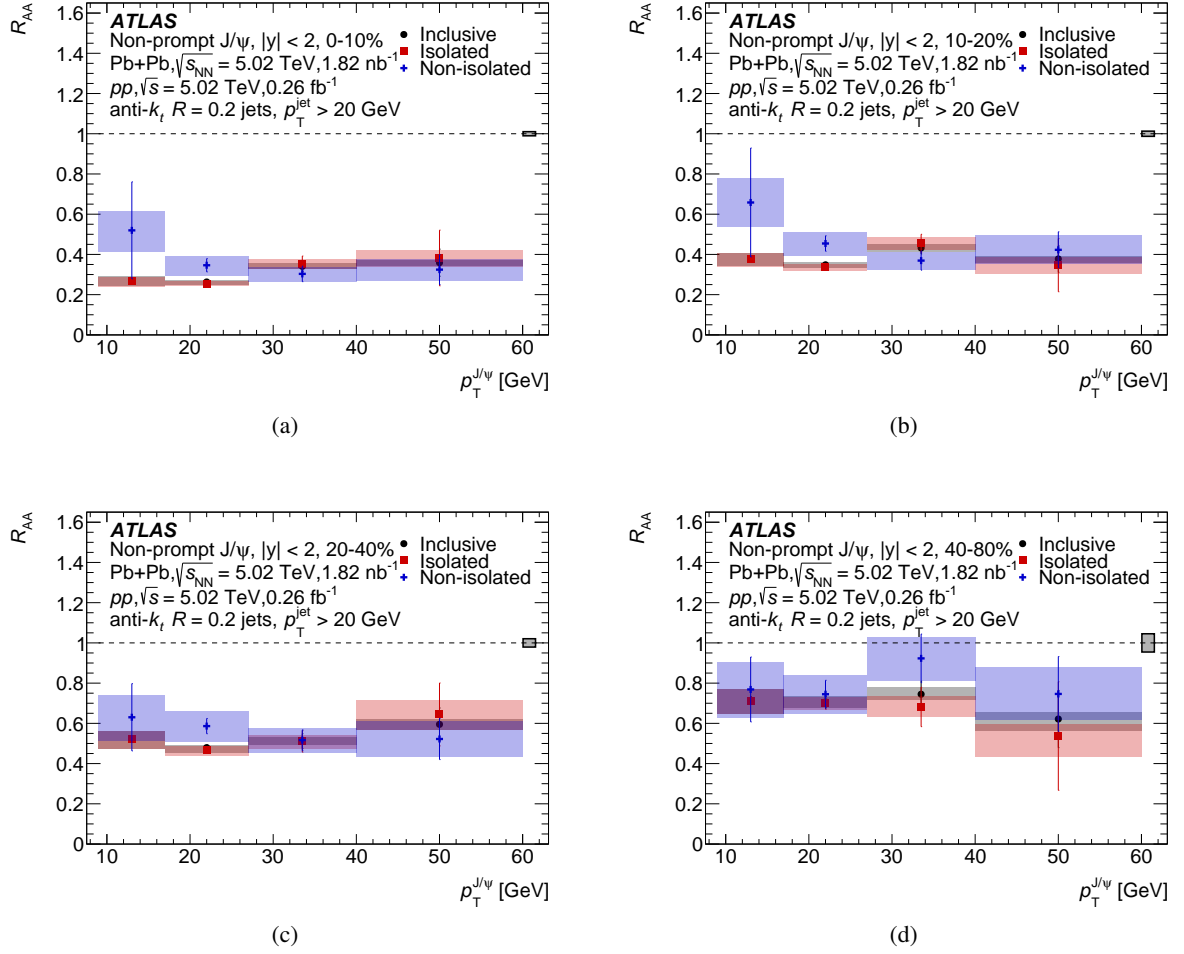


Figure 12: The nuclear modification factor as a function of p_T for Inclusive, Isolated and Non-isolated non-prompt J/ψ evaluated for four centrality intervals, namely (a) 0–10%, (b) 10–20%, (c) 20–40%, and (d) 40–80%. The error bars denote the statistical uncertainties, and the boxes represent the systematic uncertainties. Boxes at $R_{AA} = 1$ represent global scale uncertainties, namely the pp luminosity uncertainty and $\langle T_{AA} \rangle$ uncertainty.

References

- [1] H. Hahn et al., *The RHIC design overview*, *Nucl. Instrum. Meth. A* **499** (2003) 245.
- [2] L. Evans and P. Bryant, *LHC Machine*, *JINST* **3** (2008) S08001.
- [3] W. Busza, K. Rajagopal and W. van der Schee, *Heavy Ion Collisions: The Big Picture, and the Big Questions*, *Ann. Rev. Nucl. Part. Sci.* **68** (2018) 339, arXiv: 1802.04801 [hep-ph].
- [4] E. Shuryak, *Strongly coupled quark-gluon plasma in heavy ion collisions*, *Rev. Mod. Phys.* **89** (2017) 035001, arXiv: 1412.8393 [hep-ph].
- [5] M. Connors, C. Nattrass, R. Reed and S. Salur, *Jet measurements in heavy ion physics*, *Rev. Mod. Phys.* **90** (2018) 025005, arXiv: 1705.01974 [nucl-ex].
- [6] L. Cunqueiro and A. M. Sickles, *Studying the QGP with Jets at the LHC and RHIC*, *Prog. Part. Nucl. Phys.* **124** (2022) 103940, arXiv: 2110.14490 [nucl-ex].
- [7] L. Apolinário, Y.-T. Chien and L. Cunqueiro Mendez, *Jet substructure*, *Int. J. Mod. Phys. E* **33** (2024) 2430003.
- [8] N. Brambilla et al., *Heavy Quarkonium: Progress, Puzzles, and Opportunities*, *Eur. Phys. J. C* **71** (2011) 1534, arXiv: 1010.5827 [hep-ph].
- [9] ALICE Collaboration, *Measurements of inclusive J/ψ production at midrapidity and forward rapidity in Pb–Pb collisions at $\sqrt{s_{NN}} = 5.02$ TeV*, *Phys. Lett. B* **849** (2024) 138451, arXiv: 2303.13361 [nucl-ex].
- [10] ALICE Collaboration, *$\psi(2S)$ Suppression in Pb-Pb Collisions at the LHC*, *Phys. Rev. Lett.* **132** (2024) 042301, arXiv: 2210.08893 [nucl-ex].
- [11] ATLAS Collaboration, *Prompt and non-prompt J/ψ and $\psi(2S)$ suppression at high transverse momentum in 5.02 TeV Pb+Pb collisions with the ATLAS experiment*, *Eur. Phys. J. C* **78** (2018) 762, arXiv: 1805.04077 [nucl-ex].
- [12] CMS Collaboration, *Measurement of prompt and nonprompt charmonium suppression in PbPb collisions at 5.02 TeV*, *Eur. Phys. J. C* **78** (2018) 509, arXiv: 1712.08959 [hep-ex].
- [13] CMS Collaboration, *Observation of the $\Upsilon(3S)$ Meson and Suppression of Υ States in PbPb Collisions at $\sqrt{s_{NN}} = 5.02$ TeV*, *Phys. Rev. Lett.* **133** (2024) 022302, arXiv: 2303.17026 [hep-ex].
- [14] ATLAS Collaboration, *Production of $\Upsilon(nS)$ mesons in Pb+Pb and pp collisions at 5.02 TeV*, *Phys. Rev. C* **107** (2023) 054912, arXiv: 2205.03042 [nucl-ex].
- [15] ALICE Collaboration, *Υ production and nuclear modification at forward rapidity in Pb–Pb collisions at $\sqrt{s_{NN}}=5.02$ TeV*, *Phys. Lett. B* **822** (2021) 136579, arXiv: 2011.05758 [nucl-ex].
- [16] CMS Collaboration, *Measurement of nuclear modification factors of $\Upsilon(1S)$, $\Upsilon(2S)$, and $\Upsilon(3S)$ mesons in PbPb collisions at $\sqrt{s_{NN}} = 5.02$ TeV*, *Phys. Lett. B* **790** (2019) 270, arXiv: 1805.09215 [hep-ex].
- [17] Y. Makris and I. Vitev, *An Effective Theory of Quarkonia in QCD Matter*, *JHEP* **10** (2019) 111, arXiv: 1906.04186 [hep-ph].

- [18] M. Spousta, *On similarity of jet quenching and charmonia suppression*, *Phys. Lett. B* **767** (2017) 10, arXiv: [1606.00903 \[hep-ph\]](#).
- [19] F. Arleo, *Quenching of Hadron Spectra in Heavy Ion Collisions at the LHC*, *Phys. Rev. Lett.* **119** (2017) 062302, arXiv: [1703.10852 \[hep-ph\]](#).
- [20] G. T. Bodwin, E. Braaten and G. P. Lepage, *Rigorous QCD analysis of inclusive annihilation and production of heavy quarkonium*, *Phys. Rev. D* **51** (1995) 1125, [Erratum: *Phys.Rev.D* 55, 5853 (1997)], arXiv: [hep-ph/9407339](#).
- [21] P. L. Cho and A. K. Leibovich, *Color octet quarkonia production*, *Phys. Rev. D* **53** (1996) 150, arXiv: [hep-ph/9505329](#).
- [22] P. L. Cho and A. K. Leibovich, *Color octet quarkonia production. 2.*, *Phys. Rev. D* **53** (1996) 6203, arXiv: [hep-ph/9511315](#).
- [23] M. Baumgart, A. K. Leibovich, T. Mehen and I. Z. Rothstein, *Probing Quarkonium Production Mechanisms with Jet Substructure*, *JHEP* **11** (2014) 003, arXiv: [1406.2295 \[hep-ph\]](#).
- [24] R. Bain, L. Dai, A. Leibovich, Y. Makris and T. Mehen, *NRQCD Confronts LHCb Data on Quarkonium Production within Jets*, *Phys. Rev. Lett.* **119** (2017) 032002, arXiv: [1702.05525 \[hep-ph\]](#).
- [25] J.-P. Lansberg, *New Observables in Inclusive Production of Quarkonia*, *Phys. Rept.* **889** (2020) 1, arXiv: [1903.09185 \[hep-ph\]](#).
- [26] CMS Collaboration, *Fragmentation of jets containing a prompt J/ψ meson in PbPb and pp collisions at $\sqrt{s_{NN}} = 5.02$ TeV*, *Phys. Lett. B* **825** (2022) 136842, arXiv: [2106.13235 \[hep-ex\]](#).
- [27] LHCb Collaboration, *Study of J/ψ Production in Jets*, *Phys. Rev. Lett.* **118** (2017) 192001, arXiv: [1701.05116 \[hep-ex\]](#).
- [28] T. Sjöstrand, S. Mrenna and P. Skands, *A brief introduction to PYTHIA 8.1*, *Comput. Phys. Commun.* **178** (2008) 852, arXiv: [0710.3820 \[hep-ph\]](#).
- [29] CMS Collaboration, *Study of J/ψ meson production inside jets in pp collisions at $\sqrt{s} = 8$ TeV*, *Phys. Lett. B* **804** (2020) 135409, arXiv: [1910.01686 \[hep-ex\]](#).
- [30] ATLAS Collaboration, *The ATLAS Experiment at the CERN Large Hadron Collider*, *JINST* **3** (2008) S08003.
- [31] ATLAS Collaboration, *ATLAS Insertable B-Layer: Technical Design Report*, ATLAS-TDR-19; CERN-LHCC-2010-013, 2010, URL: <https://cds.cern.ch/record/1291633>, Addendum: ATLAS-TDR-19-ADD-1; CERN-LHCC-2012-009, 2012, URL: <https://cds.cern.ch/record/1451888>.
- [32] B. Abbott et al., *Production and integration of the ATLAS Insertable B-Layer*, *JINST* **13** (2018) T05008, arXiv: [1803.00844 \[physics.ins-det\]](#).
- [33] G. Avoni et al., *Upgrades of the ATLAS zero degree calorimeter system for Run 3 at the Large Hadron Collider*, *JINST* **20** (2025) P11021, arXiv: [2509.05948 \[physics.ins-det\]](#).
- [34] G. Avoni et al., *The new LUCID-2 detector for luminosity measurement and monitoring in ATLAS*, *JINST* **13** (2018) P07017.
- [35] ATLAS Collaboration, *Performance of the ATLAS trigger system in 2015*, *Eur. Phys. J. C* **77** (2017) 317, arXiv: [1611.09661 \[hep-ex\]](#).

- [36] ATLAS Collaboration, *Performance of the ATLAS muon triggers in Run 2*, [JINST **15** \(2020\) P09015](#), arXiv: [2004.13447 \[physics.ins-det\]](#).
- [37] ATLAS Collaboration, *Software and computing for Run 3 of the ATLAS experiment at the LHC*, [Eur. Phys. J. C **85** \(2025\) 234](#), arXiv: [2404.06335 \[hep-ex\]](#),
Erratum: [Eur. Phys. J. C **85** \(2025\) 907](#).
- [38] T. Sjöstrand et al., *An introduction to PYTHIA 8.2*, [Comput. Phys. Commun. **191** \(2015\) 159](#),
arXiv: [1410.3012 \[hep-ph\]](#).
- [39] E. Barberio, B. van Eijk and Z. Was,
PHOTOS: A Universal Monte Carlo for QED radiative corrections in decays,
[Comput. Phys. Commun. **66** \(1991\) 115](#).
- [40] ATLAS Collaboration, *ATLAS Pythia 8 tunes to 7 TeV data*, ATL-PHYS-PUB-2014-021, 2014,
URL: <https://cds.cern.ch/record/1966419>.
- [41] J. Pumplin et al.,
New Generation of Parton Distributions with Uncertainties from Global QCD Analysis,
[JHEP **07** \(2002\) 012](#), arXiv: [hep-ph/0201195](#).
- [42] ATLAS Collaboration, *The ATLAS Simulation Infrastructure*, [Eur. Phys. J. C **70** \(2010\) 823](#),
arXiv: [1005.4568 \[physics.ins-det\]](#).
- [43] S. Agostinelli et al., *GEANT4 – a simulation toolkit*, [Nucl. Instrum. Meth. A **506** \(2003\) 250](#).
- [44] A. Haas and on behalf of the ATLAS Collaboration,
ATLAS Simulation using Real Data: Embedding and Overlay,
[Journal of Physics: Conference Series **898** \(2017\) 042004](#).
- [45] C. Loizides, J. Kamin and D. d’Enterria,
Improved Monte Carlo Glauber predictions at present and future nuclear colliders,
[Phys. Rev. C **97** \(2018\) 054910](#), [Erratum: [Phys.Rev.C 99, 019901 \(2019\)](#)],
arXiv: [1710.07098 \[nucl-ex\]](#).
- [46] M. L. Miller, K. Reygers, S. J. Sanders and P. Steinberg,
Glauber modeling in high energy nuclear collisions, [Ann. Rev. Nucl. Part. Sci. **57** \(2007\) 205](#),
arXiv: [nucl-ex/0701025](#).
- [47] ATLAS Collaboration, *Measurement of substructure-dependent suppression of large-radius jets with charged particles in Pb+Pb collisions with ATLAS*, [Phys. Lett. B **871** \(2025\) 139929](#),
arXiv: [2504.04805 \[nucl-ex\]](#).
- [48] ATLAS Collaboration, *Muon reconstruction performance of the ATLAS detector in proton–proton collision data at $\sqrt{s} = 13$ TeV*, [Eur. Phys. J. C **76** \(2016\) 292](#), arXiv: [1603.05598 \[hep-ex\]](#).
- [49] R. Barlow and C. Beeston, *Fitting using finite Monte Carlo samples*,
[Comput. Phys. Commun. **77** \(1993\) 219](#).
- [50] ATLAS Collaboration, *Measurement of the differential cross-sections of prompt and non-prompt production of J/ψ and $\psi(2S)$ in pp collisions at $\sqrt{s} = 7$ and 8 TeV with the ATLAS detector*,
[Eur. Phys. J. C **76** \(2016\) 283](#), arXiv: [1512.03657 \[hep-ex\]](#).
- [51] LHCb Collaboration, *Measurement of J/ψ polarization in pp collisions at $\sqrt{s} = 7$ TeV*,
[Eur. Phys. J. C **73** \(2013\) 2631](#), arXiv: [1307.6379 \[hep-ex\]](#).
- [52] ALICE Collaboration, *J/ψ polarization in pp collisions at $\sqrt{s} = 7$ TeV*,
[Phys. Rev. Lett. **108** \(2012\) 082001](#), arXiv: [1111.1630 \[hep-ex\]](#).

- [53] CMS Collaboration, *Measurement of the prompt J/ψ and $\psi(2S)$ polarizations in pp collisions at $\sqrt{s} = 7$ TeV*, *Phys. Lett. B* **727** (2013) 381, arXiv: [1307.6070 \[hep-ex\]](#).
- [54] ATLAS Collaboration, *Muon reconstruction and identification efficiency in ATLAS using the full Run 2 pp collision data set at $\sqrt{s} = 13$ TeV*, *Eur. Phys. J. C* **81** (2021) 578, arXiv: [2012.00578 \[hep-ex\]](#).
- [55] ATLAS Collaboration, *Measurement of the nuclear modification factor for muons from charm and bottom hadrons in $Pb+Pb$ collisions at 5.02 TeV with the ATLAS detector*, *Phys. Lett. B* **829** (2022) 137077, arXiv: [2109.00411 \[nucl-ex\]](#).
- [56] ATLAS Collaboration, *Measurement of muon pairs produced via $\gamma\gamma$ scattering in nonultraperipheral $Pb+Pb$ collisions at $\sqrt{s_{NN}} = 5.02$ TeV with the ATLAS detector*, *Phys. Rev. C* **107** (2023) 054907, arXiv: [2206.12594 \[nucl-ex\]](#).
- [57] M. Cacciari, G. P. Salam and G. Soyez, *The anti- k_t jet clustering algorithm*, *JHEP* **04** (2008) 063, arXiv: [0802.1189 \[hep-ph\]](#).
- [58] M. Cacciari, G. P. Salam and G. Soyez, *FastJet user manual*, *Eur. Phys. J. C* **72** (2012) 1896, arXiv: [1111.6097 \[hep-ph\]](#).
- [59] ATLAS Collaboration, *Measurement of the nuclear modification factor for inclusive jets in $Pb+Pb$ collisions at $\sqrt{s_{NN}} = 5.02$ TeV with the ATLAS detector*, *Phys. Lett. B* **790** (2019) 108, arXiv: [1805.05635 \[nucl-ex\]](#).
- [60] ATLAS Collaboration, *Measurement of the jet radius and transverse momentum dependence of inclusive jet suppression in lead–lead collisions at $\sqrt{s_{NN}} = 2.76$ TeV with the ATLAS detector*, *Phys. Lett. B* **719** (2013) 220, arXiv: [1208.1967 \[hep-ex\]](#).
- [61] ATLAS Collaboration, *Jet energy scale and resolution measured in proton–proton collisions at $\sqrt{s} = 13$ TeV with the ATLAS detector*, *Eur. Phys. J. C* **81** (2021) 689, arXiv: [2007.02645 \[hep-ex\]](#).
- [62] ATLAS Collaboration, *Jet energy scale and its uncertainty for jets reconstructed using the ATLAS heavy ion jet algorithm*, ATLAS-CONF-2015-016, 2015, URL: <https://cds.cern.ch/record/2008677>.
- [63] ATLAS Collaboration, *Measurement of inclusive jet and dijet cross-sections in proton–proton collisions at $\sqrt{s} = 13$ TeV with the ATLAS detector*, *JHEP* **05** (2018) 195, arXiv: [1711.02692 \[hep-ex\]](#).
- [64] CMS Collaboration, *Measurement of the double-differential inclusive jet cross section in proton–proton collisions at $\sqrt{s} = 13$ TeV*, *Eur. Phys. J. C* **76** (2016) 451, arXiv: [1605.04436 \[hep-ex\]](#).
- [65] M. Oreglia, *A Study of the Reactions $\psi' \rightarrow \gamma\gamma\psi$* , Ph.D. Thesis, SLAC-236: Stanford University, 1980.
- [66] W. Verkerke and D. Kirkby, *The RooFit toolkit for data modeling*, 2003, arXiv: [physics/0306116 \[physics.data-an\]](#).
- [67] ATLAS Collaboration, *Measurement of inclusive jet charged-particle fragmentation functions in $Pb+Pb$ collisions at $\sqrt{s_{NN}} = 2.76$ TeV with the ATLAS detector*, *Phys. Lett. B* **739** (2014) 320, arXiv: [1406.2979 \[hep-ex\]](#).

- [68] S. Navas and others (Particle Data Group), *Review of Particle Physics*, *Phys. Rev. D* **110** (2024) 030001,
URL: <https://link.aps.org/doi/10.1103/PhysRevD.110.030001>.
- [69] ATLAS Collaboration,
Luminosity determination in pp collisions at $\sqrt{s} = 13$ TeV using the ATLAS detector at the LHC,
Eur. Phys. J. C **83** (2023) 982, arXiv: [2212.09379](https://arxiv.org/abs/2212.09379) [hep-ex].
- [70] S. A. Stouffer, E. A. Suchman, L. C. DeVinney, S. A. Star and R. M. Williams Jr, *The american soldier: Adjustment during army life.(studies in social psychology in world war ii)*, vol. 1, (1949).
- [71] S. Bityukov, N. Krasnikov, A. Nikitenko and V. Smirnova,
Two approaches to combining significances,
PoS ACAT08 (2008) 118, ed. by T. Speer, F. Carminati and M. Werlen.
- [72] ATLAS Collaboration, *ATLAS Computing Acknowledgements*, ATL-SOFT-PUB-2026-001, 2026,
URL: <https://cds.cern.ch/record/2952666>.

The ATLAS Collaboration

G. Aad ¹⁰², E. Aakvaag ¹⁷, B. Abbott ¹²¹, S. Abdelhameed ^{83b}, K. Abeling ⁵⁴, N.J. Abicht ⁴⁸, S.H. Abidi ³⁰, M. Aboeela ⁴⁴, A. Aboulhorma ^{36e}, H. Abramowicz ¹⁵⁴, B.S. Acharya ^{68a,68b,m}, A. Ackermann ^{62a}, J. Ackerschott ⁵⁵, C. Adam Bourdarios ⁴, L. Adamczyk ^{85a}, S.V. Addepalli ¹⁴⁶, M.J. Addison ¹⁰¹, J. Adelman ¹¹⁷, A. Adiguzel ^{22c}, T. Adye ¹³⁵, A.A. Affolder ¹³⁷, Y. Afik ³⁹, M.N. Agaras ¹³, A. Aggarwal ¹⁰⁰, C. Agheorghiesei ^{28c}, A. Ahmad ^{83a}, F. Ahmadov ^{38,ad}, S. Ahuja ¹⁶⁵, X. Ai ^{113c}, G. Aielli ^{75a,75b}, A. Aikot ¹⁶⁵, M. Ait Tamlihat ^{36e}, T.P.A. Åkesson ⁹⁸, D. Akiyama ¹⁷⁰, N.N. Akolkar ²⁵, S. Aktas ¹⁶⁸, G.L. Alberghi ^{24b}, J. Albert ¹⁶⁷, U. Alberti ²⁰, P. Albicocco ⁵², S. Alderweireldt ⁵¹, Z.L. Alegria ¹²², M. Aleksa ³⁷, I.N. Aleksandrov ³⁸, C. Alexa ^{28b}, T. Alexopoulos ¹⁰, F. Alfonsi ^{24b}, M. Algren ⁵⁵, M. Alhroob ¹⁶⁹, B. Ali ¹³³, H.M.J. Ali ^{91,v}, S. Ali ³², S.W. Alibocus ⁹², M. Aliev ^{34c}, G. Alimonti ^{70a}, C. Allaire ⁶⁵, B.M.M. Allbrooke ¹⁴⁹, D.R. Allen ¹²², J.S. Allen ¹⁰¹, J.F. Allen ⁵¹, C.S. Alley ¹, E.R. Almazan ¹³⁷, A. Aloisio ^{71a,71b}, F. Alonso ⁹⁰, C. Alpigiani ¹⁴⁰, A. Alvarez Fernandez ¹⁰⁰, M. Alves Cardoso ⁵⁵, M.G. Alviggi ^{71a,71b}, Y. Amaral Coutinho ^{81b}, C. Amelung ³⁷, M. Amerl ¹⁰¹, T. Amezza ¹²⁸, B. Amini ⁵³, K. Amirie ¹⁵⁸, A. Amirkhanov ³⁸, D. Amperiadou ¹⁵⁵, C. Anastopoulos ¹⁴², T. Andeen ¹¹, J.K. Anders ⁹², A.C. Anderson ⁵⁸, N. Anderson ¹⁴⁸, A. Andreazza ^{70a,70b}, S. Angelidakis ⁹, A. Angerami ⁴¹, A.V. Anisenkov ³⁸, A. Annovi ^{73a}, C. Antel ³⁷, E. Antipov ¹⁴⁸, M. Antonelli ⁵², F. Anulli ^{74a}, M. Aoki ⁸², T. Aoki ¹⁵⁶, M.A. Aparo ¹³, L. Aperio Bella ⁴⁷, M. Apicella ³¹, C. Appelt ¹⁵⁴, A. Apyan ²⁷, R. Arakida ¹²⁵, M. Arampatzi ¹⁰, S.J. Arbiol Val ⁸⁶, C. Arcangeletti ⁵², A.T.H. Arce ⁵⁰, M. Arcuri ^{43b,43a}, J-F. Arguin ¹⁰⁸, S. Argyropoulos ¹⁵⁵, J.-H. Arling ⁴⁷, O. Arnaez ⁴, H. Arnold ¹⁴⁸, G. Artoni ^{74a,74b}, H. Asada ¹¹¹, S. Asatryan ¹⁷⁵, N.A. Asbah ³⁷, R.A. Ashby Pickering ¹⁶⁹, A.M. Aslam ⁹⁵, J. Assahsah ^{36d}, K. Assamagan ³⁰, R. Astalos ^{29a}, K.S.V. Astrand ⁹⁸, S. Atashi ¹⁶², R.J. Atkin ^{34a}, H. Atmani ^{36f}, P.A. Atlasiddha ¹²⁹, K. Augsten ¹³³, A.D. Aurion ⁴⁰, V.A. Austrup ¹⁰¹, A.S. Avad ⁹⁴, G. Avolio ³⁷, A. Azzam ¹³, D. Babal ^{29b}, H. Bachacou ¹³⁶, K. Bachas ^{155,p}, A. Bachiu ³⁵, E. Bachmann ⁴⁹, M.J. Backes ^{62a}, A. Badea ³⁹, T.M. Baer ¹⁰⁶, M. Bahmani ¹⁹, D. Bahner ⁵³, K. Bai ¹²⁴, L. Baines ⁹⁴, O.K. Baker ¹⁷⁴, D. Bakshi Gupta ⁸, L.E. Balabram Filho ^{81b}, V. Balakrishnan ¹²¹, R. Balasubramanian ⁴, P. Balek ^{85a}, E. Ballabene ^{24b,24a}, F. Balli ¹³⁶, L.M. Baltés ^{62a}, W.K. Balunas ¹²⁷, I. Bamwidhi ^{83c}, E. Banas ⁸⁶, M. Bandieramonte ¹³⁰, S. Bansal ²⁵, L. Barak ¹⁵⁴, M. Barakat ⁴⁷, E.L. Barberio ¹⁰⁵, D. Barberis ^{18b}, M. Barbero ¹⁰², M.Z. Barel ¹¹⁶, T. Barillari ¹¹⁰, M-S. Barisits ³⁷, T. Barklow ¹⁴⁶, P. Baron ¹³⁴, D.A. Baron Moreno ¹⁰¹, A. Baroncelli ⁶¹, A.J. Barr ^{127,g}, J.D. Barr ⁹⁶, F. Barreiro ⁹⁹, J. Barreiro Guimarães da Costa ¹⁴, M.G. Barros Teixeira ^{131a}, F. Bartels ³⁷, R. Bartoldus ¹⁴⁶, A.E. Barton ⁹¹, P. Bartos ^{29a}, M. Baselga ⁴⁸, S. Bashiri ⁸⁶, A. Bassalat ^{65,b}, M.J. Basso ^{159a}, S. Bataju ⁴⁴, R. Bate ¹⁶⁶, R.L. Bates ⁵⁸, M. Battaglia ¹³⁷, D. Battulga ¹⁹, M. Baucé ^{74a,74b}, L. Bauckhage ⁴⁷, P. Bauer ²⁵, L.T. Bayer ⁴⁷, L.T. Bazzano Hurrell ³¹, T. Beau ¹²⁸, J.Y. Beaucamp ⁹⁰, S. Beauceron ¹²⁸, P.H. Beauchemin ¹⁶¹, P. Bechtel ²⁵, H.P. Beck ^{20,o}, K. Becker ¹⁶⁹, A.J. Beddall ⁸⁰, V.A. Bednyakov ³⁸, C.P. Bee ¹⁴⁸, L.J. Beemster ¹⁶, M. Begalli ^{81d}, M. Begel ³⁰, J.K. Behr ⁴⁷, J.F. Beirer ³⁷, F. Beisiegel ²⁵, I.B. Belean ^{28d}, M. Belfkir ^{83c}, G. Bella ¹⁵⁴, L. Bellagamba ^{24b}, A. Bellerive ³⁵, C.D. Bellgraph ⁶⁷, P. Bellos ²¹, I. Benaoumeur ²¹, D. Benckekroun ^{36a}, F. Bendebba ^{36a}, Y. Benhammou ¹⁵⁴, K.C. Benkendorfer ¹⁶⁷, L. Beresford ⁴⁷, M. Beretta ⁵², E. Bergeas Kuutmann ¹⁶³, N. Berger ⁴, B. Bergmann ¹³³, J. Beringer ^{18a}, M. Berkat ¹³⁶, G. Bernardi ⁵, C. Bernius ¹⁴⁶, F.U. Bernlochner ²⁵, A. Berrocal Guardia ¹³, T. Berry ⁹⁵, P. Berta ¹³⁴, A. Berti ^{131a}, R. Bertrand ¹⁰², S. Bethke ¹¹⁰, A. Betti ^{74a,74b}, T.F. Beumker ¹⁷³,

A.J. Bevan ⁹⁴, L. Bezio ⁵⁵, N.K. Bhalla ⁵³, S. Bharthuar ¹¹⁰, S. Bhatta ¹⁴⁸, P. Bhattarai ¹⁴⁶,
 Z.M. Bhatti ¹¹⁸, K.D. Bhide ¹⁶⁴, V.S. Bhopatkar ¹²², R.M. Bianchi ¹³⁰, G. Bianco ^{24b,24a},
 O. Biebel ¹⁰⁹, M. Biglietti ^{76a}, P. Bijl ⁵³, C.S. Billingsley ⁴⁴, Y. Bimgdi ^{36f}, M. Bindi ⁵⁴,
 A. Bingham ¹⁷³, A. Bingul ^{22b}, C. Bini ^{74a,74b}, M. Biros ¹³⁴, S. Biryukov ¹⁴⁹, T. Bisanz ⁴⁸,
 E. Bisceglie ^{24b,24a}, J.P. Biswal ¹³⁵, D. Biswas ¹⁴⁴, M. Biyabi ¹⁴, I. Bloch ⁴⁷, A. Blue ⁵⁸,
 U. Blumenschein ⁹⁴, V.S. Bobrovnikov ³⁸, L. Boccardo ^{56b,56a}, M. Boehler ⁵³, D. Bogavac ¹³,
 L.S. Boggia ¹²⁸, V. Boisvert ⁹⁵, P. Bokan ¹⁶³, T. Bold ^{85a}, M. Bomben ⁵, M. Bona ⁹⁴,
 M. Boonekamp ¹³⁶, A.G. Borbély ⁵⁸, G. Borissov ⁹¹, A. Borkar ¹⁶⁸, D. Bortoletto ¹²⁷,
 M. Borysova ¹⁷¹, D. Boscherini ^{24b}, M. Bosman ¹³, K. Bouaouda ^{36a}, L. Boudet ¹³⁶,
 J. Boudreau ¹³⁰, E.V. Bouhova-Thacker ⁹¹, D. Boumediene ⁴⁰, R. Bouquet ^{56b,56a}, A. Boveia ¹²⁰,
 D. Boye ³⁰, I.R. Boyko ³⁸, L. Bozianu ⁵⁵, J. Bracnik ²¹, N. Brahimi ⁴, G. Brandt ¹⁷³,
 O. Brandt ³³, B. Brau ¹⁰³, R. Brenner ¹⁷¹, L. Brenner ¹¹⁶, R. Brenner ¹⁶³, S. Bressler ¹⁷¹,
 M. Brettell ⁹⁶, G. Brianti ¹¹⁶, D. Britton ⁵⁸, D. Britzger ¹¹⁰, I. Brock ²⁵, R. Brock ¹⁰⁷,
 H. Bronson ¹²⁹, G. Brooijmans ⁴¹, A.J. Brooks ⁶⁷, E.M. Brooks ^{159b}, E. Brost ³⁰,
 L.M. Brown ^{167,159a}, L.E. Bruce ⁶⁰, T.L. Bruckler ¹²⁷, P.A. Bruckman de Renstrom ⁸⁶,
 B. Brüers ⁴⁷, A. Bruni ^{24b}, G. Bruni ^{24b}, D. Brunner ^{46a,46b}, M. Bruschi ^{24b}, N. Bruscinò ^{74a,74b},
 T. Buanes ¹⁷, Q. Buat ¹⁴⁰, D. Buchin ¹¹⁰, A.G. Buckley ⁵⁸, J. Bucko ¹³⁴, M. Bühring ⁴⁹,
 O. Bulekov ⁸⁰, B.A. Bullard ¹⁴⁶, T.O. Buratovich ⁹⁰, S. Burdin ⁹², C.D. Burgard ⁴⁸,
 A.M. Burger ⁸⁹, B. Burghgrave ⁸, J. Burleson ¹⁶⁴, J.C. Burzynski ¹²¹, V. Büscher ¹⁰⁰,
 P.J. Bussey ⁵⁸, O. But ²⁵, J.M. Butler ²⁶, C.M. Buttar ⁵⁸, J.M. Butterworth ⁹⁶, P. Butti ³⁷,
 W. Buttinger ¹³⁵, C.J. Buxo Vazquez ¹⁰⁷, A.R. Buzykaev ³⁸, S. Cabrera Urbán ¹⁶⁵,
 L. Cadamuro ⁶⁵, H. Cai ³⁷, Y. Cai ^{24b,112c,24a}, Y. Cai ^{112a}, M.A. Cairo ¹²⁹, V.M.M. Cairo ³⁷,
 O. Cakir ^{3a}, N. Calace ³⁷, P. Calafiura ^{18a}, G. Calderini ¹²⁸, P. Calfayan ³⁵, L. Calic ⁹⁸,
 G. Callea ⁵⁸, L.P. Caloba ^{81b}, D. Calvet ⁴⁰, S. Calvet ⁴⁰, R. Camacho Toro ¹²⁸, S. Camarda ³⁷,
 D. Camarero Munoz ²⁷, P. Camarri ^{75a,75b}, C. Camincher ³⁷, M. Campanelli ⁹⁶, A. Camplani ⁴²,
 V. Canale ^{71a,71b}, A.C. Canbay ^{3a}, E. Canonero ⁹⁵, J. Cantero ¹⁶⁵, F. Capocasa ²⁷, P. Cappelli ²⁷,
 M. Capua ^{43b,43a}, A. Carbone ^{70a,70b}, R. Cardarelli ^{75a}, J.C.J. Cardenas ⁸, M.P. Cardiff ²⁷,
 G. Carducci ^{43b,43a}, T. Carli ³⁷, G. Carlino ^{71a}, J.I. Carlotto ¹³, B.T. Carlson ^{130,q},
 E.M. Carlson ¹⁶⁷, L. Carminati ^{70a,70b}, A. Carnelli ⁴, M. Carnesale ³⁷, S. Caron ¹¹⁵,
 E.M. Carpenter ¹⁰⁶, E. Carquin ^{138g}, I.B. Carr ¹⁰⁵, S. Carrà ^{72a,72b}, G. Carratta ^{24b,24a},
 C. Carrion Martinez ¹⁶⁵, A.M. Carroll ¹²⁴, N. Cartalade ⁴⁰, M.P. Casado ^{13,h}, A. Casali ⁵⁸,
 P. Casolaro ^{71a,71b}, M. Caspar ⁴⁷, F. Cassinese ⁹⁰, F. Castiglioni ^{73a,73b}, W.R. Castiglioni ³⁹,
 F.L. Castillo ⁴, V. Castillo Gimenez ¹⁶⁵, N.F. Castro ^{131a,131e}, A. Catinaccio ³⁷, J.R. Catmore ¹²⁶,
 T. Cavaliere ⁴, V. Cavaliere ³⁰, E. Celebi ⁸⁰, S. Cella ³⁰, V. Cepaitis ⁵⁵, K. Cerny ¹²³,
 A.S. Cerqueira ^{81a}, A. Cerri ^{73a,ap}, L. Cerrito ^{75a,75b}, F. Cerutti ^{18a}, B. Cervato ^{70a,70b},
 A. Cervelli ^{24b}, G. Cesarini ⁵², S.A. Cetin ⁸⁰, V.C. Chabalala ^{34j}, P.M. Chabrilat ¹²⁸,
 R. Chakkappai ⁶⁵, S. Chakraborty ¹⁶⁹, A. Chambers ⁶⁰, J. Chan ^{18a}, J.D. Chapman ³³,
 E. Chapon ¹³⁶, D.G. Charlton ²¹, C. Chauhan ¹³², Y. Che ^{112a}, S. Chekanov ⁶,
 G.A. Chelkov ^{38,a}, H. Chen ³⁰, J. Chen ¹⁴⁵, M. Chen ⁵⁹, S. Chen ⁸⁷, S.J. Chen ^{112a},
 X. Chen ^{141a}, X. Chen ^{15,ai}, Z. Chen ⁶¹, C.L. Cheng ¹⁴⁶, H.C. Cheng ^{63a}, S. Cheong ¹⁴⁶,
 A. Cheplakov ³⁸, E. Cherepanova ¹¹⁶, E. Cheu ⁷, K. Cheung ⁶⁴, L. Chevalier ¹³⁶,
 G. Chiarelli ^{73a}, G. Chiodini ^{69a}, A.S. Chisholm ²¹, J.L. Chisholm ¹⁶⁶, A. Chitan ^{28b},
 M. Chitishvili ¹⁶⁵, M.V. Chizhov ^{38,r}, K. Chmiel ^{76a,76b}, K. Choi ¹¹, Y. Chou ¹⁴⁰,
 E.Y.S. Chow ¹¹⁵, G. Christou ⁵¹, K.L. Chu ¹⁷¹, M.C. Chu ^{63a}, Z. Chubinidze ⁵², J. Chudoba ¹³²,
 J.J. Chwastowski ⁸⁶, D. Cieri ¹¹⁰, K.M. Ciesla ^{85a}, J.P. Cifuentes Salazar ^{23b}, V. Cindro ⁹³,
 A. Ciocio ^{18a}, F. Ciotto ^{71a,71b}, Z.H. Citron ¹⁷¹, M. Citterio ^{70a}, D.A. Ciubotaru ^{28b}, A. Clark ⁵⁵,
 P.J. Clark ⁵¹, N. Clarke Hall ³⁷, C. Clarry ¹⁵⁸, S.E. Clawson ³⁷, C. Clement ^{46a,46b},

L. Clissa ^{id}24b,24a, Y. Coadou ^{id}102, M. Cobal ^{id}68a,68c, A. Coccaro ^{id}56b, M.G. Cochran Branson ^{id}140, R.F. Coelho Barrue ^{id}131a, R. Coelho Lopes De Sa ^{id}103, S. Coelli ^{id}70a, M.M. Cohen ^{id}129, L.S. Colangeli ^{id}158, B. Cole ^{id}41, P. Collado Soto ^{id}99, J. Collot ^{id}59, M.R. Coluccia ^{id}69a, I. Combes ^{id}65, P. Conde Muiño ^{id}131a,131g, L.H.J. Condren ^{id}162, M.P. Connell ^{id}34c, S.H. Connell ^{id}34c, E.I. Conroy ^{id}161, M. Contreras Cossio ^{id}11, F. Conventi ^{id}71a,ak, A.M. Cooper-Sarkar ^{id}127, L. Corazzina ^{id}74a,74b, F.A. Corchia ^{id}24b,24a, A. Cordeiro Oudot Choi ^{id}140, L.D. Corpe ^{id}40, M. Corradi ^{id}74a,74b, F. Corriveau ^{id}104,ab, A. Cortes-Gonzalez ^{id}156, M.J. Costa ^{id}165, F. Costanza ^{id}4, D. Costanzo ^{id}142, J. Couthures ^{id}4, G. Cowan ^{id}95, K. Cranmer ^{id}172, L. Cremer ^{id}48, D. Cremonini ^{id}24b,24a, S. Crépe-Renaudin ^{id}59, F. Crescioli ^{id}128, T. Cresta ^{id}72a,72b, M. Cristinziani ^{id}144, M. Cristoforetti ^{id}77a,77b, T.M. Critchley ^{id}55, E. Critelli ^{id}96, A. Cueto ^{id}99, H. Cui ^{id}96, Z. Cui ^{id}7, B.M. Cunnett ^{id}149, W.R. Cunningham ^{id}58, E. Cuppini ^{id}110, F. Curcio ^{id}14, J.R. Curran ^{id}51, J.V. Da Fonseca Pinto ^{id}81b, C. Da Via ^{id}101, W. Dabrowski ^{id}85a, T. Dado ^{id}37, S. Dahbi ^{id}151, T. Dai ^{id}106, D. Dal Santo ^{id}20, C. Dallapiccola ^{id}103, M. Dam ^{id}42, G. D'amen ^{id}30, V. D'Amico ^{id}109, J.R. Dandoy ^{id}35, M. D'Andrea ^{id}56b,56a, D. Dannheim ^{id}37, G. D'anniballe ^{id}73a,73b, M. Danninger ^{id}145, V. Dao ^{id}148, G. Darbo ^{id}56b, F. Dattola ^{id}47, S. D'Auria ^{id}70a,70b, A. D'Avanzo ^{id}71a,71b, T. Davidek ^{id}134, J. Davidson ^{id}169, I. Dawson ^{id}94, K. De ^{id}8, C. De Almeida Rossi ^{id}158, S. De Castro ^{id}24b,24a, N. De Groot ^{id}115, P. de Jong ^{id}116, H. De la Torre ^{id}117, A. De Maria ^{id}112a, S. De Miranda Rimes ^{id}81d, A. De Salvo ^{id}74a, U. De Sanctis ^{id}75a,75b, F. De Santis ^{id}69a,69b, A. De Santo ^{id}149, J.B. De Vivie De Regie ^{id}59, K.G. De Vries ^{id}116, J. Debevc ^{id}93, D.V. Dedovich ^{id}38, J. Degens ^{id}92, A.M. Deiana ^{id}44, J. Del Peso ^{id}99, L. Delagrangé ^{id}27, F. Deliot ^{id}136, C.M. Delitzsch ^{id}48, M. Della Pietra ^{id}71a,71b, D. Della Volpe ^{id}55, A. Dell'Acqua ^{id}37, L. Dell'Asta ^{id}70a,70b, M. Delmastro ^{id}4, C.C. Delogu ^{id}56b,56a, P.A. Delsart ^{id}59, S. Demers ^{id}174, M. Demichev ^{id}38, H. Denizli ^{id}22a,1, M.G. Depala ^{id}92, L. D'Eramo ^{id}40, D. Derendarz ^{id}86, L. Derin ^{id}56b,56a, F. Derue ^{id}128, P. Dervan ^{id}92,* , A.M. Desai ^{id}1, K. Desch ^{id}25, F.A. Di Bello ^{id}73a,73b, A. Di Ciaccio ^{id}75a,75b, L. Di Ciaccio ^{id}4, D. Di Croce ^{id}37, C. Di Donato ^{id}71a,71b, A. Di Girolamo ^{id}37, G. Di Gregorio ^{id}65, A. Di Luca ^{id}77a,77b, B. Di Micco ^{id}76a,76b, R. Di Nardo ^{id}76a,76b, K.F. Di Petrillo ^{id}39, M. Diamantopoulou ^{id}154, F.A. Dias ^{id}116, M.A. Diaz ^{id}138a,138b, A.R. Didenko ^{id}38, M. Didenko ^{id}165, S.D. Diefenbacher ^{id}62a, E.B. Diehl ^{id}106, S. Díez Cornell ^{id}47, C. Díez Pardos ^{id}144, C. Dimitriadi ^{id}147, A. Dimitrievska ^{id}21, A. Dimri ^{id}148, Y. Ding ^{id}61, J. Dingfelder ^{id}25, T. Dingley ^{id}127, I-M. Dinu ^{id}28b, S.J. Dittmeier ^{id}62b, F. Dittus ^{id}37, M. Divisek ^{id}134, B. Dixit ^{id}92, F. Djama ^{id}102, T. Djobava ^{id}152b, C. Doglioni ^{id}101,98, A. Dohnalova ^{id}29a, Z. Dolezal ^{id}134, K. Domijan ^{id}85a, K.M. Dona ^{id}39, M. Donadelli ^{id}81d, B. Dong ^{id}107, J. Donini ^{id}40, A. D'Onofrio ^{id}71a,71b, M. D'Onofrio ^{id}92, J. Dopke ^{id}135, A. Doria ^{id}71a, N. Dos Santos Fernandes ^{id}131a, I.A. Dos Santos Luz ^{id}81e, P. Dougan ^{id}44, M.T. Dova ^{id}90, A.T. Doyle ^{id}58, M.P. Drescher ^{id}54, E. Dreyer ^{id}171, I. Drivas-koulouris ^{id}10, M. Drnevich ^{id}118, D. Du ^{id}61, T. Du ^{id}39, T.A. du Pree ^{id}116, Z. Duan ^{id}112a, M. Dubau ^{id}4, F. Dubinin ^{id}38, M. Dubovsky ^{id}29a, E. Duchovni ^{id}171, G. Duckeck ^{id}109, P.K. Duckett ^{id}96, O.A. Ducu ^{id}28b, D. Duda ^{id}51, A. Dudarev ^{id}37, M.M. Dudek ^{id}86, E.R. Duden ^{id}27, M. D'uffizi ^{id}101, L. Duflo ^{id}65, M. Dührssen ^{id}37, I. Duminica ^{id}28g, A.E. Dumitriu ^{id}28b, M. Dunford ^{id}62a, T. Duong ^{id}4, A. Duperrin ^{id}102, A.F. Duque Bran ^{id}40, H. Duran Yildiz ^{id}3a, A. Durglishvili ^{id}152b, G.I. Dyckes ^{id}18a, M. Dyndal ^{id}85a, B.S. Dziedzic ^{id}37, G.H. Eberwein ^{id}127, B. Eckerova ^{id}29a, J.C. Egan ^{id}96, S. Eggebrecht ^{id}54, E. Egidio Purcino De Souza ^{id}81e, G. Eigen ^{id}17, K. Einsweiler ^{id}18a, T. Ekelof ^{id}163, P.A. Ekman ^{id}98, S. El Farkh ^{id}36b, Y. El Ghazali ^{id}61, H. El Jarrari ^{id}104, A. El Moussaouy ^{id}36a, I. Elbaz ^{id}154, D. Elitez ^{id}37, M. Ellert ^{id}163, F. Ellinghaus ^{id}173, T.A. Elliot ^{id}95, J. Elmsheuser ^{id}30, M. Elsayy ^{id}83b, M. Elsing ^{id}37, D. Emelianov ^{id}135, Y. Enari ^{id}82, C. Engel ^{id}100, S. Epari ^{id}108, D. Ernani Martins Neto ^{id}86, F. Ernst ^{id}37, M. Escalier ^{id}65, C. Escobar ^{id}165, R. Estevam De Paula ^{id}81c, E. Etzion ^{id}154, G. Evans ^{id}131a,131b, H. Evans ^{id}67, L.S. Evans ^{id}47, S. Ezzarqtouni ^{id}36a, F. Fabbri ^{id}24b,24a, L. Fabbri ^{id}24b,24a, G. Facini ^{id}96, V. Fadeyev ^{id}137, D. Fakoudis ^{id}100, S. Falciano ^{id}74a,

L.F. Falda Ulhoa Coelho [ID](#)²⁷, F. Fallavollita [ID](#)¹¹⁰, G. Falsetti [ID](#)^{43b,43a}, J. Faltova [ID](#)¹³⁴, K.Y. Fan [ID](#)^{63b},
 Y. Fan [ID](#)¹⁴, Y. Fang [ID](#)^{14,112c}, M. Fanti [ID](#)^{70a,70b}, M. Faraj [ID](#)^{68a,68c}, Z. Farazpay [ID](#)⁹⁷, A. Farbin [ID](#)⁸,
 A. Farilla [ID](#)^{76a}, K. Farman [ID](#)¹⁵¹, J.N. Farr [ID](#)¹⁷⁴, M.S. Farrington [ID](#)⁶⁰, S.M. Farrington [ID](#)^{135,51},
 F. Fassi [ID](#)^{36e}, D. Fassouliotis [ID](#)⁹, L. Fayard [ID](#)⁶⁵, G. Fazzino [ID](#)^{62b}, P. Federic [ID](#)¹³⁴, P. Federicova [ID](#)¹³²,
 M. Feickert [ID](#)¹⁷², L. Feligioni [ID](#)¹⁰², D.E. Fellers [ID](#)^{18a}, C. Feng [ID](#)^{113b}, Y. Feng [ID](#)¹⁴, Z. Feng [ID](#)⁶⁵,
 B. Fernandez Barbadillo [ID](#)⁹¹, P. Fernandez Martinez [ID](#)⁶⁶, C. Fernandez Ruiz [ID](#)³³, J. Ferrando [ID](#)⁹¹,
 A. Ferrari [ID](#)¹⁶³, P. Ferrari [ID](#)^{116,115}, R. Ferrari [ID](#)^{72a}, D. Ferrere [ID](#)⁵⁵, C. Ferretti [ID](#)¹⁰⁶, M.P. Fewell [ID](#)¹,
 D. Fiacco [ID](#)^{74a,74b}, F. Fiedler [ID](#)¹⁰⁰, P. Fiedler [ID](#)¹³³, S. Filimonov [ID](#)³⁸, M.S. Filip [ID](#)^{28b,s},
 M. Filipig [ID](#)^{68a,68c}, A. Filipič [ID](#)⁹³, E.K. Filmer [ID](#)^{159a}, F. Filthaut [ID](#)¹¹⁵, M.C.N. Fiolhais [ID](#)^{131a,131c,c},
 L. Fiorini [ID](#)¹⁶⁵, W.C. Fisher [ID](#)¹⁰⁷, T. Fitschen [ID](#)¹⁰¹, I. Fleck [ID](#)¹⁴⁴, P. Fleischmann [ID](#)¹⁰⁶, T. Flick [ID](#)¹⁷³,
 M. Flores [ID](#)^{34d,ag}, L.R. Flores Castillo [ID](#)^{63a}, M. Foll [ID](#)¹²⁶, F.M. Follega [ID](#)^{77a,77b}, N. Fomin [ID](#)³³,
 A. Formica [ID](#)¹³⁶, M. Fornasiero [ID](#)¹⁴⁹, A.C. Forti [ID](#)¹⁰¹, N. Forti [ID](#)^{24b,24a}, E. Fortin [ID](#)¹⁰²,
 A.W. Fortman [ID](#)^{18a}, L. Foster [ID](#)^{18a}, L. Fountas [ID](#)⁹, H. Fox [ID](#)⁹¹, P. Francavilla [ID](#)^{73a,73b},
 S. Francescato [ID](#)⁶⁰, S. Franchellucci [ID](#)²⁰, M. Franchini [ID](#)^{24b,24a}, S. Franchino [ID](#)^{62a}, D. Francis [ID](#)³⁷,
 L. Franco [ID](#)⁴⁷, L. Franconi [ID](#)⁴⁷, M. Franklin [ID](#)⁶⁰, G. Frattari [ID](#)³⁷, Y.Y. Frid [ID](#)¹⁵⁴, N. Fritzsche [ID](#)³⁷,
 A. Froch [ID](#)⁵⁵, D. Froidevaux [ID](#)³⁷, J.A. Frost [ID](#)¹³⁵, Y. Fu [ID](#)¹⁰⁷, S. Fuenzalida Garrido [ID](#)^{138g},
 Y.C. Fujikake [ID](#)¹³⁷, M. Fujimoto [ID](#)¹⁴⁸, K.Y. Fung [ID](#)^{63a}, E. Furtado De Simas Filho [ID](#)^{81e},
 M. Furukawa [ID](#)¹⁵⁶, M. Fuste Costa [ID](#)⁴⁷, P. Fuste Martin [ID](#)¹³, J. Fuster [ID](#)¹⁶⁵, A. Gaa [ID](#)⁵⁴,
 A. Gabrielli [ID](#)^{24b,24a}, A. Gabrielli [ID](#)¹⁵⁸, G. Gagliardi [ID](#)^{56b,56a}, L.G. Gagnon [ID](#)¹⁴⁶, S. Galantzan [ID](#)¹⁵⁴,
 J. Gallagher [ID](#)¹, E.J. Gallas [ID](#)¹²⁷, A.L. Gallen [ID](#)¹⁶³, B.J. Gallop [ID](#)¹³⁵, K.K. Gan [ID](#)¹²⁰, Y. Gao [ID](#)⁵¹,
 Z. Gao [ID](#)^{112a}, A. Garabaglu [ID](#)¹⁴⁰, F.M. Garay Walls [ID](#)^{138a,138b}, C. García [ID](#)¹⁶⁵, A. Garcia Alonso [ID](#)¹¹⁶,
 A.G. Garcia Caffaro [ID](#)¹⁷⁴, J.E. García Navarro [ID](#)¹⁶⁵, M.A. Garcia Ruiz [ID](#)^{23b}, M. Garcia-Sciveres [ID](#)^{18a},
 G.L. Gardner [ID](#)¹²⁹, R.W. Gardner [ID](#)³⁹, N. Garelli [ID](#)¹⁶¹, R.B. Garg [ID](#)¹⁴⁶, J.M. Gargan [ID](#)³³, C.A. Garner [ID](#)¹⁵⁸,
 C.M. Garvey [ID](#)^{34a}, V.K. Gassmann [ID](#)¹⁶¹, G. Gaudio [ID](#)^{72a}, A.J. Gavin [ID](#)⁹⁴, J. Gavranovic [ID](#)⁹³,
 I.L. Gavrilenko [ID](#)^{131a}, C. Gay [ID](#)¹⁶⁶, G. Gaycken [ID](#)¹²⁴, A. Gekow [ID](#)¹²⁰, C. Gemme [ID](#)^{56b}, M.H. Genest [ID](#)⁵⁹,
 A.D. Gentry [ID](#)¹¹⁴, S. George [ID](#)⁹⁵, T. Geralis [ID](#)⁴⁵, A.A. Gerwin [ID](#)¹²¹, P. Gessinger-Befurt [ID](#)³⁷,
 M. Ghani [ID](#)¹⁶⁹, K. Ghorbanian [ID](#)⁹⁴, A. Ghosal [ID](#)¹⁴⁴, A. Ghosh [ID](#)¹⁶², A. Ghosh [ID](#)⁷, B. Giacobbe [ID](#)^{24b},
 S. Giagu [ID](#)^{74a,74b}, A. Giannini [ID](#)⁶¹, S.M. Gibson [ID](#)⁹⁵, D.T. Gil [ID](#)^{85b}, B.J. Gilbert [ID](#)⁴¹, D. Gillberg [ID](#)³⁵,
 G. Gilles [ID](#)¹¹⁶, D.M. Gingrich [ID](#)^{2,aj}, M.P. Giordani [ID](#)^{68a,68c}, P.F. Giraud [ID](#)¹³⁶, G. Giugliarelli [ID](#)^{68a,68c},
 D. Giugni [ID](#)^{70a}, F. Giuli [ID](#)^{75a,75b,al}, I. Gkialas [ID](#)^{9,i}, B.C. Gladwyn [ID](#)¹²⁷, C. Glasman [ID](#)⁹⁹,
 M. Glazewska [ID](#)²⁰, R.M. Gleason [ID](#)¹⁶², G. Glemža [ID](#)⁴⁷, I. Gnesi [ID](#)^{24b,24a,am}, Y. Go [ID](#)³⁰,
 M. Goblirsch-Kolb [ID](#)³⁷, B. Gocke [ID](#)⁴⁸, D. Godin [ID](#)¹⁰⁸, B. Gokturk [ID](#)^{22a}, S. Goldfarb [ID](#)¹⁰⁵, T. Golling [ID](#)⁵⁵,
 M.G.D. Gololo [ID](#)^{34c}, A. Golub [ID](#)¹⁴⁰, J.P. Gombas [ID](#)¹⁰⁷, A. Gomes [ID](#)^{131a,131b}, G. Gomes Da Silva [ID](#)¹⁴⁴,
 A.J. Gomez Delegido [ID](#)³⁷, R. Gonçalo [ID](#)^{131a}, A. Gongadze [ID](#)^{152c}, F. Gonnella [ID](#)²¹, J.L. Gonski [ID](#)¹⁴⁶,
 R.Y. González Andana [ID](#)⁵¹, S. González de la Hoz [ID](#)¹⁶⁵, M.V. Gonzalez Rodrigues [ID](#)⁴⁷,
 R. Gonzalez Suarez [ID](#)¹⁶³, S. Gonzalez-Sevilla [ID](#)⁵⁵, L. Goossens [ID](#)³⁷, B. Gorini [ID](#)³⁷, E. Gorini [ID](#)^{69a,69b},
 A. Gorišek [ID](#)⁹³, T.C. Gosart [ID](#)¹²⁹, A.T. Goshaw [ID](#)⁵⁰, M.I. Gostkin [ID](#)³⁸, S. Goswami [ID](#)¹²²,
 C.A. Gottardo [ID](#)³⁷, S.A. Gotz [ID](#)¹⁰⁹, M. Gouighri [ID](#)^{36b}, A.G. Goussiou [ID](#)¹⁴⁰, N. Govender [ID](#)^{34c},
 R.P. Grabarczyk [ID](#)¹²⁷, I. Grabowska-Bold [ID](#)^{85a}, K. Graham [ID](#)³⁵, E. Gramstad [ID](#)¹²⁶,
 S. Grancagnolo [ID](#)^{69a,69b}, C.M. Grant [ID](#)¹, P.M. Gravila [ID](#)^{28f}, F.G. Gravili [ID](#)^{69a,69b}, H.M. Gray [ID](#)^{18a},
 M. Greco [ID](#)¹¹⁰, M.J. Green [ID](#)¹, C. Grefe [ID](#)²⁵, A.S. Grefsrud [ID](#)³⁷, I.M. Gregor [ID](#)⁴⁷, K.T. Greif [ID](#)¹⁶²,
 P. Grenier [ID](#)¹⁴⁶, S.G. Grewe [ID](#)¹¹⁰, K. Grimm [ID](#)³², S. Grinstein [ID](#)^{13,x}, E. Gross [ID](#)¹⁷¹, J. Grosse-Knetter [ID](#)⁵⁴,
 L.H. Grossman [ID](#)^{18b}, L. Guan [ID](#)¹⁰⁶, G. Guerrieri [ID](#)³⁷, R. Guevara [ID](#)¹²⁶, R. Gugel [ID](#)¹⁰⁰,
 J.A.M. Guhit [ID](#)¹⁰⁶, A. Guida [ID](#)¹⁹, E. Guilloton [ID](#)¹⁶⁹, S. Guindon [ID](#)³⁷, F. Guo [ID](#)^{14,112c}, J. Guo [ID](#)^{141a},
 L. Guo [ID](#)⁴⁷, L. Guo [ID](#)^{112b,u}, Y. Guo [ID](#)¹⁰⁶, Y. Guo [ID](#)⁴¹, A. Gupta [ID](#)⁴⁸, R. Gupta [ID](#)¹³⁰, S. Gupta [ID](#)²⁷,
 S. Gurbuz [ID](#)²⁵, S.S. Gurdasani [ID](#)⁴⁷, G. Gustavino [ID](#)^{74a,74b}, P. Gutierrez [ID](#)¹²¹,
 L.F. Gutierrez Zagazeta [ID](#)¹²⁹, M. Gutsche [ID](#)⁴⁹, C. Gutschow [ID](#)⁹⁶, W. Guérin [ID](#)⁸⁹, C. Gwenlan [ID](#)¹²⁷,

C.B. Gwilliam ^{id}92, E.S. Haaland ^{id}126, A. Haas ^{id}118, M. Habedank ^{id}58, C. Haber ^{id}18a,
 R.J. Haberle ^{id}171, H.K. Hadavand ^{id}8, A. Haddad ^{id}40, A. Hadeef ^{id}49, K.E. Haeussler ^{id}53,
 A.I. Hagan ^{id}91, J.J. Hahn ^{id}144, M. Haleem ^{id}168, J. Haley ^{id}122, G.D. Hallewell ^{id}102, J.A. Hallford ^{id}47,
 H. Hamdaoui ^{id}163, M. Hamer ^{id}25, S.E.D. Hammoud ^{id}65, E.J. Hampshire ^{id}95, L. Han ^{id}112a, L. Han ^{id}61,
 S. Han ^{id}14, K. Hanagaki ^{id}82, M. Hance ^{id}137, D.A. Hangal ^{id}41, H. Hanif ^{id}145, M.D. Hank ^{id}129,
 J.B. Hansen ^{id}42, P.H. Hansen ^{id}42, T. Harenberg ^{id}173, S. Harkusha ^{id}175, M.L. Harris ^{id}103,
 Y.T. Harris ^{id}25, J. Harrison ^{id}13, P.F. Harrison ^{id}169, M.L.E. Hart ^{id}96, N.M. Hartman ^{id}110,
 N.M. Hartmann ^{id}109, R.Z. Hasan ^{id}95,135, Y. Hasegawa ^{id}143, D. Hashimoto ^{id}111, F. Haslbeck ^{id}37,
 S. Hassan ^{id}126, R. Hauser ^{id}107, M. Haviernik ^{id}134, C.M. Hawkes ^{id}21, R.J. Hawkings ^{id}37,
 Y. Hayashi ^{id}156, D. Hayden ^{id}107, R.L. Hayes ^{id}116, C.P. Hays ^{id}127, J.M. Hays ^{id}94, H.S. Hayward ^{id}92,
 M. He ^{id}14,112c, Y. He ^{id}47, Y. He ^{id}96, V. Hedberg ^{id}98, J. Heilman ^{id}35, S. Heim ^{id}47, T. Heim ^{id}18a,
 J.J. Heinrich ^{id}124, L. Heinrich ^{id}110, J. Hejbal ^{id}132, M. Helbig ^{id}49, A. Held ^{id}172, S. Hellesund ^{id}17,
 C.M. Helling ^{id}166, F.N.E. Henry ^{id}58, H. Herde ^{id}98, Y. Hernández Jiménez ^{id}148, G. Hertén ^{id}53,
 R. Herténberger ^{id}109, L. Hervás ^{id}37, M.E. Hesping ^{id}100, N.P. Hessey ^{id}159a, J. Hessler ^{id}110,
 R. Hicks ^{id}129, M. Hidaoui ^{id}36b, N. Hidic ^{id}134, E. Hill ^{id}158, T.S. Hillersoy ^{id}17, S.J. Hillier ^{id}21,
 J.R. Hinds ^{id}107, F. Hinterkeuser ^{id}25, M. Hirose ^{id}125, S. Hirose ^{id}170, D. Hirschbuehl ^{id}173, B. Hiti ^{id}93,
 J. Hobbs ^{id}148, R. Hobincu ^{id}28e, N. Hod ^{id}171, A.M. Hodges ^{id}164, M.C. Hodgkinson ^{id}142,
 B.H. Hodgkinson ^{id}37, A. Hoecker ^{id}37, D.D. Hofer ^{id}106, J. Hofer ^{id}165, J. Hofner ^{id}100, M. Holzbock ^{id}37,
 L.B.A.H. Hommels ^{id}33, V. Homsak ^{id}127, J.J. Hong ^{id}67, T.M. Hong ^{id}130, R. Honscheid ^{id}127,
 B.H. Hooberman ^{id}164, W.H. Hopkins ^{id}6, M.C. Hoppesch ^{id}164, Y. Horii ^{id}111, M.E. Horstmann ^{id}110,
 M.M. Horzela ^{id}54, S. Hou ^{id}151, M.R. Housenga ^{id}164, J. Howarth ^{id}58, J. Hoya ^{id}6, M. Hrabovsky ^{id}123,
 T. Hryn'ova ^{id}4, P.J. Hsu ^{id}64, S.-C. Hsu ^{id}140, T. Hsu ^{id}65, M. Hu ^{id}18a, P. Hu ^{id}63b, Q. Hu ^{id}61,
 S. Huang ^{id}33, X. Huang ^{id}14,112c, Y. Huang ^{id}134, Y. Huang ^{id}112b, Y. Huang ^{id}14, Z. Huang ^{id}65,
 Z. Hubacek ^{id}133, F. Huegging ^{id}25, T.B. Huffman ^{id}127, M. Hufnagel Maranha De Faria ^{id}81a,
 C.A. Hugli ^{id}47, M. Huhtinen ^{id}37, S.K. Huiberts ^{id}17, R. Hulsken ^{id}104, C.E. Hultquist ^{id}18a,
 D.L. Humphreys ^{id}103, N. Huseynov ^{id}12, J. Huston ^{id}107, B. Huth ^{id}37, J. Huth ^{id}60, L. Huth ^{id}47,
 R. Hyneman ^{id}7, G. Iacobucci ^{id}55, G. Iakovidis ^{id}30, L. Iconomidou-Fayard ^{id}65, J.P. Iddon ^{id}165,
 P. Iengo ^{id}71a,71b, Y. Iiyama ^{id}156, T. Iizawa ^{id}156, Y. Ikegami ^{id}82, D. Iliadis ^{id}155, N. Ilic ^{id}158,
 H. Imam ^{id}36a, G. Inacio Goncalves ^{id}81d, S.A. Infante Cabanas ^{id}138c, T. Ingebretsen Carlson ^{id}46a,46b,
 J.M. Inglis ^{id}94, G. Introzzi ^{id}72a,72b, M. Iodice ^{id}76a, V. Ippolito ^{id}74a,74b, R.K. Irwin ^{id}92, M. Ishino ^{id}156,
 W. Islam ^{id}172, C. Issever ^{id}19, O.N. Istantia ^{id}65,b, S. Istin ^{id}22a,ar, K. Itabashi ^{id}125, H. Ito ^{id}170,
 R. Iuppa ^{id}77a,77b, A. Ivina ^{id}171, F. Ivone ^{id}37, S. Izumiyama ^{id}111, V. Izzo ^{id}71a, P. Jacka ^{id}133,
 P. Jackson ^{id}1, P.R. Jacobson ^{id}50, P. Jain ^{id}47, K. Jakobs ^{id}53, J. Jamieson ^{id}58, W. Jang ^{id}156,
 S. Jankovych ^{id}116, B.K. Jashal ^{id}135, M. Javurkova ^{id}103, P. Jawahar ^{id}101, L. Jeanty ^{id}124,
 J. Jejelava ^{id}152a,ae, P. Jenni ^{id}53,f, L. Jerala ^{id}93, C.E. Jessiman ^{id}35, H. Jia ^{id}166, J. Jia ^{id}148, K. Jia ^{id}146,
 X. Jia ^{id}110,112c, C. Jiang ^{id}51, D.G. Jiang ^{id}164, Q. Jiang ^{id}63b, S. Jiggins ^{id}47, M. Jimenez Ortega ^{id}165,
 J. Jimenez Pena ^{id}13, S. Jin ^{id}112a, A. Jinaru ^{id}28b, O. Jinnouchi ^{id}139, P. Johansson ^{id}142, K.A. Johns ^{id}7,
 J.W. Johnson ^{id}137, F.A. Jolly ^{id}47, D.M. Jones ^{id}149, E. Jones ^{id}47, P. Jones ^{id}33, R.W.L. Jones ^{id}91,
 T.J. Jones ^{id}92, H.L. Joos ^{id}37, R. Joshi ^{id}120, J. Jovicevic ^{id}16, X. Ju ^{id}18a, J.J. Jungburth ^{id}37,
 T. Junkermann ^{id}62a, A. Juste Rozas ^{id}13,x, M.K. Juzek ^{id}86, S. Kabana ^{id}138f, A. Kaczmarska ^{id}86,
 S.A. Kadir ^{id}146, M. Kado ^{id}110, P. Kafle ^{id}107, H. Kagan ^{id}120, M. Kagan ^{id}146, A. Kahn ^{id}129,
 C. Kahra ^{id}100, T. Kaji ^{id}156, E. Kajomovitz ^{id}153, N. Kakati ^{id}171, N. Kakoty ^{id}13, S. Kandel ^{id}8,
 E. Kanellaki ^{id}45, N. Kanellos ^{id}10, S. Kang ^{id}50, D. Kar ^{id}34j,* , E. Karentzos ^{id}25, K. Karki ^{id}8,
 O. Karkout ^{id}116, S.N. Karpov ^{id}38, Z.M. Karpova ^{id}38, V. Kartvelishvili ^{id}91,152b, E. Kasimi ^{id}155,
 S. Katsarov ^{id}47, J. Katzy ^{id}47, S. Kaur ^{id}35, R. Kavak ^{id}37, K. Kawade ^{id}143, M.P. Kawale ^{id}121,
 C. Kawamoto ^{id}87, E.F. Kay ^{id}37, S. Kazakos ^{id}107, K. Kazakova ^{id}102, J.M. Keaveney ^{id}34a,
 R. Keeler ^{id}167, G.V. Kehris ^{id}60, J.S. Keller ^{id}35, J.M. Kelly ^{id}167, J.I. Kelsey ^{id}164, K. Kemp ^{id}1,

J.J. Kempster ¹⁴⁹, O. Kepka ¹³², J. Kerr ^{159b}, B.P. Kerridge ¹³⁵, B.P. Kerševan ⁹³,
 L. Keszeghova ^{29a}, M.B. Khan ⁹³, R.A. Khan ¹³⁰, A. Khanov ¹²², M. Kholodenko ^{131a},
 T.J. Khoo ¹⁹, G. Khoriali ¹⁶⁸, Y. Khouli ^{36a}, Y.A.R. Khwaira ¹²⁸, D. Kim ⁶, D.W. Kim ^{18b},
 Y.K. Kim ³⁹, N. Kimura ⁹⁶, M.K. Kingston ⁵⁴, F. Kirfel ²⁵, J. Kirk ¹³⁵, A.E. Kiryunin ¹¹⁰,
 S. Kita ¹⁵⁶, O. Kivernyk ²⁵, M. Klassen ³⁷, C. Klein ³⁵, L. Klein ¹⁶⁸, M.H. Klein ⁴⁴,
 U. Klein ⁹², A. Klimentov ³⁰, P. Kluit ¹¹⁶, S. Kluth ¹¹⁰, E. Kneringer ⁷⁸, T.M. Knight ¹⁵⁸,
 A. Knue ⁴⁸, M. Kobel ⁴⁹, D. Kobylanski ¹⁷¹, S.F. Koch ³⁷, M. Kocian ¹⁴⁶, P. Kodyš ¹³⁴,
 D.M. Koeck ¹²⁴, T. Koffas ³⁵, K. Kojima ⁸², O. Kolay ⁴⁹, I. Koletsou ⁴, T. Komarek ⁸⁶,
 S. Kondo ¹⁵⁶, K. Köneke ⁵⁴, A.X.Y. Kong ¹, T. Kono ¹¹⁹, N. Konstantinidis ⁹⁶,
 P. Kontaxakis ⁵⁵, B. Konya ⁹⁸, R. Kopeliansky ⁴¹, S. Koperny ^{85a}, R. Koppenhofer ⁵³,
 I. Kopsalis ¹⁰, K. Korcyl ⁸⁶, K. Kordas ^{155,d}, A. Korn ⁹⁶, S. Korn ⁵⁴, I. Korolkov ¹³,
 O. Kortner ¹¹⁰, S. Kortner ¹¹⁰, W.H. Kostecka ¹¹⁷, M. Kostov ^{29a}, V.V. Kostyukhin ¹⁴⁴,
 A. Kotsokechagia ³⁷, A. Kotwal ⁵⁰, A. Koulouris ³⁷, A. Kourkoumeli-Charalampidi ^{72a,72b},
 O. Kovanda ¹²⁴, R. Kowalewski ¹⁶⁷, W. Kozanecki ¹²⁴, G. Kramberger ⁹³, P. Kramer ²⁵,
 A. Krasznahorkay ¹⁰³, A.C. Kraus ¹¹⁷, J.W. Kraus ¹⁷³, J.A. Kremer ⁴⁷, N.B. Krengel ¹⁴⁴,
 T. Kresse ¹⁵⁸, L. Kretschmann ¹⁷³, J. Kretschmar ⁹², P. Krieger ¹⁵⁸, K. Krizka ²¹,
 K. Kroeninger ⁴⁸, H. Kroha ¹¹⁰, J. Kroll ¹³², J. Kroll ¹²⁹, K.S. Krowpman ¹⁰⁷, U. Kruchonak ³⁸,
 H. Krüger ²⁵, N. Krumnack ⁷⁹, J. Krupa ¹⁴⁶, M.C. Kruse ⁵⁰, O. Kuchinskaia ³⁸, S. Kuday ^{3a},
 S. Kuehn ³⁷, R. Kuesters ⁵³, T. Kuhl ⁴⁷, V. Kukhtin ³⁸, Y. Kulchitsky ³⁸, S. Kuleshov ^{138d,138b},
 J. Kull ¹, E.V. Kumar ¹⁰⁹, M. Kumar ^{34j}, N. Kumari ⁴⁷, P. Kumari ^{159b}, A. Kupco ¹³²,
 O. Kuprash ⁵³, H. Kurashige ⁸⁴, L.L. Kurchaninov ^{159a}, O. Kurdysh ⁴, M. Kuze ¹³⁹,
 A.K. Kvam ¹⁰³, J. Kvita ¹²³, N.G. Kyriacou ¹⁴⁰, M. Laassiri ³⁰, C. Lacasta ¹⁶⁵, H. Lacker ¹⁹,
 D. Lacour ¹²⁸, E. Ladygin ³⁸, A. Lafarge ⁴⁰, B. Laforge ¹²⁸, T. Lagouri ¹⁷⁴, F.Z. Lahbabi ^{36a},
 S. Lai ⁵⁴, W.S. Lai ⁹⁶, I.K. Lakomic ⁵⁴, J.E. Lambert ¹⁶⁷, S. Lammers ⁶⁷, W. Lampl ⁷,
 C. Lampoudis ¹⁵⁵, G. Lamprinoudis ¹⁶⁸, A.N. Lancaster ¹¹⁷, U. Landgraf ⁵³, M.P.J. Landon ⁹⁴,
 V.S. Lang ⁵³, A.J. Lankford ¹⁶², F. Lanni ³⁷, C.S. Lantz ¹⁶⁴, K. Lantzsch ²⁵, A. Lanza ^{72a},
 M. Lanzac Berrocal ¹⁶⁵, T. Lari ^{70a}, D. Larsen ¹⁷, L. Larson ¹¹, F. Lasagni Manghi ^{24b},
 M. Lassnig ³⁷, H.C. Lau ¹⁶⁷, S.D. Lawlor ¹⁴², R. Lazaridou ¹⁶², M. Lazzaroni ^{70a,70b},
 E.T.T. Le ¹⁶², H.D.M. Le ¹⁰⁷, E.M. Le Boulicaut ¹⁷⁴, D.O. Le Guennec ¹³⁶, L.T. Le Pottier ^{18a},
 B. Leban ^{24b,24a}, F. Ledroit-Guillon ⁵⁹, T.F. Lee ^{159b}, L.L. Leeuw ^{34h}, M. Lefebvre ¹⁶⁷,
 C. Leggett ^{18a}, L.M. Lehmann ¹¹⁶, W.A. Leight ¹⁰³, W. Leinonen ¹¹⁵, A. Leisos ^{155,t},
 M.A.L. Leite ^{81c}, C.E. Leitgeb ¹⁹, R. Leitner ¹³⁴, E. Lelak ¹³⁴, K.J.C. Leney ⁴⁴, T. Lenz ²⁵,
 S. Leone ^{73a}, C. Leonidopoulos ⁵¹, A. Leopold ¹⁴⁷, J. LePage-Bourbonnais ³⁵, R. Les ⁶⁵,
 C.G. Lester ³³, J. Levêque ⁴, L.J. Levinson ¹⁷¹, G. Levrini ^{24b,24a}, M.P. Lewicki ⁸⁶, C. Lewis ¹⁴⁰,
 D.J. Lewis ⁴, L. Lewitt ¹⁴², A. Li ³⁰, B. Li ^{113b}, C. Li ¹⁰⁶, C. Li ⁶¹, C-Q. Li ¹¹⁰, H. Li ^{113b},
 H. Li ¹⁰¹, H. Li ¹⁵, H. Li ⁶¹, H. Li ^{113b}, J. Li ^{141a}, L. Li ^{141a}, R. Li ¹⁷⁴, S. Li ^{141b,141a}, Y. Li ¹⁴,
 Z. Li ^{14,112c}, Z. Li ⁶¹, S. Liang ^{14,112c}, Z. Liang ¹⁴, M. Liberatore ¹³⁶, B. Liberti ^{75a},
 G.B. Libotte ^{81d}, K. Lie ^{63c}, J. Lieber Marin ^{81e}, H. Lien ⁶⁷, H. Lin ¹⁰⁶, S.F. Lin ¹⁴⁸,
 L. Linden ¹⁰⁹, R.E. Lindley ⁷, J.H. Lindon ³⁷, J. Ling ⁶⁰, M. Linkert ¹⁰⁰, E. Lipeles ¹²⁹,
 A. Lipniacka ¹⁷, A. Lister ¹⁶⁶, J.D. Little ⁶⁷, B. Liu ^{113a}, B.X. Liu ^{112b}, D. Liu ¹⁵³, D. Liu ¹³⁷,
 E.H.L. Liu ²¹, H. Liu ^{112b}, J.K.K. Liu ¹¹⁸, K. Liu ^{141b}, K. Liu ^{141b}, M. Liu ⁶¹, M.Y. Liu ⁶¹,
 P. Liu ^{113b}, Q. Liu ¹⁴⁶, S. Liu ¹⁴⁸, X. Liu ^{113b}, Y. Liu ^{112b,112c}, Y. Liu ¹⁶⁴, Y.L. Liu ^{113b},
 Y.W. Liu ⁶¹, Z. Liu ^{65j}, S.L. Lloyd ⁹⁴, E.M. Lobodzinska ⁴⁷, P. Loch ⁷, E. Lodhi ¹⁵⁸,
 K. Lohwasser ¹⁴², E. Loiacono ¹²², J.D. Lomas ²¹, I. Longarini ¹⁶², R. Longo ^{24b,24a,am},
 A. Lopez Solis ¹³, N.A. Lopez-canelas ⁷, N. Lorenzo Martinez ⁴, A.M. Lory ¹⁰⁹, M. Losada ^{83b},
 G. Löschke Centeno ⁴, X. Lou ^{14,112c}, P.A. Love ⁹¹, H. Lu ¹⁴, M. Lu ⁶⁵, S. Lu ¹²⁹,
 Y.J. Lu ¹⁵¹, H.J. Lubatti ¹⁴⁰, C. Luci ^{74a,74b}, F.L. Lucio Alves ^{112a}, J.A. Lue ¹²⁴, F. Luehring ⁶⁷,




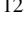





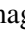








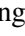

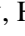


D. Lumb ¹³⁵, B.S. Lunday ¹²⁹, O. Lundberg ¹⁴⁷, J. Lunde ³⁷, N.A. Luongo ⁶, M.S. Lutz ¹⁵⁸,
 A.B. Lux ²⁶, D. Lynn ³⁰, R. Lysak ¹³², V. Lysenko ¹³³, E. Lytken ⁹⁸, V. Lyubushkin ³⁸,
 T. Lyubushkina ³⁸, M.M. Lyukova ¹⁴⁸, H. Ma ³⁰, K. Ma ⁶¹, L.L. Ma ^{113b}, W. Ma ⁶¹,
 Y. Ma ^{113b}, P.C. Machado De Abreu Farias ^{81e}, D. Macina ³⁷, R. Madar ⁴⁰, T. Madula ⁹⁶,
 J. Maeda ⁸⁴, S. Maeland ¹⁷, T. Maeno ³⁰, P.T. Mafa ^{34f}, G. Magni ⁶⁵, H. Maguire ¹⁴²,
 M. Maheshwari ³³, V. Maiboroda ⁶⁵, G. Maineri ^{70a,70b}, A. Maio ^{131a,131b,131d}, A. Maiza ¹⁶⁸,
 K. Maj ^{85a}, O. Majersky ⁴⁷, S. Majewski ¹²⁴, A. Makita ¹⁵⁶, N. Makovec ⁶⁵, V. Maksimovic ¹⁶,
 B. Malaescu ¹²⁸, J. Malamant ¹²⁶, Pa. Malecki ⁸⁶, F. Malek ^{59,n}, M. Mali ⁹³, D. Malito ⁹⁵,
 A. Maloizel ⁵, A. Malvezzi Lopes ^{81d}, S. Malyukov ³⁸, J. Mamuzic ⁹³, G. Mancini ⁵²,
 M.N. Mancini ²⁷, G. Manco ^{72a,72b}, S.S. Mandarry ¹⁴⁹, I. Mandić ⁹³,
 L. Manhaes de Andrade Filho ^{81a}, I.M. Maniatis ¹⁷¹, J. Manjarres Ramos ⁸⁹, D.C. Mankad ¹⁷¹,
 A. Mann ¹⁰⁹, T. Manoussos ¹⁰⁰, M.N. Mantinan ³⁹, S. Manzoni ³⁷, L. Mao ^{141a},
 X. Mapekula ^{34c}, A. Marantis ¹⁵⁵, R.R. Marcelo Gregorio ¹, G. Marchiori ⁵, C. Marcon ^{70a},
 E. Maricic ¹⁶, M. Marinescu ⁴⁷, S. Marium ⁴⁷, M. Marjanovic ¹²¹, A. Markhoos ⁵³,
 M. Markovitch ⁶⁵, M.K. Maroun ¹⁰³, M.C. Marr ¹⁴⁵, T.L. Marsault ¹³⁶, G.T. Marsden ¹⁰¹,
 Z. Marshall ^{18a}, S. Marti-Garcia ¹⁶⁵, J. Martin ⁹⁶, T.A. Martin ¹³⁵, V.J. Martin ⁵¹,
 B. Martin dit Latour ¹⁷, L. Martinelli ^{74a,74b}, V.I. Martinez Outschoorn ¹⁰³, P. Martinez Suarez ³⁷,
 S. Martin-Haugh ¹³⁵, G. Martinovicova ¹³⁴, V.S. Martoiu ^{28b}, A. Martone ⁸⁹, A.C. Martyniuk ⁹⁶,
 A. Marzin ³⁷, D. Mascione ^{77a,77b}, L. Masetti ¹⁰⁰, J. Masik ¹⁰¹, A.L. Maslennikov ³⁸,
 S.L. Mason ⁴¹, P. Massarotti ^{71a,71b}, P. Mastrandrea ^{73a,73b}, A. Mastroberardino ^{43b,43a},
 R. Mastrofrancesco ^{72a,72b}, T. Masubuchi ¹²⁵, T.T. Mathew ¹²⁴, J. Matousek ¹³⁴, D.M. Mattern ⁴⁸,
 K. Mauer ⁴⁷, J. Maurer ^{28b}, T. Maurin ⁵⁸, B. Maček ⁹³, C. Mavungu Tsava ¹⁰², A.E. May ¹⁰¹,
 E. Mayer ⁴⁰, R. Mazini ^{34j}, S.M. Mazza ¹³⁷, E. Mazzeo ³⁷, J.P. Mc Gowan ¹⁶⁷, S.P. Mc Kee ¹⁰⁶,
 C.C. McCracken ¹⁶⁶, E.F. McDonald ¹⁰⁵, L.F. Mcelhinney ⁹¹, J.A. Mcfayden ¹⁴⁹,
 R.P. McGovern ¹⁶⁷, R.P. Mckenzie ^{34j}, D.J. Mclaughlin ⁹⁶, S.J. McMahon ¹³⁵,
 C.M. Mcpartland ⁹², R.A. McPherson ^{167,ab}, S. Mehlhase ¹⁰⁹, A. Mehta ⁹², D. Melini ¹⁶⁵,
 B.R. Mellado Garcia ^{14,ah}, A.H. Melo ⁵⁴, F. Meloni ⁴⁷, A.M. Mendes Jacques Da Costa ¹⁰¹,
 L. Meng ⁹¹, S. Menke ¹¹⁰, M. Mentink ³⁷, E. Meoni ^{43b,43a}, G. Mercado ¹¹⁷, S. Merianos ¹⁵⁵,
 C. Merlassino ^{68a,68c}, C. Meroni ^{70a,70b}, J. Metcalfe ⁶, A.S. Mete ⁶, E. Meuser ¹⁰⁰, C. Meyer ⁶⁷,
 J-P. Meyer ¹³⁶, O. Mezhska ^{29b}, Y. Miao ^{112a}, R.P. Middleton ¹³⁵, M. Mihovilovic ⁶⁵,
 L. Mijović ⁵¹, G. Mikenberg ¹⁷¹, M. Mikestikova ¹³², M. Mikuž ⁹³, H. Mildner ¹⁰⁰, A. Milic ³⁷,
 D.W. Miller ³⁹, E.H. Miller ¹⁴⁶, A. Milov ¹⁷¹, D.A. Milstead ^{46a,46b}, T. Min ^{112a}, I.A. Minashvili ^{152b},
 A.I. Mincer ¹¹⁸, B. Mindur ^{85a}, M. Mineev ³⁸, L.M. Mir ¹³, M. Miralles Lopez ⁵⁸,
 M. Mironova ^{18a}, M. Missio ⁴⁰, A. Mitra ¹⁶⁹, P. Mitra ¹³, V.A. Mitsou ¹⁶⁵, P.S. Miyagawa ⁹⁴,
 R. Mizuhiki ⁸⁴, T. Mkrtychyan ³⁷, M. Mlinarevic ⁹⁶, T. Mlinarevic ⁹⁶, M. Mlynarikova ¹³⁴,
 L. Mlynarska ^{85a}, C. Mo ^{141a}, H. Mobius ⁴⁷, S. Mobius ²⁰, M.H. Mohamed Farook ¹¹⁴,
 S. Mohapatra ⁴¹, M.F. Mohd Soberi ⁵¹, S. Mohiuddin ¹²², G. Mokgatitswane ^{34j}, R. Mole ²¹,
 L. Moleri ¹⁷¹, U. Molinatti ¹²⁷, M.E. Mollerach ³¹, L.G. Mollier ²⁰, L. Monaco ^{37,58},
 B. Mondal ¹³², S. Mondal ¹³⁴, K. Mönig ⁴⁷, E. Monnier ¹⁰², L. Monsonis Romero ¹⁶⁵,
 A. Montella ^{46a,46b}, M. Montella ¹²⁰, F. Montekali ^{76a,76b}, F. Monticelli ⁹⁰, S. Monzani ^{68a,68c},
 M.E.E. Moors ²⁵, A. Morancho Tarda ⁴², N. Morange ⁶⁵, M. Moreno Llácer ¹⁶⁵,
 C. Moreno Martinez ⁵⁵, J.M. Moreno Perez ^{23b}, P. Morettini ^{56b}, S. Morgenstern ^{62a}, M. Morii ⁶⁰,
 M. Morinaga ¹⁵⁶, F. Morodei ^{74a,74b}, P. Moschovakos ³⁷, B. Moser ⁵³, M. Mosidze ^{152b},
 T. Moskalets ⁴⁴, P. Moskvitina ¹¹⁵, C.J. Mosomane ^{34b}, J. Moss ³², T. Motta Quirino ^{81d},
 A. Moussa ^{36d}, Y. Moyal ^{171,k}, H. Moyano Gomez ¹³, E.J.W. Moyse ¹⁰³, T.G. Mroz ⁸⁶,
 S. Muanza ¹⁰², M. Mucha ²⁵, P. Mucha ⁹⁶, J. Mueller ¹³⁰, B.J. Mughal ¹⁷, D. Muller ¹⁴⁴,
 G.A. Mullier ¹⁶³, A.J. Mullin ³³, J.J. Mullin ⁵⁰, A.C. Mullins ⁴⁴, A.E. Mulski ⁶⁰, D.P. Mungo ¹⁵⁸,

D. Munoz Perez ¹²², F.J. Munoz Sanchez ¹⁰¹, W.J. Murray ^{169,135}, E. Musajan ⁶¹,
 M. Muškinja ⁹³, C. Mwewa ⁴⁷, A.J. Myers ⁸, G. Myers ¹⁰⁶, M. Myska ¹³³, B.P. Nachman ¹⁴⁶,
 I.A. Nadas ^{28d}, K. Nagai ¹²⁷, K. Nagano ⁸², R. Nagasaka ¹⁵⁶, J.L. Nagle ^{30,ao}, E. Nagy ¹⁰²,
 A.M. Nairz ³⁷, T. Nakagawa ⁸⁷, Y. Nakahama ⁸², K. Nakamura ⁸², A. Nandi ^{62b}, H. Nanjo ¹²⁵,
 E.A. Narayanan ⁴⁴, V.A. Narendran ¹²⁷, Y. Narukawa ¹⁵⁶, L. Nasella ²⁷, S. Nasri ^{83c}, C. Nass ²⁵,
 G. Navarro ^{23a}, A. Nayaz ¹⁹, S. Nechaeva ^{24b,24a}, F. Nechansky ¹³², A. Negri ^{72a,72b},
 M. Negrini ^{24b}, C. Nellist ¹¹⁶, C. Nelson ¹⁰⁴, K. Nelson ¹⁰⁶, S. Nemecek ¹³², M. Nessi ^{37,g},
 M.S. Neubauer ¹⁶⁴, J. Newell ⁹², P.R. Newman ²¹, Y.W.Y. Ng ¹⁶⁴, B. Ngair ^{83b},
 H.D.N. Nguyen ¹⁰⁸, J.D. Nichols ¹²¹, R. Nicolaidou ¹³⁶, J. Nielsen ¹³⁷, M. Niemeyer ⁵⁴,
 J. Niermann ³⁷, N. Nikiforou ³⁷, I. Nikolic-Audit ¹²⁸, P. Nilsson ³⁰, G. Ninio ¹⁵⁴, A. Nisati ^{74a},
 D. Nishimura ¹⁵⁶, R. Nisius ¹¹⁰, N. Nitika ¹⁷¹, E.K. Nkadimeng ^{34j}, T. Nobe ¹⁵⁶, D. Noll ¹⁴⁶,
 T. Nommensen ¹⁵⁰, M.B. Norfolk ¹⁴², B.J. Norman ³⁵, L.C. Nosler ^{18a}, M. Noury ^{36a}, J. Novak ⁹³,
 T. Novak ⁹³, P. Novotny ¹⁷¹, R. Novotny ¹³³, L. Nozka ¹²³, K. Ntekas ³⁷, D. Ntounis ¹⁴⁶,
 N.M.J. Nunes De Moura Junior ^{81b}, J. Ocariz ¹²⁸, I. Ochoa ^{131a}, A. Odella Rodriguez ¹³,
 S. Oerdek ⁴⁷, A. Ogrodnik ⁸⁶, A. Oh ¹⁰¹, C.C. Ohm ¹⁴⁷, H. Oide ⁸², M.L. Ojeda ³⁷,
 Y. Okumura ¹⁵⁶, L.F. Oleiro Seabra ^{131a}, I. Oleksiyuk ⁵⁵, G. Oliveira Correa ¹³,
 D. Oliveira Damazio ³⁰, J.L. Oliver ¹, R. Omar ⁶⁷, A.P. O'Neill ²⁰, Y. Onoda ¹³⁹,
 A. Onofre ^{131a,131e,e}, P.U.E. Onyisi ¹¹, M.J. Oreglia ³⁹, D. Orestano ^{76a,76b}, R. Orlandini ^{76a,76b},
 R.S. Orr ¹⁵⁸, L.M. Osojnak ⁴¹, Y. Osumi ¹¹¹, G. Otero y Garzón ³¹, H. Otono ⁸⁸,
 M. Ouchrif ^{36d}, F. Ould-Saada ¹²⁶, T. Ovsianikova ¹⁴⁰, M. Owen ⁵⁸, R.E. Owen ¹³⁵,
 S.A. Oyeniran ¹¹⁴, V.E. Ozcan ^{22a}, F. Ozturk ⁸⁶, N. Ozturk ⁸, S. Ozturk ⁸⁰, H.A. Pacey ¹²⁷,
 K. Pachal ^{159a}, A. Pacheco Pages ¹³, C. Padilla Aranda ¹³, G. Padovano ^{74a,74b},
 S. Pagan Griso ^{18a}, L. Pagani ^{75a,75b}, J. Pampel ²⁵, D.K. Panchal ¹¹, C.E. Pandini ⁵⁹,
 J.G. Panduro Vazquez ¹³⁵, H.D. Pandya ¹, H. Pang ¹³⁶, P. Pani ⁴⁷, G. Panizzo ^{68a,68c},
 L. Panwar ^{128,w}, L. Paolozzi ²¹, S. Parajuli ¹⁶⁴, A. Paramonov ⁶, C. Paraskevopoulos ⁵²,
 D. Paredes Hernandez ^{63b}, S.R. Paredes Saenz ⁵¹, A. Pareti ^{72a,72b}, K.R. Park ⁴¹, T.H. Park ¹¹⁰,
 F. Parodi ^{56b,56a}, J.A. Parsons ⁴¹, J.A. Partridge ¹³⁷, U. Parzefall ⁵³, B.A. Paschen ^{18a},
 B. Pascual Dias ⁴⁰, L. Pascual Dominguez ⁹⁹, E. Pasqualucci ^{74a}, S. Passaggio ^{56b}, F. Pastore ⁹⁵,
 P. Patel ⁸⁶, U.M. Patel ⁵⁰, J.R. Pater ¹⁰¹, T. Pauly ³⁷, A. Paunovic ¹⁶, F. Pauwels ¹³⁴,
 C.I. Pazos ¹⁶¹, M. Pedersen ¹²⁶, R. Pedro ^{131a}, O. Penc ¹³², C.C. Penelaud ¹²⁸, S. Peng ¹⁵,
 G.D. Penn ¹⁷⁴, B.S. Peralva ^{81d}, A.P. Pereira Peixoto ¹⁴⁰, L. Pereira Sanchez ¹⁴⁶,
 D.V. Perpelitsa ^{30,ao}, G. Perera ¹⁰³, E. Perez Codina ³⁷, M. Perganti ¹⁰, H. Pernegger ³⁷,
 S. Perrella ^{74a,74b}, K. Peters ⁴⁷, R.F.Y. Peters ¹⁰¹, B.A. Petersen ³⁷, T.C. Petersen ⁴², E. Petit ¹⁰²,
 V. Petousis ¹³³, A.R. Petri ^{70a,70b}, V.A. Petrovic ⁹⁶, T. Petru ¹³⁴, M. Pettee ^{18a}, A. Petukhov ⁸⁰,
 K. Petukhova ³⁷, R. Pezoa ^{138g}, L. Pezzotti ^{24b,24a}, G. Pezzullo ¹⁷⁴, L. Pfaffenbichler ³⁷,
 A.J. Pflieger ⁷⁸, T.M. Pham ¹⁷², T. Pham ¹⁰⁵, P.W. Phillips ¹³⁵, G. Piacquadio ¹⁴⁸, E. Pianori ^{18a},
 F. Piazza ¹²⁴, R. Piegai ³¹, D. Pietreanu ^{28b}, A.D. Pilkington ¹⁰¹, T. Pilusa ^{34j},
 M. Pinamonti ^{68a,68c}, J.L. Pinfeld ², G. Pinheiro Matos ⁴¹, B.C. Pinheiro Pereira ^{131a},
 J. Pinol Bel ¹³, A.E. Pinto Pinoargote ¹²⁸, L. Pintucci ^{68a,68c}, K.M. Piper ¹⁴⁹, A. Pirttikoski ⁵⁵,
 D.A. Pizzi ³⁵, L. Pizzimento ^{63b}, A. Plebani ³³, M.-A. Pleier ³⁰, V. Pleskot ¹³⁴, E. Plotnikova ³⁸,
 G. Poddar ⁹⁴, R. Poettgen ⁹⁸, L. Poggioli ¹²⁸, N.A. Pohl ¹²⁰, S. Polacek ¹³⁴, G. Polesello ^{72a},
 A. Poley ¹⁴⁵, A. Polini ^{24b}, C.S. Pollard ¹⁶⁹, Z.B. Pollock ¹²⁰, E. Pompa Pacchi ¹²¹, N.I. Pond ⁹⁶,
 D. Ponomarenko ⁶⁷, L. Pontecorvo ³⁷, S. Popa ^{28a}, G.A. Popeneciu ^{28d}, A. Poreba ³⁷,
 D.M. Portillo Quintero ^{159a}, S. Pospisil ¹³³, M.A. Postill ¹⁴², P. Postolache ^{28c}, K. Potamianos ¹⁶⁹,
 P.A. Potepa ^{85a}, I.N. Potrap ³⁸, C.J. Potter ³³, H. Potti ¹⁵⁰, J. Poveda ¹⁶⁵,
 M.E. Pozo Astigarraga ³⁷, R. Pozzi ³⁷, A. Prades Ibanez ^{75a,75b}, S.R. Pradhan ¹⁴², J. Preston ⁹⁵,
 J. Pretel ¹⁶⁷, D. Price ¹⁰¹, M. Primavera ^{69a}, L. Primomo ^{68a,68c}, M.A. Principe Martin ⁹⁹,

R. Privara ¹²³, T. Procter ^{85b}, M.L. Proffitt ¹⁴⁰, N. Proklova ¹²⁹, K. Prokofiev ^{63c}, G. Proto ¹¹⁰, J. Proudfoot ⁶, M. Przybycien ^{85a}, W.W. Przygoda ^{85b}, A. Psallidas ⁴⁵, D. Pudzha ⁵², P. Puhl ⁵⁷, H.I. Purnell ¹, D. Pyatiizbyantseva ¹¹⁵, J. Qian ¹⁰⁶, R. Qian ¹⁰⁷, D. Qichen ¹²⁷, Y. Qin ¹³, T. Qiu ⁵¹, A. Quadt ⁵⁴, M. Queitsch-Maitland ¹⁰¹, G. Quetant ⁵⁵, R.P. Quinn ¹⁶⁶, D. Rafanoharana ¹¹⁰, J.L. Rainbolt ³⁹, S. Rajagopalan ³⁰, E. Ramakoti ³⁸, L. Rambelli ^{56b,56a}, I.A. Ramirez-Berend ³⁵, K. Ran ^{106,112c}, S.D. Randles ⁹², D.S. Rankin ¹²⁹, N.P. Rapheeha ^{34j}, H. Rasheed ^{28b}, A. Rastogi ^{18a}, S. Rave ¹⁰⁰, S. Ravera ^{56b,56a}, B. Ravina ³⁷, I. Ravinovich ¹⁷¹, M. Raymond ³⁷, A.L. Read ¹²⁶, N.P. Readioff ¹⁴², D.M. Rebuzzi ^{72a,72b}, A.S. Reed ⁵⁸, K. Reeves ²⁷, D. Reikher ³⁷, T. Reisch ⁵⁵, A. Rej ⁴⁸, H. Ren ⁶¹, M. Renda ^{28b}, F. Renner ⁴⁷, A.G. Rennie ⁵⁸, M. Repik ⁵⁵, A.L. Rescia ^{43b,43a}, S. Resconi ^{70a}, M. Ressegotti ^{56b}, S. Rettie ¹¹⁶, W.F. Rettie ³⁵, M.M. Revering ³³, O.L. Rezanova ³⁸, P. Reznicek ¹³⁴, H. Riani ^{36d}, N. Ribaric ³⁷, B. Ricci ^{68a,68c}, E. Ricci ^{77a,77b}, R. Richter ¹¹⁰, E. Richter-Was ^{85b}, M. Ridel ¹²⁸, S. Ridouani ^{36d}, P. Riedler ³⁷, E.M. Riefel ^{46a,46b}, J.O. Rieger ¹¹⁶, M. Rimoldi ^{34c}, L. Rinaldi ^{24b,24a}, P. Rincke ^{163,54}, G. Ripellino ¹⁶³, I. Riu ¹³, J.C. Rivera Vergara ¹⁶⁷, F. Rizatdinova ¹²², E. Rizvi ⁹⁴, B.R. Roberts ³⁹, S.S. Roberts ¹³⁷, D. Robinson ³³, A. Robson ⁵⁸, A. Rocchi ^{75a,75b}, C. Roda ^{73a,73b}, F.A. Rodriguez ¹¹⁷, S. Rodriguez Bosca ³⁷, Y. Rodriguez Garcia ^{23a}, A.M. Rodríguez Vera ¹¹⁷, S. Roe ³⁷, J.T. Roemer ³⁷, O. Røhne ¹²⁶, R.A. Rojas ³⁷, Z. Rokavec ⁹³, C.P.A. Roland ¹²⁸, A. Romaniouk ⁷⁸, E. Romano ^{72a,72b}, M. Romano ^{24b}, N. Rompotis ⁹², L. Roos ¹²⁸, S. Rosati ^{74a}, L. Roscher ⁴⁷, B.J. Rosser ³⁹, E. Rossi ¹²⁷, E. Rossi ^{71a,71b}, L.P. Rossi ⁶⁰, L. Rossini ⁵³, R. Rosten ¹²⁰, M. Rotaru ^{28b}, R. Roth ³⁷, F.A. Rothen ⁵⁵, D. Rousseau ⁶⁵, D. Rousso ⁴⁷, S. Roy-Garand ⁵⁵, A. Rozanov ¹⁰², Z.M.A. Rozario ⁵⁸, Y. Rozen ¹⁵³, A. Rubio Jimenez ¹⁶⁵, V.H. Ruelas Rivera ¹⁹, T.A. Ruggeri ¹, A. Ruggiero ¹²⁷, A. Ruiz-Martinez ¹⁶⁵, A. Rummler ³⁷, G.B. Rupnik Boero ³⁷, N.A. Rusakovich ³⁸, S. Ruscelli ⁴⁸, H.L. Russell ¹⁶⁷, G. Russo ¹³⁷, J.P. Rutherford ⁷, S. Rutherford Colmenares ¹¹⁸, M. Rybar ¹³⁴, P. Rybczynski ^{85a}, A. Ryzhov ⁴⁴, M.A.E. Saadawy ⁴⁴, F. Safai Tehrani ^{74a}, S. Saha ¹, B. Sahoo ¹⁷¹, B.T. Saifuddin ¹²¹, M. Saimpert ¹³⁶, I. Sainz Saenz Diez ^{62a}, G.T. Saito ^{81c}, M. Saito ¹⁵⁶, T. Saito ¹⁵⁶, A. Sala ^{70a,70b}, O.T. Salin ⁶⁵, A. Salnikov ¹⁴⁶, J. Salt ¹⁶⁵, A. Salvador Salas ¹⁵⁴, F. Salvatore ¹⁴⁹, G. Salvi ¹⁰⁶, A. Salzburger ³⁷, D. Sammel ⁵³, E. Sampson ⁹¹, D. Sampsonidis ^{155,d}, D. Sampsonidou ¹²⁴, M.A.A. Samy ⁵⁸, J. Sánchez ¹⁶⁵, H. Sandaker ¹²⁶, C.O. Sander ⁴⁷, J.A. Sandesara ¹⁷², M. Sandhoff ¹⁷³, C. Sandoval ^{23b}, L. Sanfilippo ^{62a}, D.P.C. Sankey ¹³⁵, T. Sano ⁸⁷, A. Sansar ^{22c}, A. Sansoni ⁵², M. Santana Queiroz ^{18b}, L. Santi ³⁷, C. Santoni ⁴⁰, G. Santoro ^{43b,43a}, H. Santos ^{131a,131b}, L. Santos Pereira Trigo ⁴⁷, E. Sanzani ^{24b,24a}, K.A. Saoucha ^{83d}, J.G. Saraiva ^{131a,131d}, J. Sardain ⁷, S. Sarkar ⁵⁰, O. Sasaki ⁸², K. Sato ¹⁶⁰, C. Sauer ³⁷, E. Sauvan ⁴, P. Savard ^{158,aj}, M. Savic ¹⁶⁴, R. Sawada ¹⁵⁶, C. Sawyer ¹³⁵, L. Sawyer ⁹⁷, A.M. Sayed ²⁷, C. Sbarra ^{24b}, A. Sbrizzi ^{24b,24a}, R. Scaglioni ^{72a,72b}, T. Scanlon ⁹⁶, J. Schaarschmidt ¹⁴⁰, U. Schäfer ¹⁰⁰, A.C. Schaffer ^{65,44}, D. Schaile ¹⁰⁹, R.D. Schamberger ¹⁴⁸, C. Scharf ¹⁹, M.M. Schefer ²⁰, D. Scheirich ¹³⁴, M. Schernau ^{138f}, C. Scheulen ⁵⁵, C. Schiavi ^{56b,56a}, M. Schioppa ^{43b,43a}, S. Schlenker ³⁷, T. Schlomer ⁵⁴, J. Schmeing ¹⁷³, C.R. Schmidt ⁴⁹, E. Schmidt ¹¹⁰, M.A. Schmidt ¹⁷³, K. Schmieden ²⁵, C. Schmitt ¹⁰⁰, N. Schmitt ¹⁰⁰, S. Schmitt ⁴⁷, N.A. Schneider ¹⁰⁹, L. Schoeffel ¹³⁶, A. Schoening ^{62b}, P.G. Scholer ³⁵, E. Schopf ¹⁴⁴, M. Schott ²⁵, S. Schramm ⁵⁵, T. Schroer ⁵⁵, H-C. Schultz-Coulon ^{62a}, M. Schumacher ⁵³, B.A. Schumm ¹³⁷, Ph. Schune ¹³⁶, H.R. Schwartz ⁷, A. Schwartzman ¹⁴⁶, T.A. Schwarz ¹⁰⁶, Ph. Schwemling ¹³⁶, R. Schwienhorst ¹⁰⁷, F.G. Sciacca ²⁰, A. Sciandra ³⁰, G. Sciolla ²⁷, S.A. Scoville ¹³⁰, F. Scuri ^{73a}, C.D. Sebastiani ³⁷, K. Sedlaczek ¹¹⁷, A. Sehrawat ^{138b}, S.C. Seidel ¹¹⁴, B.D. Seidlitz ⁴¹, C. Seitz ⁴⁷, J.M. Seixas ^{81b}, G. Sekhniaidze ^{71a}, L. Selem ¹²⁸, N. Semprini-Cesari ^{24b,24a}, A. Semushin ¹⁷⁵,

V. Senthilkumar ¹¹⁶, L. Serin ⁶⁵, M. Sessa ^{71a,71b}, H. Severini ¹²¹, F. Sforza ^{56b,56a}, A. Sfyrla ⁵⁵, Q. Sha ¹⁴, H. Shaddix ¹¹⁷, A.H. Shah ³³, R. Shaheen ¹⁴⁷, J.D. Shahinian ¹²⁹, M. Shamim ³⁷, L.Y. Shan ¹⁴, M. Shapiro ^{18a}, A. Sharma ³⁷, A.S. Sharma ¹⁶⁶, P. Sharma ³⁰, K. Shaw ¹⁴⁹, S.M. Shaw ¹⁰¹, D. Shemyakin ¹⁷¹, Q. Shen ¹⁴, D.J. Sheppard ¹⁴⁵, P. Sherwood ⁹⁶, L. Shi ^{112b}, X. Shi ¹⁴, E.B. Shields ¹⁷¹, S. Shimizu ⁸², S. Shirabe ⁸⁸, M. Shiyakova ^{38,z}, M.J. Shochet ³⁹, D.R. Shope ¹²⁶, S. Shrestha ^{120,aq}, I. Shreyber ³⁸, M.J. Shroff ¹⁰⁴, P. Sicho ¹³², A.M. Sickles ¹⁶⁴, E. Sideras Haddad ^{34j}, A.C. Sidley ¹¹⁶, A. Sidoti ^{24b}, F. Siegert ⁴⁹, Dj. Sijacki ¹⁶, F. Sili ⁶¹, J.M. Silva ⁵¹, I. Silva Ferreira ^{81b}, M.V. Silva Oliveira ³⁰, S.B. Silverstein ^{46a}, S. Simion ⁶⁵, R. Simoniello ³⁷, E.L. Simpson ¹⁰¹, H. Simpson ¹⁴⁹, L.R. Simpson ⁶, S. Simsek ⁸⁰, S.N. Singh ²⁷, S. Singh ³⁰, S. Sinha ⁴⁷, S. Sinha ¹⁰¹, M. Sioli ^{24b,24a}, K. Sioulas ⁹, E. Sitnikova ⁴⁷, J. Sjölin ^{46a,46b}, A. Skaf ⁵⁴, E. Skorda ²¹, P. Skubic ¹²¹, M. Slawinska ⁸⁶, I. Slazyk ¹⁷, I. Sliusar ¹²⁶, V. Smakhtin ¹⁷¹, B.H. Smart ¹³⁵, Y. Smirnov ^{34c}, O. Smirnova ⁹⁸, J.L. Smith ¹⁰¹, M.B. Smith ³⁵, R. Smith ¹⁴⁶, H. Smitmanns ¹⁰⁰, M. Smizanska ⁹¹, K. Smolek ¹³³, P. Smolyanskiy ¹³³, A.A. Snesarev ³⁸, H.L. Snoek ¹¹⁶, R.M. Snyder ⁵⁰, S. Snyder ³⁰, R. Sobie ^{167,ab}, A. Soffer ¹⁵⁴, C.A. Solans Sanchez ³⁷, E.Yu. Soldatov ³⁸, U. Soldevila ¹⁶⁵, A.A. Solodkov ^{34j}, S. Solomon ²⁷, A. Soloshenko ³⁸, O.V. Solovyanov ⁴⁰, P. Sommer ⁴⁹, A. Sopczak ¹³³, A.L. Sopio ⁵¹, F. Sopkova ^{29b}, J.D. Sorenson ¹¹⁴, I.R. Sotarriva Alvarez ¹³⁹, V. Sothilingam ^{62a}, O.J. Soto Sandoval ^{138c,138b}, S. Sottocornola ⁶⁷, R. Soualah ^{83a}, D. South ⁴⁷, N. Soybelman ¹⁷¹, S. Spagnolo ^{69a,69b}, A.S. Spellman ¹²⁴, D. Sperlich ⁵³, B. Spisso ^{71a,71b}, L. Splendori ¹⁰², M. Spousta ¹³⁴, E.J. Staats ³⁵, R. Stamen ^{62a}, E. Stanecka ⁸⁶, W. Stanek-Maslouska ⁴⁷, M.V. Stange ⁴⁹, B. Stanislaus ^{18a}, M.M. Stanitzki ⁴⁷, G.H. Stark ¹³⁷, J. Stark ⁸⁹, P. Staroba ¹³², P. Starovoitov ^{83d}, R. Staszewski ⁸⁶, C. Stauch ¹⁰⁹, G. Stavropoulos ⁴⁵, A. Stefl ³⁷, A. Stein ¹⁰⁰, P. Steinberg ³⁰, B. Stelzer ^{145,159a}, H.J. Stelzer ¹³⁰, O. Stelzer ^{159a}, H. Stenzel ⁵⁷, T.J. Stevenson ¹⁴⁹, G.A. Stewart ⁴⁷, G. Stoicea ^{28b}, M. Stolarski ^{131a}, S. Stonjek ¹¹⁰, A. Straessner ⁴⁹, J. Strandberg ¹⁴⁷, S. Strandberg ^{46a,46b}, M. Stratmann ¹⁷³, M. Strauss ¹²¹, T. Strebler ¹⁰², P. Strizenec ^{29b}, R. Ströhmer ¹⁶⁸, D.M. Strom ¹²⁴, R. Stroynowski ⁴⁴, A. Strubig ^{46a,46b}, S.A. Stucci ³⁰, B. Stugu ¹⁷, J. Stupak ¹²¹, N.A. Styles ⁴⁷, D. Su ¹⁴⁶, S. Su ⁶¹, X. Su ⁶¹, D. Suchy ^{29a}, A.D. Sudhakar Ponnuru ⁵⁴, L. Sudit ¹⁷¹, Y. Sue ⁸², K. Sugizaki ¹²⁹, D.M.S. Sultan ¹²⁷, L. Sultanaliyeva ²⁵, S. Sultansoy ^{3b}, S. Sun ¹⁷², W. Sun ¹⁴, S. Sundar Raman ¹⁶⁶, N. Sur ⁹⁸, J.P. Surdutovich ¹²⁰, N. Suri Jr ¹⁷⁴, M.R. Sutton ¹⁴⁹, M. Svatos ¹³², P.N. Swallow ³³, S.N. Swatman ³⁷, M. Swiatlowski ^{159a}, A. Swoboda ³⁷, I. Sykora ^{29a}, M. Sykora ¹³⁴, T. Sykora ¹³⁴, D. Ta ¹⁰⁰, K. Tackmann ^{47,y}, A. Taffard ¹⁶², R. Tafirout ^{159a}, Y. Takubo ⁸², M. Talby ¹⁰², N.M. Tamir ¹³, A. Tanaka ¹⁵⁶, J. Tanaka ¹⁵⁶, R. Tanaka ⁶⁵, M. Tanasini ¹⁴⁸, Z. Tao ¹⁶⁶, S. Tapia Araya ^{138g}, S. Tapprogge ¹⁰⁰, A. Tarek Abouelfadl Mohamed ³⁷, S. Tarem ¹⁵³, K. Tariq ¹⁴, G. Tarna ³⁷, G.F. Tartarelli ^{70a}, M.J. Tartarin ^{141b}, P. Tas ¹³⁴, M. Tasevsky ¹³², E. Tassi ^{43b,43a}, Y. Tayalati ^{36e,aa}, G.N. Taylor ¹⁰⁵, W. Taylor ^{159b}, R.J. Taylor Vara ¹⁶⁵, A.S. Tegetmeier ⁸⁹, P. Teixeira-Dias ⁹⁵, J.J. Teoh ¹⁵⁸, K. Terashi ¹⁵⁶, J. Terron ⁹⁹, S. Terzo ¹³, M. Testa ⁵², R.J. Teuscher ^{158,ab}, A. Thaler ⁷⁸, T. Theveneaux-Pelzer ¹⁰², J.P. Thomas ²¹, E.A. Thompson ^{18a}, P.D. Thompson ²¹, E. Thomson ¹²⁹, R.E. Thornberry ³⁰, T.M. Thory-Rao ²¹, C.N. Thotamuna Wijewardhana ¹⁴⁸, C. Tian ⁶¹, Y. Tian ⁵⁵, V. Tikhomirov ⁸⁰, Yu.A. Tikhonov ³⁸, D. Timoshyn ¹³⁴, E.X.L. Ting ¹, P. Tipton ¹⁷⁴, A. Tishelman-Charny ³⁰, K. Todome ¹³⁹, S. Todorova-Nova ¹³⁴, L. Toffolin ^{68a,68c}, M. Togawa ⁸², J. Tojo ⁸⁸, S. Tokár ^{29a}, O. Toldaiev ⁶⁷, A.J. Toler ¹⁰³, G. Tolkachev ¹⁰², M. Tomoto ⁸², L. Tompkins ¹⁴⁶, E. Torrence ¹²⁴, H. Torres ⁸⁹, D.I. Torres Arza ^{138g}, E. Torres Reoyo ¹⁶⁵, E. Torró Pastor ¹⁶⁵, M. Toscani ³¹, C. Toscirri ³⁹, M. Tost ¹¹, D.R. Tovey ¹⁴², T. Trefzger ¹⁶⁸, P.M. Tricarico ¹³, A. Tricoli ³⁰, I.M. Trigger ^{159a}, S. Trincaz-Duvoid ¹²⁸, D.A. Trischuk ¹⁶⁷, A. Tropina ³⁸, D. Truncali ^{75a,75b}, L. Truong ^{34c}, M. Trzebinski ⁸⁶,

A. Trzupiek ⁸⁶, F. Tsai ¹⁴⁸, A. Tsiamis ¹⁵⁵, P.V. Tsiareshka ³⁸, S. Tsigaridas ^{159a}, A. Tsigotis ^{155,t},
 V. Tsiskaridze ^{152a}, E.G. Tskhadadze ^{152a}, H.F. Tsoi ¹²⁹, Y. Tsujikawa ⁸⁷, V. Tsulaia ^{18a},
 K. Tsuru ¹¹⁹, D. Tsybychev ¹⁴⁸, Y. Tu ^{63b}, A. Tudorache ^{28b}, V. Tudorache ^{28b}, S.B. Tuncay ¹²⁷,
 S. Turchikhin ^{56b,56a}, I. Turk Cakir ^{3a}, R. Turra ^{70a}, T. Turtuvshin ^{38,ac}, P.M. Tuts ⁴¹,
 Y. Uematsu ⁸², F. Ukegawa ¹⁶⁰, P.A. Ulloa Poblete ^{138c,138b}, G. Unal ³⁷, A. Undrus ³⁰,
 J. Urban ^{29b}, P. Urrejola ^{138e}, G. Usai ⁸, R. Ushioda ¹⁵⁷, M. Usman ¹⁰⁸, F. Ustuner ⁵¹,
 Z. Uysal ⁸⁰, V. Vacek ¹³³, B. Vachon ¹⁰⁴, A. Vaitkus ⁹⁶, C. Valderanis ¹⁰⁹,
 E. Valdes Santurio ^{46a,46b}, M. Valente ³⁷, S. Valentinetti ^{24b,24a}, A. Valero ¹⁶⁵,
 E. Valiente Moreno ¹⁶⁵, A. Vallier ⁸⁹, J.A. Valls Ferrer ¹⁶⁵, D.R. Van Arneman ¹¹⁶,
 R. Van Den Broucke ¹²⁸, A. Van Der Graaf ⁴⁸, H.Z. Van Der Schyf ^{34j}, P. Van Gemmeren ⁶,
 M. Van Rijnbach ³⁷, S. Van Stroud ⁹⁶, I. Van Vulpen ¹¹⁶, P. Vana ¹³⁴, M. Vanadia ^{75a,75b},
 U.M. Vande Voorde ¹⁴⁷, W. Vandelli ³⁷, E.R. Vandewall ¹⁴⁶, D. Vannicola ¹⁵⁴, R. Vari ^{74a},
 M. Varma ¹⁷⁴, E.W. Varnes ⁷, C. Varni ^{85a}, D. Varouchas ⁶⁵, L. Varriale ¹⁶⁵, K.E. Varvell ¹⁵⁰,
 M.E. Vasile ^{28b}, A. Vasileiadou ⁹, L. Vaslin ⁸², M.D. Vassilev ¹⁴⁶, A. Vasyukov ³⁸,
 L.M. Vaughan ¹²², R. Vavricka ¹³⁴, T. Vazquez Schroeder ¹³, J. Veatch ³², V. Vecchio ¹⁰¹,
 M.J. Veen ¹⁰³, I. Veliscek ³⁰, I. Velkovska ⁹³, L.M. Veloce ¹⁵⁸, F. Veloso ^{131a,131c},
 A.G. Veltman ⁵¹, S.H. Venetianer ¹⁶¹, S. Veneziano ^{74a}, A. Ventura ^{69a,69b}, A. Verbitskyi ¹¹⁰,
 M. Verducci ^{73a,73b}, C. Vergis ⁹⁴, M. Verissimo De Araujo ^{81b}, W. Verkerke ¹¹⁶,
 J.C. Vermeulen ¹¹⁶, C. Vernieri ¹⁴⁶, M. Vessella ¹⁶², M.C. Vetterli ^{145,aj}, A. Vgenopoulos ¹⁰⁰,
 N. Viaux Maira ^{138g,af}, L. Vicens ¹³³, T. Vickey ¹⁴², O.E. Vickey Boeriu ¹⁴²,
 G.H.A. Viehhauser ¹²⁷, L. Vigani ^{62b}, M. Vigil ¹¹⁰, M. Villa ^{24b,24a}, M. Villaplana Perez ¹⁶⁵,
 E.M. Villhauer ³⁹, E. Vilucchi ⁵², M. Vincent ¹⁶⁵, M.G. Vincter ³⁵, A. Visibile ^{46a,46b},
 A. Visive ¹¹⁶, C. Vittori ^{24b,24a}, I. Vivarelli ^{24b,24a}, M.I. Vivas Albornoz ⁴⁷, E. Voevodina ¹¹⁰,
 F. Vogel ¹⁰⁹, J.C. Voigt ¹³⁶, P. Vokac ¹³³, Yu. Volkotrub ^{85b}, L. Vomberg ²⁵, E. Von Toerne ²⁵,
 B. Vormwald ³⁷, K. Vorobev ⁵⁰, M. Vos ¹⁶⁵, K. Voss ¹⁴⁴, M. Vozak ³⁷, L. Vozdecky ¹²¹,
 N. Vranjes ¹⁶, M. Vranjes Milosavljevic ¹⁶, M. Vreeswijk ¹¹⁶, N.K. Vu ^{112a}, R. Vuillermet ³⁷,
 I. Vukotic ³⁹, I.K. Vyas ³⁵, J.F. Wack ³³, A. Wada ¹¹¹, S. Wada ¹⁶⁰, C. Wagner ¹⁴⁶,
 J.M. Wagner ^{18a}, W. Wagner ¹⁷³, S. Wahdan ¹⁷³, H. Wahlberg ⁹⁰, C.H. Waits ¹²¹, R. Walker ¹⁰⁹,
 K. Walkingshaw Pass ⁵⁸, W. Walkowiak ¹⁴⁴, A. Wall ¹²⁹, E.J. Wallin ⁹⁸, T. Wamorkar ¹⁴⁶,
 K. Wandall-Christensen ¹⁶⁵, A. Wang ⁶¹, A.Z. Wang ¹³⁷, C. Wang ⁴⁷, C. Wang ¹¹, H. Wang ^{18a},
 J. Wang ^{63c}, P. Wang ¹⁰¹, P. Wang ⁹⁶, R. Wang ⁶⁰, R. Wang ¹⁰⁶, R. Wang ⁶, S.M. Wang ¹⁵¹,
 S. Wang ^{14,an}, T. Wang ¹¹⁵, T. Wang ⁶¹, W.T. Wang ¹²⁷, W. Wang ^{113c}, X. Wang ¹⁶⁴,
 X. Wang ^{141a}, X. Wang ⁴⁷, Y. Wang ¹⁴⁸, Y. Wang ¹¹⁴, Y. Wang ⁶¹, Z. Wang ¹⁴, Z. Wang ^{63b},
 C. Wanotayaroj ⁸², A. Warburton ¹⁰⁴, A.L. Warnerbring ¹⁴⁴, S. Waterhouse ⁹⁶, A.T. Watson ²¹,
 H. Watson ⁵¹, M.F. Watson ²¹, E. Watton ³⁷, G. Watts ¹⁴⁰, B.M. Waugh ⁹⁶, J.M. Webb ⁵³,
 C. Weber ³⁰, M.S. Weber ²⁰, C. Wei ⁶¹, Y. Wei ⁵³, A.R. Weidberg ¹²⁷, E.J. Weik ¹¹⁸,
 J. Weingarten ⁴⁸, C. Weiser ⁵³, C.J. Wells ⁴⁷, P.S. Wells ³⁷, T. Wenaus ³⁰, T. Wengler ³⁷,
 N.S. Wenke ¹¹⁰, N. Wermes ²⁵, D. Werner ⁴⁷, M. Wessels ^{62a}, A.M. Wharton ⁹¹, A.S. White ³⁷,
 A. White ⁸, M.J. White ¹, D. Whiteson ¹⁶², W. Wiedenmann ¹⁷², M. Wielers ¹³⁵, R. Wierda ¹⁴⁷,
 C. Wiglesworth ⁴², H.G. Wilkens ³⁷, J.J.H. Wilkinson ³³, S. Williams ³³, S. Willocq ¹⁰³,
 L.F. Wills ¹¹⁷, D.J. Wilson ¹⁰¹, P.J. Windischhofer ³⁹, F.I. Winkel ³¹, F. Winklmeier ¹²⁴,
 B.T. Winter ⁵³, M. Wittgen ¹⁴⁶, M. Wobisch ⁹⁷, T. Wojtkowski ⁵⁹, Z. Wolffs ¹¹⁶, J. Wollrath ³⁷,
 M.W. Wolter ⁸⁶, H. Wolters ^{131a,131c}, M.C. Wong ¹³⁷, E.L. Woodward ⁴¹, S.D. Worm ⁴⁷,
 B.K. Wosiek ⁸⁶, K.A. Wozniak ⁵⁵, K.W. Woźniak ⁸⁶, S. Wozniewski ⁵⁴, K. Wraight ⁵⁸,
 C. Wu ¹⁵⁸, J. Wu ¹⁵⁶, M. Wu ^{112b}, M. Wu ¹¹⁵, S.L. Wu ¹⁷², S. Wu ^{14,an}, X. Wu ⁶¹,
 Y.Q. Wu ¹⁵⁸, Y. Wu ⁶¹, Z. Wu ¹⁰², Z. Wu ^{112a}, J. Wuerzinger ¹¹⁰, T.R. Wyatt ¹⁰¹,
 B.M. Wynne ⁵¹, L. Xia ^{112a}, M. Xie ⁶¹, A. Xiong ¹²⁴, I. Xiotidis ³⁷, D. Xu ¹⁴, H. Xu ⁶¹,

L. Xu , R. Xu , T. Xu , W. Xu , Y. Xu , Z. Xu , R. Xue , B. Yabsley , S. Yacoob , Y. Yamaguchi , E. Yamashita , H. Yamauchi , T. Yamazaki , Y. Yamazaki , F. Yan , S. Yan , Z. Yan , C. Yang , H.J. Yang , H.T. Yang , S. Yang , X. Yang , X. Yang , Y. Yang , Y. Yang , W-M. Yao , C.L. Yardley , J. Ye , S. Ye , X. Ye , I. Yeletsikh , B. Yeo , M.R. Yexley , T.P. Yildirim , K. Yorita , C.J.S. Young , C. Young , I.N.L. Young , N.D. Young , D. Yu , Y. Yu , J. Yuan , M. Yuan , R. Yuan , L. Yue , M. Zaazoua , B. Zabinski , I. Zahir , Q.U.A. Zahoor , A. Zaio , Z.K. Zak , T. Zakareishvili , S. Zambito , J. Zang , R. Zanzottera , O. Zaplatilek , I. Zatocilova , E. Zaya , C. Zeitnitz , H. Zeng , T. Ženiš , S. Zenz , W. Zhan , B. Zhang , D.F. Zhang , G. Zhang , J. Zhang , J. Zhang , L. Zhang , L. Zhang , P. Zhang , R. Zhang , S. Zhang , Y. Zhang , Y. Zhang , Y. Zhang , Y. Zhang , Y. Zhang , Y. Zhang , Y. Zhang , Z. Zhang , Z. Zhang , Z. Zhang , Z. Zhang , Z. Zhang , Z. Zhang , H. Zhao , T. Zhao , Y. Zhao , Z. Zhao , Z. Zhao , A. Zhemchugov , J. Zheng , L. Zheng , X. Zheng , Z. Zheng , D. Zhong , B. Zhou , B. Zhou , N. Zhou , Y. Zhou , Y. Zhou , Y. Zhou , Z. Zhou , J. Zhu , X. Zhu , Y. Zhu , X. Zhuang , K. Zhukov , P. Ziakas , N.I. Zimine , J. Zinsser , M. Ziolkowski , L. Živković , A. Zoccoli , K. Zoch , A. Zografos , T.G. Zorbas , O. Zormpa , D. Zubov , L. Zwalinski .

¹Department of Physics, University of Adelaide, Adelaide; Australia.

²Department of Physics, University of Alberta, Edmonton AB; Canada.

^{3(a)}Department of Physics, Ankara University, Ankara; ^(b)Division of Physics, TOBB University of Economics and Technology, Ankara; Türkiye.

⁴LAPP, Université Savoie Mont Blanc, CNRS/IN2P3, Annecy; France.

⁵APC, Université Paris Cité, CNRS/IN2P3, Paris; France.

⁶High Energy Physics Division, Argonne National Laboratory, Argonne IL; United States of America.

⁷Department of Physics, University of Arizona, Tucson AZ; United States of America.

⁸Department of Physics, University of Texas at Arlington, Arlington TX; United States of America.

⁹Physics Department, National and Kapodistrian University of Athens, Athens; Greece.

¹⁰Physics Department, National Technical University of Athens, Zografou; Greece.

¹¹Department of Physics, University of Texas at Austin, Austin TX; United States of America.

¹²Institute of Physics, Azerbaijan Academy of Sciences, Baku; Azerbaijan.

¹³Institut de Física d'Altes Energies (IFAE), Barcelona Institute of Science and Technology, Barcelona; Spain.

¹⁴Institute of High Energy Physics, Chinese Academy of Sciences, Beijing; China.

¹⁵Physics Department, Tsinghua University, Beijing; China.

¹⁶Institute of Physics, University of Belgrade, Belgrade; Serbia.

¹⁷Department for Physics and Technology, University of Bergen, Bergen; Norway.

^{18(a)}Physics Division, Lawrence Berkeley National Laboratory, Berkeley CA; ^(b)University of California, Berkeley CA; United States of America.

¹⁹Institut für Physik, Humboldt Universität zu Berlin, Berlin; Germany.

²⁰Albert Einstein Center for Fundamental Physics and Laboratory for High Energy Physics, University of Bern, Bern; Switzerland.

²¹School of Physics and Astronomy, University of Birmingham, Birmingham; United Kingdom.

^{22(a)}Department of Physics, Bogazici University, Istanbul; ^(b)Department of Physics Engineering, Gaziantep University, Gaziantep; ^(c)Department of Physics, Istanbul University, Istanbul; Türkiye.

- ^{23(a)} Facultad de Ciencias y Centro de Investigaciones, Universidad Antonio Nariño, Bogotá; ^(b) Departamento de Física, Universidad Nacional de Colombia, Bogotá; Colombia.
- ^{24(a)} Dipartimento di Fisica e Astronomia A. Righi, Università di Bologna, Bologna; ^(b) INFN Sezione di Bologna; Italy.
- ²⁵ Physikalisches Institut, Universität Bonn, Bonn; Germany.
- ²⁶ Department of Physics, Boston University, Boston MA; United States of America.
- ²⁷ Department of Physics, Brandeis University, Waltham MA; United States of America.
- ^{28(a)} Transilvania University of Brasov, Brasov; ^(b) Horia Hulubei National Institute of Physics and Nuclear Engineering, Bucharest; ^(c) Department of Physics, Alexandru Ioan Cuza University of Iasi, Iasi; ^(d) National Institute for Research and Development of Isotopic and Molecular Technologies, Physics Department, Cluj-Napoca; ^(e) National University of Science and Technology Politehnica, Bucharest; ^(f) West University in Timisoara, Timisoara; ^(g) Faculty of Physics, University of Bucharest, Bucharest; Romania.
- ^{29(a)} Faculty of Mathematics, Physics and Informatics, Comenius University, Bratislava; ^(b) Department of Subnuclear Physics, Institute of Experimental Physics of the Slovak Academy of Sciences, Kosice; Slovak Republic.
- ³⁰ Physics Department, Brookhaven National Laboratory, Upton NY; United States of America.
- ³¹ Universidad de Buenos Aires, Facultad de Ciencias Exactas y Naturales, Departamento de Física, y CONICET, Instituto de Física de Buenos Aires (IFIBA), Buenos Aires; Argentina.
- ³² California State University, CA; United States of America.
- ³³ Cavendish Laboratory, University of Cambridge, Cambridge; United Kingdom.
- ^{34(a)} Department of Physics, University of Cape Town, Cape Town; ^(b) iThemba Labs, Western Cape; ^(c) Department of Mechanical Engineering Science, University of Johannesburg, Johannesburg; ^(d) National Institute of Physics, University of the Philippines Diliman (Philippines); ^(e) Department of Physics, Stellenbosch University, Matieland; ^(f) University of KwaZulu-Natal, School of Agriculture and Science, Mathematics, Westville; ^(g) University of South Africa, Department of Physics, Pretoria; ^(h) University of Pretoria, Department of Mechanical and Aeronautical Engineering, Pretoria; ⁽ⁱ⁾ University of Zululand, KwaDlangezwa; ^(j) School of Physics, University of the Witwatersrand, Johannesburg; South Africa.
- ³⁵ Department of Physics, Carleton University, Ottawa ON; Canada.
- ^{36(a)} Faculté des Sciences Ain Chock, Université Hassan II de Casablanca; ^(b) Faculté des Sciences, Université Ibn-Tofail, Kénitra; ^(c) Faculté des Sciences Semlalia, Université Cadi Ayyad, LPHEA-Marrakech; ^(d) LPMR, Faculté des Sciences, Université Mohamed Premier, Oujda; ^(e) Faculté des sciences, Université Mohammed V, Rabat; ^(f) Institute of Applied Physics, Mohammed VI Polytechnic University, Ben Guerir; Morocco.
- ³⁷ CERN, Geneva; Switzerland.
- ³⁸ Affiliated with an international laboratory covered by a cooperation agreement with CERN.
- ³⁹ Enrico Fermi Institute, University of Chicago, Chicago IL; United States of America.
- ⁴⁰ LPC, Université Clermont Auvergne, CNRS/IN2P3, Clermont-Ferrand; France.
- ⁴¹ Nevis Laboratory, Columbia University, Irvington NY; United States of America.
- ⁴² Niels Bohr Institute, University of Copenhagen, Copenhagen; Denmark.
- ^{43(a)} Dipartimento di Fisica, Università della Calabria, Rende; ^(b) INFN Gruppo Collegato di Cosenza, Laboratori Nazionali di Frascati; Italy.
- ⁴⁴ Physics Department, Southern Methodist University, Dallas TX; United States of America.
- ⁴⁵ National Centre for Scientific Research "Demokritos", Agia Paraskevi; Greece.
- ^{46(a)} Department of Physics, Stockholm University; ^(b) Oskar Klein Centre, Stockholm; Sweden.
- ⁴⁷ Deutsches Elektronen-Synchrotron DESY, Hamburg and Zeuthen; Germany.
- ⁴⁸ Fakultät Physik, Technische Universität Dortmund, Dortmund; Germany.

- ⁴⁹Institut für Kern- und Teilchenphysik, Technische Universität Dresden, Dresden; Germany.
- ⁵⁰Department of Physics, Duke University, Durham NC; United States of America.
- ⁵¹SUPA - School of Physics and Astronomy, University of Edinburgh, Edinburgh; United Kingdom.
- ⁵²INFN e Laboratori Nazionali di Frascati, Frascati; Italy.
- ⁵³Physikalisches Institut, Albert-Ludwigs-Universität Freiburg, Freiburg; Germany.
- ⁵⁴II. Physikalisches Institut, Georg-August-Universität Göttingen, Göttingen; Germany.
- ⁵⁵Département de Physique Nucléaire et Corpusculaire, Université de Genève, Genève; Switzerland.
- ⁵⁶(^a) Dipartimento di Fisica, Università di Genova, Genova; (^b) INFN Sezione di Genova; Italy.
- ⁵⁷II. Physikalisches Institut, Justus-Liebig-Universität Giessen, Giessen; Germany.
- ⁵⁸SUPA - School of Physics and Astronomy, University of Glasgow, Glasgow; United Kingdom.
- ⁵⁹LPSC, Université Grenoble Alpes, CNRS/IN2P3, Grenoble INP, Grenoble; France.
- ⁶⁰Laboratory for Particle Physics and Cosmology, Harvard University, Cambridge MA; United States of America.
- ⁶¹Department of Modern Physics and State Key Laboratory of Particle Detection and Electronics, University of Science and Technology of China, Hefei; China.
- ⁶²(^a) Kirchhoff-Institut für Physik, Ruprecht-Karls-Universität Heidelberg, Heidelberg; (^b) Physikalisches Institut, Ruprecht-Karls-Universität Heidelberg, Heidelberg; Germany.
- ⁶³(^a) Department of Physics, Chinese University of Hong Kong, Shatin, N.T., Hong Kong; (^b) Department of Physics, University of Hong Kong, Hong Kong; (^c) Department of Physics and Institute for Advanced Study, Hong Kong University of Science and Technology, Clear Water Bay, Kowloon, Hong Kong; China.
- ⁶⁴Department of Physics, National Tsing Hua University, Hsinchu; Taiwan.
- ⁶⁵IJCLab, Université Paris-Saclay, CNRS/IN2P3, 91405, Orsay; France.
- ⁶⁶Centro Nacional de Microelectrónica (IMB-CNM-CSIC), Barcelona; Spain.
- ⁶⁷Department of Physics, Indiana University, Bloomington IN; United States of America.
- ⁶⁸(^a) INFN Gruppo Collegato di Udine, Sezione di Trieste, Udine; (^b) ICTP, Trieste; (^c) Dipartimento Politecnico di Ingegneria e Architettura, Università di Udine, Udine; Italy.
- ⁶⁹(^a) INFN Sezione di Lecce; (^b) Dipartimento di Matematica e Fisica, Università del Salento, Lecce; Italy.
- ⁷⁰(^a) INFN Sezione di Milano; (^b) Dipartimento di Fisica, Università di Milano, Milano; Italy.
- ⁷¹(^a) INFN Sezione di Napoli; (^b) Dipartimento di Fisica, Università di Napoli, Napoli; Italy.
- ⁷²(^a) INFN Sezione di Pavia; (^b) Dipartimento di Fisica, Università di Pavia, Pavia; Italy.
- ⁷³(^a) INFN Sezione di Pisa; (^b) Dipartimento di Fisica E. Fermi, Università di Pisa, Pisa; Italy.
- ⁷⁴(^a) INFN Sezione di Roma; (^b) Dipartimento di Fisica, Sapienza Università di Roma, Roma; Italy.
- ⁷⁵(^a) INFN Sezione di Roma Tor Vergata; (^b) Dipartimento di Fisica, Università di Roma Tor Vergata, Roma; Italy.
- ⁷⁶(^a) INFN Sezione di Roma Tre; (^b) Dipartimento di Matematica e Fisica, Università Roma Tre, Roma; Italy.
- ⁷⁷(^a) INFN-TIFPA; (^b) Università degli Studi di Trento, Trento; Italy.
- ⁷⁸Universität Innsbruck, Department of Astro and Particle Physics, Innsbruck; Austria.
- ⁷⁹Department of Physics and Astronomy, Iowa State University, Ames IA; United States of America.
- ⁸⁰Istinye University, Sariyer, Istanbul; Türkiye.
- ⁸¹(^a) Departamento de Engenharia Elétrica, Universidade Federal de Juiz de Fora (UFJF), Juiz de Fora; (^b) Universidade Federal do Rio De Janeiro COPPE/EE/IF, Rio de Janeiro; (^c) Instituto de Física, Universidade de São Paulo, São Paulo; (^d) Rio de Janeiro State University, Rio de Janeiro; (^e) Federal University of Bahia, Bahia; Brazil.
- ⁸²KEK, High Energy Accelerator Research Organization, Tsukuba; Japan.
- ⁸³(^a) Khalifa University of Science and Technology, Abu Dhabi; (^b) New York University Abu Dhabi, Abu Dhabi; (^c) United Arab Emirates University, Al Ain; (^d) University of Sharjah, Sharjah; United Arab

Emirates.

⁸⁴Graduate School of Science, Kobe University, Kobe; Japan.

⁸⁵(^a) AGH University of Krakow, Faculty of Physics and Applied Computer Science, Krakow; (^b) Marian Smoluchowski Institute of Physics, Jagiellonian University, Krakow; Poland.

⁸⁶Institute of Nuclear Physics Polish Academy of Sciences, Krakow; Poland.

⁸⁷Faculty of Science, Kyoto University, Kyoto; Japan.

⁸⁸Research Center for Advanced Particle Physics and Department of Physics, Kyushu University, Fukuoka ; Japan.

⁸⁹L2IT, Université de Toulouse, CNRS/IN2P3, UPS, Toulouse; France.

⁹⁰Instituto de Física La Plata, Universidad Nacional de La Plata and CONICET, La Plata; Argentina.

⁹¹Physics Department, Lancaster University, Lancaster; United Kingdom.

⁹²Oliver Lodge Laboratory, University of Liverpool, Liverpool; United Kingdom.

⁹³Department of Experimental Particle Physics, Jožef Stefan Institute and Department of Physics, University of Ljubljana, Ljubljana; Slovenia.

⁹⁴Department of Physics and Astronomy, Queen Mary University of London, London; United Kingdom.

⁹⁵Department of Physics, Royal Holloway University of London, Egham; United Kingdom.

⁹⁶Department of Physics and Astronomy, University College London, London; United Kingdom.

⁹⁷Louisiana Tech University, Ruston LA; United States of America.

⁹⁸Fysiska institutionen, Lunds universitet, Lund; Sweden.

⁹⁹Departamento de Física Teórica C-15 and CIAFF, Universidad Autónoma de Madrid, Madrid; Spain.

¹⁰⁰Institut für Physik, Universität Mainz, Mainz; Germany.

¹⁰¹School of Physics and Astronomy, University of Manchester, Manchester; United Kingdom.

¹⁰²CPPM, Aix-Marseille Université, CNRS/IN2P3, Marseille; France.

¹⁰³Department of Physics, University of Massachusetts, Amherst MA; United States of America.

¹⁰⁴Department of Physics, McGill University, Montreal QC; Canada.

¹⁰⁵School of Physics, University of Melbourne, Victoria; Australia.

¹⁰⁶Department of Physics, University of Michigan, Ann Arbor MI; United States of America.

¹⁰⁷Department of Physics and Astronomy, Michigan State University, East Lansing MI; United States of America.

¹⁰⁸Group of Particle Physics, University of Montreal, Montreal QC; Canada.

¹⁰⁹Fakultät für Physik, Ludwig-Maximilians-Universität München, München; Germany.

¹¹⁰Max-Planck-Institut für Physik (Werner-Heisenberg-Institut), München; Germany.

¹¹¹Graduate School of Science and Kobayashi-Maskawa Institute, Nagoya University, Nagoya; Japan.

¹¹²(^a) Department of Physics, Nanjing University, Nanjing; (^b) School of Science, Shenzhen Campus of Sun Yat-sen University; (^c) University of Chinese Academy of Science (UCAS), Beijing; China.

¹¹³(^a) School of Physics, Nankai University, Tianjin; (^b) Institute of Frontier and Interdisciplinary Science and Key Laboratory of Particle Physics and Particle Irradiation (MOE), Shandong University, Qingdao; (^c) School of Physics, Zhengzhou University; China.

¹¹⁴Department of Physics and Astronomy, University of New Mexico, Albuquerque NM; United States of America.

¹¹⁵Institute for Mathematics, Astrophysics and Particle Physics, Radboud University/Nikhef, Nijmegen; Netherlands.

¹¹⁶Nikhef National Institute for Subatomic Physics and University of Amsterdam, Amsterdam; Netherlands.

¹¹⁷Department of Physics, Northern Illinois University, DeKalb IL; United States of America.

¹¹⁸Department of Physics, New York University, New York NY; United States of America.

¹¹⁹Ochanomizu University, Otsuka, Bunkyo-ku, Tokyo; Japan.

- ¹²⁰Ohio State University, Columbus OH; United States of America.
- ¹²¹Homer L. Dodge Department of Physics and Astronomy, University of Oklahoma, Norman OK; United States of America.
- ¹²²Department of Physics, Oklahoma State University, Stillwater OK; United States of America.
- ¹²³Palacký University, Joint Laboratory of Optics, Olomouc; Czech Republic.
- ¹²⁴Institute for Fundamental Science, University of Oregon, Eugene, OR; United States of America.
- ¹²⁵Graduate School of Science, University of Osaka, Osaka; Japan.
- ¹²⁶Department of Physics, University of Oslo, Oslo; Norway.
- ¹²⁷Department of Physics, Oxford University, Oxford; United Kingdom.
- ¹²⁸LPNHE, Sorbonne Université, Université Paris Cité, CNRS/IN2P3, Paris; France.
- ¹²⁹Department of Physics, University of Pennsylvania, Philadelphia PA; United States of America.
- ¹³⁰Department of Physics and Astronomy, University of Pittsburgh, Pittsburgh PA; United States of America.
- ¹³¹(^a) Laboratório de Instrumentação e Física Experimental de Partículas - LIP, Lisboa; (^b) Departamento de Física, Faculdade de Ciências, Universidade de Lisboa, Lisboa; (^c) Departamento de Física, Universidade de Coimbra, Coimbra; (^d) Centro de Física Nuclear da Universidade de Lisboa, Lisboa; (^e) Departamento de Física, Escola de Ciências, Universidade do Minho, Braga; (^f) Departamento de Física Teórica y del Cosmos, Universidad de Granada, Granada (Spain); (^g) Departamento de Física, Instituto Superior Técnico, Universidade de Lisboa, Lisboa; Portugal.
- ¹³²Institute of Physics of the Czech Academy of Sciences, Prague; Czech Republic.
- ¹³³Czech Technical University in Prague, Prague; Czech Republic.
- ¹³⁴Charles University, Faculty of Mathematics and Physics, Prague; Czech Republic.
- ¹³⁵Particle Physics Department, Rutherford Appleton Laboratory, Didcot; United Kingdom.
- ¹³⁶IRFU, CEA, Université Paris-Saclay, Gif-sur-Yvette; France.
- ¹³⁷Santa Cruz Institute for Particle Physics, University of California Santa Cruz, Santa Cruz CA; United States of America.
- ¹³⁸(^a) Departamento de Física, Pontificia Universidad Católica de Chile, Santiago; (^b) Millennium Institute for Subatomic physics at high energy frontier (SAPHIR), Santiago; (^c) Instituto de Investigación Multidisciplinario en Ciencia y Tecnología, y Departamento de Física, Universidad de La Serena; (^d) Universidad Andres Bello, Department of Physics, Santiago; (^e) Universidad San Sebastian, Recoleta; (^f) Instituto de Alta Investigación, Universidad de Tarapacá, Arica; (^g) Departamento de Física, Universidad Técnica Federico Santa María, Valparaíso; Chile.
- ¹³⁹Department of Physics, Institute of Science, Tokyo; Japan.
- ¹⁴⁰Department of Physics, University of Washington, Seattle WA; United States of America.
- ¹⁴¹(^a) State Key Laboratory of Dark Matter Physics, School of Physics and Astronomy, Shanghai Jiao Tong University, Key Laboratory for Particle Astrophysics and Cosmology (MOE), SKLPPC, Shanghai; (^b) State Key Laboratory of Dark Matter Physics, Tsung-Dao Lee Institute, Shanghai Jiao Tong University, Shanghai; China.
- ¹⁴²Department of Physics and Astronomy, University of Sheffield, Sheffield; United Kingdom.
- ¹⁴³Department of Physics, Shinshu University, Nagano; Japan.
- ¹⁴⁴Department Physik, Universität Siegen, Siegen; Germany.
- ¹⁴⁵Department of Physics, Simon Fraser University, Burnaby BC; Canada.
- ¹⁴⁶SLAC National Accelerator Laboratory, Stanford CA; United States of America.
- ¹⁴⁷Department of Physics, Royal Institute of Technology, Stockholm; Sweden.
- ¹⁴⁸Departments of Physics and Astronomy, Stony Brook University, Stony Brook NY; United States of America.
- ¹⁴⁹Department of Physics and Astronomy, University of Sussex, Brighton; United Kingdom.

- ¹⁵⁰School of Physics, University of Sydney, Sydney; Australia.
- ¹⁵¹Institute of Physics, Academia Sinica, Taipei; Taiwan.
- ¹⁵²^(a) E. Andronikashvili Institute of Physics, Iv. Javakhishvili Tbilisi State University, Tbilisi; ^(b) High Energy Physics Institute, Tbilisi State University, Tbilisi; ^(c) University of Georgia, Tbilisi; Georgia.
- ¹⁵³Department of Physics, Technion, Israel Institute of Technology, Haifa; Israel.
- ¹⁵⁴Raymond and Beverly Sackler School of Physics and Astronomy, Tel Aviv University, Tel Aviv; Israel.
- ¹⁵⁵Department of Physics, Aristotle University of Thessaloniki, Thessaloniki; Greece.
- ¹⁵⁶International Center for Elementary Particle Physics and Department of Physics, University of Tokyo, Tokyo; Japan.
- ¹⁵⁷Graduate School of Science and Technology, Tokyo Metropolitan University, Tokyo; Japan.
- ¹⁵⁸Department of Physics, University of Toronto, Toronto ON; Canada.
- ¹⁵⁹^(a) TRIUMF, Vancouver BC; ^(b) Department of Physics and Astronomy, York University, Toronto ON; Canada.
- ¹⁶⁰Division of Physics and Tomonaga Center for the History of the Universe, Faculty of Pure and Applied Sciences, University of Tsukuba, Tsukuba; Japan.
- ¹⁶¹Department of Physics and Astronomy, Tufts University, Medford MA; United States of America.
- ¹⁶²Department of Physics and Astronomy, University of California Irvine, Irvine CA; United States of America.
- ¹⁶³Department of Physics and Astronomy, University of Uppsala, Uppsala; Sweden.
- ¹⁶⁴Department of Physics, University of Illinois, Urbana IL; United States of America.
- ¹⁶⁵Instituto de Física Corpuscular (IFIC), Centro Mixto Universidad de Valencia - CSIC, Valencia; Spain.
- ¹⁶⁶Department of Physics, University of British Columbia, Vancouver BC; Canada.
- ¹⁶⁷Department of Physics and Astronomy, University of Victoria, Victoria BC; Canada.
- ¹⁶⁸Fakultät für Physik und Astronomie, Julius-Maximilians-Universität Würzburg, Würzburg; Germany.
- ¹⁶⁹Department of Physics, University of Warwick, Coventry; United Kingdom.
- ¹⁷⁰Waseda University, Tokyo; Japan.
- ¹⁷¹Department of Particle Physics and Astrophysics, Weizmann Institute of Science, Rehovot; Israel.
- ¹⁷²Department of Physics, University of Wisconsin, Madison WI; United States of America.
- ¹⁷³Fakultät für Mathematik und Naturwissenschaften, Fachgruppe Physik, Bergische Universität Wuppertal, Wuppertal; Germany.
- ¹⁷⁴Department of Physics, Yale University, New Haven CT; United States of America.
- ¹⁷⁵Yerevan Physics Institute, Yerevan; Armenia.
- ^a Also at Affiliated with an institute formerly covered by a cooperation agreement with CERN.
- ^b Also at An-Najah National University, Nablus; Palestine.
- ^c Also at Borough of Manhattan Community College, City University of New York, New York NY; United States of America.
- ^d Also at Center for Interdisciplinary Research and Innovation (CIRI-AUTH), Thessaloniki; Greece.
- ^e Also at Centre of Physics of the Universities of Minho and Porto (CF-UM-UP); Portugal.
- ^f Also at CERN, Geneva; Switzerland.
- ^g Also at Département de Physique Nucléaire et Corpusculaire, Université de Genève, Genève; Switzerland.
- ^h Also at Departament de Física de la Universitat Autònoma de Barcelona, Barcelona; Spain.
- ⁱ Also at Department of Financial and Management Engineering, University of the Aegean, Chios; Greece.
- ^j Also at Department of Modern Physics and State Key Laboratory of Particle Detection and Electronics, University of Science and Technology of China, Hefei; China.
- ^k Also at Department of Physics, Ben Gurion University of the Negev, Beer Sheva; Israel.
- ^l Also at Department of Physics, Bolu Abant İzzet Baysal University, Bolu; Türkiye.

- m* Also at Department of Physics, King's College London, London; United Kingdom.
- n* Also at Department of Physics, Stellenbosch University; South Africa.
- o* Also at Department of Physics, University of Fribourg, Fribourg; Switzerland.
- p* Also at Department of Physics, University of Thessaly; Greece.
- q* Also at Department of Physics, Westmont College, Santa Barbara; United States of America.
- r* Also at Faculty of Physics, Sofia University, 'St. Kliment Ohridski', Sofia; Bulgaria.
- s* Also at Faculty of Physics, University of Bucharest; Romania.
- t* Also at Hellenic Open University, Patras; Greece.
- u* Also at Henan University; China.
- v* Also at Imam Mohammad Ibn Saud Islamic University; Saudi Arabia.
- w* Also at Indian Institute of Technology (IIT), Jodhpur; India.
- x* Also at Institutio Catalana de Recerca i Estudis Avancats, ICREA, Barcelona; Spain.
- y* Also at Institut für Experimentalphysik, Universität Hamburg, Hamburg; Germany.
- z* Also at Institute for Nuclear Research and Nuclear Energy (INRNE) of the Bulgarian Academy of Sciences, Sofia; Bulgaria.
- aa* Also at Institute of Applied Physics, Mohammed VI Polytechnic University, Ben Guerir; Morocco.
- ab* Also at Institute of Particle Physics (IPP); Canada.
- ac* Also at Institute of Physics and Technology, Mongolian Academy of Sciences, Ulaanbaatar; Mongolia.
- ad* Also at Institute of Physics, Azerbaijan Academy of Sciences, Baku; Azerbaijan.
- ae* Also at Institute of Theoretical Physics, Iliia State University, Tbilisi; Georgia.
- af* Also at Millennium Institute for Subatomic physics at high energy frontier (SAPHIR), Santiago; Chile.
- ag* Also at National Institute of Physics, University of the Philippines Diliman (Philippines); Philippines.
- ah* Also at School of Physics, University of the Witwatersrand, Johannesburg; South Africa.
- ai* Also at The Collaborative Innovation Center of Quantum Matter (CICQM), Beijing; China.
- aj* Also at TRIUMF, Vancouver BC; Canada.
- ak* Also at Università di Napoli Parthenope, Napoli; Italy.
- al* Also at Università degli Studi Link; Italy.
- am* Also at University and INFN Torino, Torino; Italy.
- an* Also at University of Chinese Academy of Sciences (UCAS), Beijing; China.
- ao* Also at University of Colorado Boulder, Department of Physics, Colorado; United States of America.
- ap* Also at University of Siena; Italy.
- aq* Also at Washington College, Chestertown, MD; United States of America.
- ar* Also at Yeditepe University, Physics Department, Istanbul; Türkiye.
- * Deceased